

Layer-by-layer self-assembly of nanofiltration membrane for water and wastewater treatment

by

Jingjing Sun

A thesis

presented to the University of Waterloo

in fulfillment of the

thesis requirement for the degree of

Master of Applied Science

in

Chemical Engineering

Waterloo, Ontario, Canada, 2015

©Jingjing Sun 2015

Author's Declaration

I hereby declare that I am the sole author of this thesis. This is a true copy of the thesis, including any required final revisions, as accepted by my examiners.

I understand that my thesis may be made electronically available to the public.

Abstract

In this study, polyelectrolyte composite membranes were prepared using layer-by-layer (LbL) self-assembly of chitosan/poly(acrylic acid) (chitosan/PAA) on polyethersulfone (PES) substrates. These thin-film-composite (TFC) membranes were used for salt rejection.

The performance of the chitosan/PAA composite membranes showed good separation performance for salt solutions. With an increase in the chitosan/PAA bilayers, the salt rejection of the membrane increased and permeation flux decreased, which indicated the growth of the polyelectrolyte thin film on PES substrates. By varying such preparation conditions as polyelectrolyte concentration, deposition time and the outermost layer in LbL assembly, membranes with different separation performances were obtained. Therefore, LbL assembly of polyelectrolytes can be used to tailor the membrane structure with the desired separation performances.

Although the chitosan/PAA composite membranes possessed favorable salt retention, these membranes could not afford a long-term operation in salt solutions. Membrane swelling would take place during a long period of nanofiltration (NF) application. To improve the NF performance and stability of the CS/PAA composite membranes in salt solutions, two post-treatment methods (i.e., heat treatment and crosslinking) were used in membrane preparation. An improvement in the membrane selectivity was accomplished by increasing the heating temperature and duration. When the heating temperature reached 150°C, the salt rejection of membranes had markedly enhanced. A heat treatment time of

60 min seemed to be sufficient to produce membranes with high separation performance. In addition, the stability of membrane was also enhanced by the heat treatment.

Chemical crosslinking of chitosan/PAA multilayers was also applied in membrane preparation process. Glutaraldehyde was utilized as a crosslinking agent for membrane modification of chitosan terminated composite membranes. The resulting membranes showed improved stability and salt rejection. A 2³ factorial experimental design was used in this study to evaluate the main crosslinking effects (i.e., crosslinking temperature, crosslinking time, and glutaraldehyde concentration) and their interactions on the separation performance of the membrane. The crosslinking temperature, glutaraldehyde concentration, and their interaction showed more significant influence on membrane performance than other effects. Moreover, the stability of the chitosan/PAA composite membrane were enhanced considerably by crosslinking of membrane with glutaraldehyde.

Keywords: Nanofiltration, salt rejection, polyelectrolyte, self-assembly, crosslinking, chitosan, glutaraldehyde, factorial design.

Acknowledgements

First and foremost, I would like to give my gratitude to my supervisor Professor Xianshe Feng, for his precious guidance, supervision, comments and provisions that benefited me much throughout my master's study. Thanks to him for giving me the chance to explore new knowledge as well as giving me precious advice in order to improve myself to become a better person.

I would like to express my eternal appreciation towards the examination committee for their comments and suggestions on my thesis.

I would like to thank my dear friends and colleagues, especially fellow students in the Feng's group for their support and assistance.

I must give my endless thanks to my family for their immeasurable support and love throughout my lifetime. This thesis is inscribed to them.

Table of Contents

Author’s Declaration	ii
Abstract.....	iii
Acknowledgements.....	v
Table of Contents.....	vi
List of Figures.....	ix
List of Tables.....	xii
CHAPTER 1.....	1
Introduction	1
1.1 Background	1
1.2 Research objectives	4
1.3 Outline of the thesis.....	5
CHAPTER 2.....	7
Literature Review.....	7
2.1 Principles of Nanofiltration	8
2.1.1 Features of Nanofiltration	8
2.1.2 Mass transport through NF membranes	9
2.1.3 NF membrane characterization	10
2.2 NF membrane materials, preparation, and applications	13
2.2.1 NF membrane materials	13
2.2.2 NF membrane preparation.....	15
2.2.3 Applications of NF membranes.....	16
2.3 Polyelectrolyte composite membranes	19
2.3.1 Formation of LbL polyelectrolyte composite membranes	20
2.3.2 Materials for polyelectrolyte composite membranes	22
2.3.3 LbL Assembly for membrane separation.....	26
2.4 Factors affecting the separation performance of LbL membranes	28

2.4.1 Number of deposited polyelectrolyte bilayers	28
2.4.2 pH and ionic strength of polyelectrolyte solutions.....	28
2.4.3 Molecular weight of polyelectrolytes.....	29
2.5 Post-treatment procedures for optimizing membrane performance	31
2.5.1 Heat treatment	31
2.5.2 Surface modification by crosslinking.....	32
CHAPTER 3.....	35
Studies of LbL assembly of chitosan/PAA on PES substrates for salt rejection	35
3.1 Introduction.....	35
3.2 Experimental	36
3.2.1 Materials.....	36
3.2.2 Preparation of chitosan/PAA composite membranes.....	37
3.2.3 Nanofiltration	38
3.2.4 Heat treatment	40
3.2.5 Stability test of the polyelectrolyte composite membranes.....	40
3.3 Results and discussion	41
3.3.1 Effect of number of polyelectrolyte bilayers.....	41
3.3.2 Effect of polyelectrolyte deposition time	45
3.3.3 Effects of concentration of polyelectrolyte solution	47
3.3.4 Effects of the outermost layer of the membrane	51
3.3.5 Effects of heat treatment temperature	54
3.3.6 Effects of heat treatment time	56
3.3.7 Effects of operating pressure in nanofiltration.....	58
3.3.8 Effects of feed salt concentration in nanofiltration	62
3.3.9 Stability of chitosan/PAA composite membrane without heat treatment	65
3.3.10 Stability of heat-treated CS/PAA composite membrane.....	68
3.4 Conclusions.....	70
CHAPTER 4.....	72
Studies of chemical crosslinking on performance of chitosan/PAA composite	

membranes	72
4.1 Introduction.....	72
4.2 Experimental	73
4.2.1 Materials and membrane preparation.....	73
4.2.2 Crosslinking of chitosan/PAA composite membranes.....	74
4.2.3 Experimental Design.....	74
4.2.4 Stability test of crosslinked chitosan/PAA composite membrane	75
4.3 Results and discussion	75
4.3.1 Pareto charts for the factorial design.....	75
4.3.2 Analysis of variance.....	79
4.3.3 Effect of concentration of glutaraldehyde solution	83
4.3.4 Effect of crosslinking temperature	86
4.3.5 Effect of crosslinking time	88
4.3.6 Effect of operating pressure in nanofiltration	90
4.3.7 Effect of feed salt concentration in nanofiltration.....	92
4.3.8 Stability of crosslinked chitosan/PAA composite membrane	94
4.4 Conclusions.....	96
CHAPTER 5.....	98
General conclusions and Recommendations	98
5.1 General conclusions	98
5.2 Recommendations.....	99
5.2.1 Preparation conditions in LbL assembly	100
5.2.2 Modification of LbL-assembled membranes	102
5.2.3 Membrane separation in a complex system	102
References.....	104
Appendix A.....	116
A-1. Sample calculations of the permeation flux and salt rejection.....	116
A-2. Yates Algorithm for a 2 ^k factorial Design to compute the linear contrasts of the effects and their sum of squares (S.S.).....	120

List of Figures

Figure 2.1 Membrane and conventional process overview [Schäfer et al., 2005]	8
Figure 2.2 Cross-section of an asymmetric membrane [Bergman, 2007]	13
Figure 2.3 Cross-section of a thin-film composite membrane [Bergman, 2007]	14
Figure 2.4 Scheme of Layer-by-Layer adsorption of polyelectrolytes [Tieke et al., 2001]....	20
Figure 2.5 Dissolution of chitosan in dilute acetic acid [Feng and Huang, 1996].....	25
Figure 2.6 Separation characteristic of PVA/PVS membranes in ethanol/water feed mixture prepared at different pH, with or without addition of NaCl [Toutianoush and Tieke, 2002] .	29
Figure 2.7 Dependence of separation performance on water content in ethanol/water mixture for PVA/PAA membranes with PAA of molecular weight 5000 or 250,000 [Toutianoush and Tieke, 2002]	30
Figure 2.8 Effect of annealing temperature on flux and water content in the permeate for separation of ethanol/water mixture with 6.2% water [Krasemann and Tieke, 1998].....	31
Figure 2.9 Schematic diagram of heat-induced cross-linking of PAH/PAA film via amidation [Harris et al., 1999]	33
Figure 3.1 LbL-assembly steps in a cap device	38
Figure 3.2 Schematic diagram of nanofiltration experiment	39
Figure 3.3 Effects of number of bilayers on (a) salt rejection and (b) permeation flux for the [chitosan/PAA] _n membranes (Operating pressure: 0.7 MPa; Salt concentration: 500 ppm) ..	43
Figure 3.4 Effects of polyelectrolyte deposition time on (a) salt rejection and (b) permeation flux of the resulting polyelectrolyte membranes (Operating pressure: 0.7 MPa; Salt concentration: 500 ppm)	46
Figure 3.5 Effects of polyelectrolyte concentration on (a) salt rejection and (b) permeation flux of the [CS/PAA] ₄ membranes (Operating pressure: 0.7 MPa; Salt concentration: 500ppm)	49
Figure 3.6 Effects of number of bilayers on (a) salt rejection and (b) permeation flux for [CS/PAA] _n CS membranes (Operating pressure: 0.7 MPa; Salt concentration: 500 ppm).....	52

Figure 3.7 Effects of heat treatment temperature on (a) salt rejection and (b) permeation flux for the [CS/PAA] ₄ membrane (Polyelectrolyte concentration: 1000 ppm; Deposition time: 60 min; Heat treatment time: 90 min; Operating pressure: 0.7 MPa; Salt concentration: 500 ppm)	55
Figure 3.8 Effects of heat treatment time on (a) salt rejection and (b) permeation flux for the [CS/PAA] ₄ membrane (Polyelectrolyte concentration: 1000 ppm; Deposition time: 60 min; Heat treatment temperature: 150°C; Operating pressure: 0.7 MPa; Salt concentration: 500 ppm)	57
Figure 3.9 Effect of operating pressure on (a) salt rejection and (b) permeation flux for the [CS/PAA] ₄ membrane without heat treatment (Polyelectrolyte concentration : 1000 ppm; Deposition time : 60 min)	60
Figure 3.10 Effects of operating pressure on (a) salt rejection and (b) permeation flux for the heat-treated [CS/PAA] ₄ membrane (Polyelectrolyte concentration : 1000 ppm; Deposition time : 60 min; Heat treatment temperature: 150°C; Heat treatment time: 60 min).....	61
Figure 3.11 Effects of feed salt concentration on (a) salt rejection and (b) permeation flux for the [CS/PAA] ₄ membrane without heat treatment (Polyelectrolyte concentration : 1000 ppm; Deposition time : 60 min)	63
Figure 3.12 Effects of feed concentration on (a) salt rejection and (b) permeation flux for the heat-treated [CS/PAA] ₄ membrane (Polyelectrolyte concentration : 1000 ppm; Deposition time : 60 min; Heat treatment temperature: 150°C; Heat treatment time: 60 min).....	64
Figure 3.13 Stability of the [CS/PAA] ₄ membrane without heat treatment, (a) salt rejection and (b) permeation flux (Polyelectrolyte concentration : 1000 ppm; Deposition time : 60 min; Operating pressure: 0.7 MPa; Salt concentration: 500 ppm).....	67
Figure 3.14 Stability of the heat-treated [CS/PAA] ₄ membrane, (a) salt rejection and (b) permeation flux (Polyelectrolyte concentration : 1000 ppm; Deposition time : 60 min; Heat treatment temperature: 150°C; Heat treatment time: 60 min; Operating pressure: 0.7 MPa; Salt concentration: 500 ppm)	69
Figure 4.1 Structure of crosslinked chitosan molecular.....	73
Figure 4.2 Pareto charts of the crosslinking effects on salt rejection for (a) Na ₂ SO ₄ , (b) MgSO ₄ , (c), NaCl and (d) MgCl ₂ . (A) Crosslinking temperature; (B) Crosslinking time; and (C) Glutaraldehyde concentration.....	77
Figure 4.3 Pareto charts of the crosslinking effects on permeation flux for (a) Na ₂ SO ₄ , (b) MgSO ₄ , (c), NaCl and (d) MgCl ₂ . (A) Crosslinking temperature; (B) Crosslinking time; and (C) Glutaraldehyde concentration.....	78

Figure 4.4 Effects of glutaraldehyde concentrations on (a) salt rejection and (b) permeation flux (Operating pressure: 0.7 MPa; Salt concentration: 500 ppm)	84
Figure 4.5 Effects of crosslinking temperature on (a) salt rejection and (b) permeation flux (Operating pressure: 0.7 MPa; Salt concentration: 500 ppm).....	87
Figure 4.6 Effects of crosslinking time on (a) salt rejection and (b) permeation flux (Operating pressure: 0.7 MPa; Salt concentration: 500 ppm).....	89
Figure 4.7 Effects of operating pressure on (a) salt rejection and (b) permeation flux for the crosslinked [CS/PAA] ₄ CS membrane (Polyelectrolyte concentration : 1000 ppm; Deposition time : 60 min; Crosslinking temperature: 25 °C; Crosslinking time: 60 min; Glutaraldehyde concentration: 1.0 wt%)	91
Figure 4.8 Effects of feed salt concentration on (a) salt rejection and (b) permeation flux for the crosslinked [CS/PAA] ₄ CS membrane (Polyelectrolyte concentration : 1000 ppm ; Deposition time : 60 min; Crosslinking temperature: 25 °C; Crosslinking time: 60 min; Glutaraldehyde concentration: 1.0 wt%)	93
Figure 4.9 Stability of the crosslinked [CS/PAA] ₄ CS membrane, (a) salt rejection and (b) permeation flux (Operating pressure: 0.7 MPa; Salt concentration: 500 ppm; Crosslinking temperature: 25 °C; Crosslinking time: 60 min; Glutaraldehyde concentration: 1.0 wt%)	95
Figure A-1 Linear relationship between salt concentration and its electrical conductivity..	119

List of Tables

Table 2.1 Characterization methods for NF membranes [Schäfer et al., 2005]	11
Table 2.2 Polyelectrolytes used for LbL assembly of thin films [Tieke et al., 2001]	24
Table 3.1 Diffusion Coefficient D_i of salts in water at 25°C [Schaep et al., 1998]	45
Table 4.1 Variables investigated and their levels in the experimental design	74
Table 4.2 Design arrangement and experimental results	75
Table 4.3 The p -values and coded coefficients from ANOVA for salt rejection	81
Table 4.4 The p -values and coded coefficients from ANOVA for permeation flux	81
Table A-1 Signs for calculating the effects in the 2^3 factorial Design	120
Table A-2 Yate's algorithm for the 2^3 factorial design	121

CHAPTER 1

Introduction

1.1 Background

Nanofiltration (NF) is a pressure-driven membrane process for removal of inorganic and organic chemicals from a liquid mixture. It started and developed in the 1970s as a variant of reverse osmosis (RO) process. By the late 1980s, NF had become established, and the first application of NF was reported [Conlon and McClellan, 1989]. Compared with RO, NF requires relatively low operating pressure and low maintenance costs while offering high permeation flux and reasonable rejection to multivalent salts and large organic molecules ($MW > 300$). Nowadays, NF has been widely used in water and wastewater treatment, oil process, organic recovery, and food Industry [Bessarabov and Twardowski, 2002; Daufin et al., 2001; Hussain and Al-Rawajfeh, 2009].

NF membranes can be classified according to their structure as homogeneous, asymmetric and composite membranes [Schäfer et al., 2005]. Composite membranes are generally formed by coating ultrathin films on porous substrates. The ultrathin films and the substrates can be chosen separately to optimize overall performance of the membranes. Since Cadotte [1981] fabricated the first thin-film-composite (TFC) membrane by interfacial polymerization, TFC membranes have been widely used,

particularly in RO and NF processes. Several techniques may be employed for the fabrication of TFC membrane preparation, including sol-gel process, vapor deposition, layer-by-layer assembly, and crosslinking method [Abu Seman et al., 2010; Bessarabov and Twardowski, 2002; Bonekamp et al., 2008; Du et al., 2007; Li et al., 2002; Wu et al., 2014; Xu et al., 2010].

Layer-by-layer (LbL) assembly is a simple technique for TFC membrane preparation. It was firstly proposed by Decher and Hong [1991]. A typical process of LbL assembly involves alternating immersions of a porous substrate into two oppositely charged polyelectrolyte solutions to form multilayered thin films [Decher and Schlenoff, 2006]. A variety of polyelectrolytes are used in the LbL assembly of multilayers [Krasemann and Tieke, 1999; Meier-Haack et al., 2001]. The driving forces for build-up of ultrathin multilayers are mainly based on electrostatic attraction and other intermolecular interactions (e.g., hydrogen bonding and charge transfer). Tailoring the thickness and morphology of the multilayers could be achieved by changing such membrane fabrication conditions as the number of bilayers, deposition time, and polyelectrolyte concentrations [Buron et al., 2009; McAloney et al., 2001; Quinn and Caruso, 2004]. LbL assembly provides a simple, potentially economical, and environmentally friendly approach to construct charged ultrathin skin layers, and thus has a great potential for preparation of separation membranes [Lu et al., 2008; Van Ackern et al., 1998; Zhu et al., 2006].

Recently, chitosan, which is a natural polymeric material, has been increasingly used for the fabrication of separation membranes [Feng and Huang, 1996; Toutianoush et al., 2002]. Chitosan is derived from chitin and can become cationic when dissolved in an acid. It offers the advantages of easy accessibility, inexpensiveness, non-toxicity, good chemical resistance and good film-forming properties. Thus, it is a popular material for TFC membranes. The structural stability of chitosan membranes, however, is often not good enough for long-term use. This is because membrane swelling occurs when the amine and hydroxyl groups in chitosan chains are hydrated in water. Membrane swelling is a process due to solvent uptake in the polymers. When the polymer-polymer interactions are strong intermolecular forces (i.e., crosslinking, crystallinity and strong hydrogen bonding), a slow diffusion of solvent molecules into the polymer can only lead to the formation of swollen gels. However, if the polymer-solvent interactions can overcome the polymer-polymer interactions, partial dissolution of polymers into solvent may take place [Fred, 1984]. Membrane swelling, accompanied by decomposition of membrane structure, usually weakens the separation performance of the membrane. Crosslinking is commonly used to restrict the degree of membrane swelling.

Crosslinking refers to the process of chemically linking one polymer chain to another by covalent bonds to form a three-dimensional network. In this process, the crosslinking agents are often required to form intermolecular cationic/ionic bridges

between the polymer chains. For chitosan membranes, several crosslinking agents can be employed for surface modification [Cui et al., 2008; Ghazali et al., 1997; Jegal and Lee, 1999; Wan et al., 2003]. Glutaraldehyde is a bifunctional crosslinking agent that can bridge amino groups between two adjacent polypeptide chains. Thanks to its water solubility, high crosslinking efficiency, and low cost, glutaraldehyde has become the predominant choice in surface crosslinking of chitosan thin films [Anjali Devi et al., 2005; Uragami et al., 1993].

1.2 Research objectives

The purpose of this study was to investigate NF performance of TFC membranes fabricated by the LbL assembly of chitosan/PAA on polyethersulfone (PES) substrates. Different preparation and operating parameters that affect membrane performance were studied. Glutaraldehyde as a crosslinking agent was used in this study to modify the chitosan/PAA composite membranes. The detailed research objectives were as follows:

- 1). To fabricate chitosan/PAA composite membranes by the LbL assembly of chitosan (as a cationic polyelectrolyte) and PAA (as an anionic one) on PES substrates.
- 2). To investigate the preparation conditions of LbL assembly (i.e., number of bilayers, deposition time, polyelectrolyte concentration and the outermost layer) and operating conditions (i.e., pressure and feed concentration) on

NF performance of the membranes.

- 3). To evaluate the influences of heat treatment on the stability and separation performance of the membranes.
- 4). To modify the chitosan/PAA composite membranes by surface crosslinking of chitosan sublayer with glutaraldehyde and to examine the crosslinking effects (i.e., glutaraldehyde concentration, crosslinking time and temperature) and their interactions on stability and separation performance of the membranes.

1.3 Outline of the thesis

This thesis consists of five chapters, and they are organized as follows:

Chapter 1 is an introduction to this thesis work, and the objectives of the research were described.

To have a comprehensive understanding of the fundamentals of nanofiltration, LbL assembly, and crosslinking of polyelectrolyte-based composite membranes, a literature review was presented in Chapter 2.

Chapter 3 focused on the LbL assembly of chitosan/PAA thin films on PES substrates for salt rejections by NF. The effects of parameters involved in LbL assembly and operating conditions in NF experiments on separation performance of the membranes were investigated. Heat treatment was also applied in the membrane preparation to improve stability and separation performance of the TFC membranes.

Crosslinking of the chitosan/PAA composite membranes by glutaraldehyde was found to be effective to improve the membrane selectivity and stability. The main crosslinking effects and their interactions on membrane performance were studied by using a 2^3 full factorial experimental design, and the results were shown in Chapter 4.

Chapter 5 summarized the general conclusions drawn from this study and provided the recommendations for future work.

CHAPTER 2

Literature Review

Nanofiltration (NF) is a membrane filtration process used for liquid separation. NF membranes are commonly applied in water treatments including water softening, wastewater treatment for reuse, and dye-salt separation [Ghizellaoui et al., 2005; Koyuncu, 2002; Zhang et al., 2009]. One of the most important methods to prepare NF membranes is via surface coating. Layer-by-Layer (LbL) assembly of polyelectrolytes is a relatively new technique to create charged, nanometer-scale coatings. It has been proved to be a potential method to fabricate NF membranes [Hong et al., 2009; Stanton et al., 2003; Su et al., 2012; Tieke et al., 2005]. To enhance the performance and stability of separation membranes, crosslinking of polymer chains on the membrane surface is commonly used [Huang et al., 2006; Ju et al., 2008; Robinson et al., 2005].

This chapter attempts to provide a review of the principles of NF, NF membranes, and their applications. Since the LbL assembly was used in this study to prepare NF membranes, the prior work of LbL assembly of polyelectrolytes is also reviewed.

2.1 Principles of Nanofiltration

2.1.1 Features of Nanofiltration

Nanofiltration is a pressure-driven membrane process for liquid separations with two features:

- Capacity of rejecting organic components from aqueous solutions with the molecular weight cut-off (MWCO) in the range of 300 kg/kmol.
- Capacity of rejecting low molecular weight ions of different valency [Rautenbach and Groschl, 1990].

NF is one of the five membrane processes commonly used in water and wastewater treatment, and Figure 2.1 shows a spectrum of the solute sizes and molecular weights.

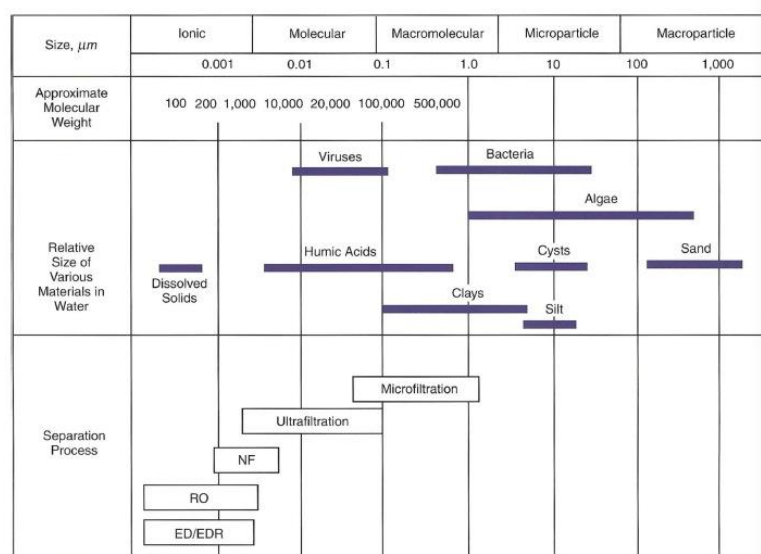


Figure 2.1 Membrane and conventional process overview [Schäfer et al., 2005]

NF is a membrane process between UF where the mechanism of separation is assumed to be size exclusion and RO where the mass transport is governed by a solution-diffusion mechanism. The pore size in NF membranes is so small (nominally-1nm) that uncharged solutes can be highly retained. The electrostatic properties of NF membrane surface allow monovalent ions to be reasonably transmitted while multivalent ions mostly rejected. The mechanism of NF process, therefore, can be regarded as a combination of the size and electrical exclusion of UF and the ion interaction mechanisms of RO.

2.1.2 Mass transport through NF membranes

NF transport is a complex process, and mathematical models that can predict membrane performance is important for industrial application of NF membranes. In the past 30 years, a great deal of work is done on mathematical modeling of mass transport through NF membranes [Al-Zoubi et al., 2007; Hagemeyer and Gimbel, 1998; Nghiem et al., 2004; Patel and Nath, 2014; Vanderhorst et al., 1995].

The widely adapted models of NF transport are based on the extended Nernst-Planck equation proposed by Dresner and Schlögl [1972; 1966]. The equation can be written as:

$$j_i = -D_{i,p} \frac{dc_i}{dx} - \frac{z_i c_i D_{i,p}}{RT} F \frac{d\psi}{dx} + K_{i,c} c_i V \quad (2-1)$$

$$D_{i,p} = K_{i,d} D_{i,\infty} \quad (2-2)$$

where:

c_i — concentration in membrane (mol/ m³)

$D_{i,p}$ — hindered diffusivity (m²/s)

- $D_{i,\infty}$ — bulk diffusivity (m^2/s)
- F — Faraday constant (C/mol)
- j_i — ion flux (based on membrane area)($\text{mol/ m}^2\text{s}$)
- $K_{i,c}$ — hinder factor for convection
- $K_{i,d}$ — hinder factor for diffusion
- R — gas constant (J /mol K)
- T — absolute temperature (K)
- V — solute velocity (m/s)
- x — distance normal to membrane (m)
- z_i — valence of ion
- ψ — electric potential in axial direction (V)

j_i is the flux of ion i and the terms on the right hand side in Eq.(2-1) represent mass transport due to diffusion, electric field gradient and convection respectively. The terms of $K_{i,d}$ and $K_{i,c}$ represents the hindered nature of diffusion and convection of the ions inside the membrane, the value of which are depending on the assumptions made about the membrane (i.e., porous or homogenous, the fluxes, concentrations, and the potentials).

2.1.3 NF membrane characterization

The characterization methods applied to NF membranes can be classified based on the following parameters:

1. Performance parameters;

2. Morphology parameters

3. Charge parameters.

The membrane characterization methods are summarized in Table 2.1:

Table 2.1 Characterization methods for NF membranes[Schäfer et al., 2005]

	Method	Characteristic(s)
Performance parameters	<ul style="list-style-type: none"> • Retention measurements with charged molecules • Retention measurements with uncharged molecules • Water permeability measurement: permeability coefficient • Solvent permeability measurement: Permeability coefficient 	Surface charge, mesh size, pore size Mesh-, pore size Membrane resistance Membrane resistance
Morphology Parameters	<ul style="list-style-type: none"> • Gas adsorption/desorption • Permporometry • Microscopy Field emission microscopy (FEM), Scanning electron microscopy (SEM) Atomic force microscopy (AFM) • Spectroscopy ATR-FTIR ESR/NMR Raman spectroscopy XPS(ESCA) • Contact angle Captive(air) bubble method Sessile drop method 	Pore size, surface area Pore size/porosity Pore size/ porosity Surface roughness, pore size,porosity Chemical composition Hydrophobicity
Charge Parameters	<ul style="list-style-type: none"> • Electro-kinetic measurements • Titration • Impedance spectroscopy 	Zeta potential, surface charge Ion exchange capacity/overall charge Ionic conductivity

Performance parameters include retention measurements (of both charged and uncharged solutes) and permeability measurements (both for water and organic solvents).

The simplest characterization experiment is the determination of the pure water permeability. Since the water flux as a function of the pressure normally exhibits a linear relationship, the permeability coefficient can be determined from the slope

The solute retention of a membrane is defined as in equation:

$$R = \frac{c_f - c_p}{c_f} \quad (2-3)$$

where c refers to the concentration in the feed (f) and permeate (p), respectively.

For retention measurements of charged molecules, Donnan effects frequently dominate or contribute to the separation performance. The standard reference materials are various salts such as Na_2SO_4 , NaCl , and MgCl_2 . Conductivity measurements can determine the concentrations of the feed and permeate. For the rejection of uncharged solutes, the separation performance is determined by a combined effect of size effects and interaction between solute and membrane. The range of a molecular weight retained by NF membranes is typically 200 to 2000. Solutes used for membrane characterization include dextrans, polyethylene glycols, dyes and saccharides (glucose, sucrose, raffinose). Molecular weight cut-off (MWCO) is used as a characteristic parameter for NF membranes. MWCO refers to the lowest molecular weight of the solute that is 90% retained by the membrane.

2.2 NF membrane materials, preparation, and applications

2.2.1 NF membrane materials

A wide variety of materials can be used to manufacture NF membranes, with two primary materials being cellulose acetate (and its derivatives) and various polyamides (eg., aromatic polyamides). Cellulose acetate is commonly used to prepare asymmetric membrane. Figure 2.2 illustrates the structure of asymmetric homogeneous membranes. The dense surface skin of the membrane gives the membrane its rejection characteristics, and the porous substrate supports the skin to withstand pressure differentials across the NF membranes.

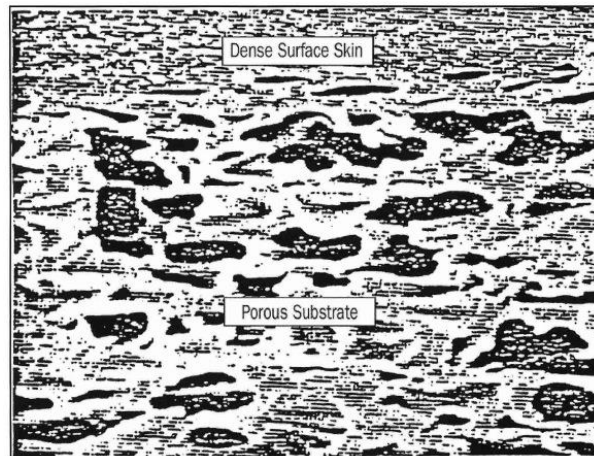


Figure 2.2 Cross-section of an asymmetric membrane [Bergman, 2007]

More recently-developed membranes are thin-film composite membranes (TFC) made of various polymers. TFC usually consists of an ultrathin (i.e., 250 to 2,000 Å) salt barrier layer supported by a separate microporous substrate, as shown in Figure 2.3. A variety of polymers are used for preparing the barrier layer, including the most commonly used aromatic polyamides [Kim et al., 2002; Tang et al., 2009]. Primarily due to high pH tolerance, high organics removal ability, low operating pressures and high rejection characteristics, TFC membranes are most commonly used in water treatment applications.

In addition to polymer membranes, ceramic is another promising material to prepare NF membranes [Childress and Elimelech, 2000; Peeters et al., 1998; Van Gestel et al., 2002]. Ceramic membranes have the advantages of higher chemical, structural and thermal stability than polymeric membrane. They can withstand a high tolerance to pressure, do not swell and can be cleaned easily.

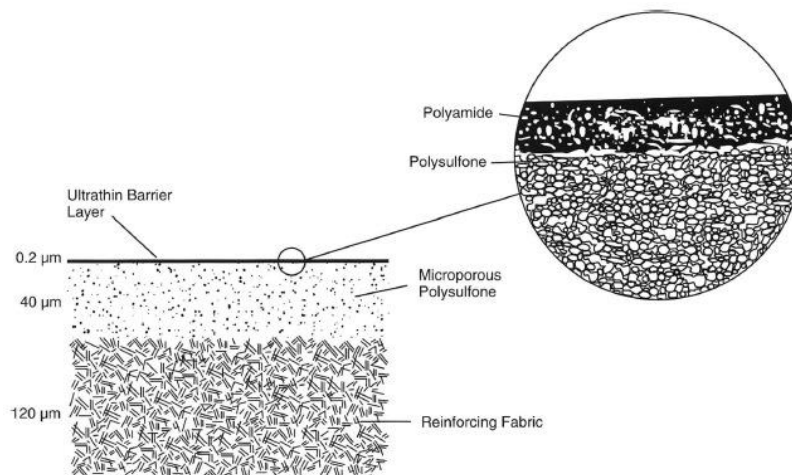


Figure 2.3 Cross-section of a thin-film composite membrane [Bergman, 2007]

2.2.2 NF membrane preparation

The methods to prepare NF membranes include phase inversion, interfacial polymerization, and surface coating.

Phase inversion is a controlled transformation of a cast polymeric solution from a liquid into a solid state. During the phase inversion process, the solvent from the polymer solution was gradually removed to induce phase separation of the polymer solution, thereby forming a polymer-rich and polymer-lean phases. The phase inversion can be accomplished by immersion precipitation, controlled evaporation, thermal precipitation and precipitation from the vapor phase [Mulder, 1996].

Interfacial polymerization has become an important technology to synthesize composite NF membranes. The polymerization reaction occurs at the interface between two immiscible phases, which contain the reactants. Taking the preparation of polyamide composite membrane as an example, a microporous substrate (e.g. a polysulfone UF membrane) is immersed in an aqueous diamine solution. After removing the excess of solution on the membrane surface, the substrate is contacted with an organic phase, which contains an acyl chloride. As a consequence, these two monomers react on the surface of the substrate to form a thin layer (1 to 0.1μ) of PA [Son and Jegal, 2011].

Surface coating is a relatively simple technique for membrane formation. The choice of the polymer for coating a layer depends on many factors, including strength and stability of the polymer, solubility in solvents and crosslinking abilities. In general, the

viscosity of the coating solutions influences the performance of NF membranes formed. Normally, viscous coating solutions result in thick membranes, and thus lead to reduced fluxes while the solute rejections remain the same [Cisneros- Zevallos and Krochta, 2003]. Thanks to its advantages of easy operating, environmentally benign, and potentially economical, LbL assembly has become a promising coating technique for membrane fabrication [Jin et al., 2003; Zhu et al., 2007].

Surface modification can be used to further improve the performance of a prepared NF membrane. The surface modification methods include surface crosslinking, plasma treatment, polymer grafting and photochemical modification [Hu et al., 2002; Pieracci et al., 1999; Ray, 1970]. By modifying the membrane surface, the pore structure, hydrophilicity and stability of the membrane can be enhanced. When the membrane surface is crosslinked, membranes will be less permeable but more selective for solute retention. A proper cross-linking will give the membrane more stability and sometimes better separation properties [Zeng and Ruckenstein, 1998].

2.2.3 Applications of NF membranes

NF membranes can be used a wide variety of applications, including water treatment, food industry, pulp and paper industry, textile dye effluents and bioreactor.

The primary application of NF membrane is water treatment of saline surface water, groundwater, seawater, tertiary treated wastewater, or industrial process water.

Nanofiltration started to be used for drinking water treatment in the late 1980s, and it has now been used to removal of many different contaminant components in water including:

- Dissolved mineral components (nitrate, sulphate, As, Ni) [Le Gouellec and Elimelech, 2002; Tsuru et al., 1998; Van der Bruggen et al., 2001]
- Dissolved organic components (algal toxins) [Hall et al., 2000; Hitzfeld et al., 2000]
- Organic micropollutants (pesticides, endocrine disruptors) [Hayes et al., 2006; Moore and Waring, 1998]
- Taste and odor compounds (2-methylisoborneol, 2,4,6-trichloroanisole) [Smith et al., 2002]

With the constantly increasing need for clean water and decreasing available water supply, NF has become an important choice for water treatment in the future.

The main application of NF in the dairy industry is for concentration and demineralization of whey, in line with other membrane filtration processes. NF applications for salty-, acid- and sweet whey have been reported [Kelly and Kelly, 1995; Rektor and Vatai, 2004].

Large amounts of water used in pulp, bleaching and paper industry can be reused after filtration treatment with membrane processes [Rosa and de Pinho, 1995; Zaidi et al., 1992]. A main advantage of NF in the recovery of water for reuse in pulp and paper industry is that NF process uses a lower operating pressure than RO process. As a result, NF is

possibly more economical to operate. In addition, NF is also able to produce cleaner water than UF, and the clean water can be used in many places in the mill. NF can be used to reduce the chemical oxygen demand (COD) by 70-90%, adsorbable organic halides by 90-97% and most multivalent metals by more than 90%.

Membrane filtration is one of the most popular techniques for wastewater treatment in the textile industry. Dyes used in the textile industry typically have a molecular weight in the range 700-1000 Daltons, and they are ideally suited for NF separation. Based on a few nanofiltration installations used for textile wastewater treatment, it is reported that the capital payout is less than three years [Chakraborty et al., 2003; Tang and Chen, 2002].

In many cell- or enzyme-based industrial processes, the conversion and the separation processes are in general carried out separately. In the last few decades, however, more and more attention is paid to the development of membrane reactors to integrate the bioconversion and product separation. There are many advantages of membrane reactors, including better opportunities for developing continuous processes, better possibilities for process control, less variations in product quality, and higher productivity than traditional continuous processes. There are different types of membrane reactors. For example, a membrane fermenter is a membrane reactor in which whole cells from plant, bacterial or mammalian origins can be applied. NF-based fermenters are mainly used in bacterial cell-based process, and they can be targeted at product formation or wastewater treatment [Jeantet et al., 1996; Valadez-Blanco et al., 2008].

These days, the interest in using nanofiltration expands rapidly in the separation of low molecular weight substances from non-aqueous solutions. The success of membrane technology in the processing of aqueous feeds inspires researchers to develop membranes for non-aqueous separations. Traditional polymeric and ceramic membranes, however, are often not satisfactory for organic applications. Polymeric membranes tend to have different degrees of swelling in organic solvents, but the structure of ceramic membranes can be influenced little by the organic solvents. In recent years, many studies focus on solvent resistant membranes. However, it seems that time and patience are needed before membrane filtration becomes an accepted unit operation in non-aqueous processing [Tsuru et al., 2001].

2.3 Polyelectrolyte composite membranes

The LbL assembly of polyelectrolytes to produce multilayered thin films on porous substrates, originally attempted by Decher and Hong [1991; 1997], is a simple approach to produce charged, ultrathin membrane skin. The LbL assembly involves alternating immersions of a charged substrate into two solutions containing oppositely charged polyelectrolytes to produce thin film composite membranes. By changing the number of bilayers as well as the pH and salt concentration of polyelectrolyte solutions, the thickness and structure of LbL-assembled thin films can be tailored. Theoretically, any polyelectrolyte can be used to produce multilayered thin films, and the LbL assembly of polyelectrolytes is capable of forming a wide variety of membranes.

2.3.1 Formation of LbL polyelectrolyte composite membranes

The LbL assembly consists of four steps, as shown in Figure 2.4.

- 1) The negatively charged surface of a substrate is immersed in a cationic polyelectrolyte solution until a thin layer of polycation is adsorbed, and the surface charge was reversed;
- 2) The substrate is washed with de-ionized water to remove the excess polycation molecules on the surface that are not strongly adsorbed on the substrate surface;
- 3) Immersing the surface of the substrate into an anionic polyelectrolyte solution where the negative charge is adsorbed.
- 4) Washing the substrate surface with de-ionized water.

By repeating these four steps, multiple polyelectrolyte bilayers can be assembled on the substrate. If the substrate surface is positively charged, then an anionic polyelectrolyte will be deposited on the substrate surface first, followed by rinsing with water and deposition of polycations.

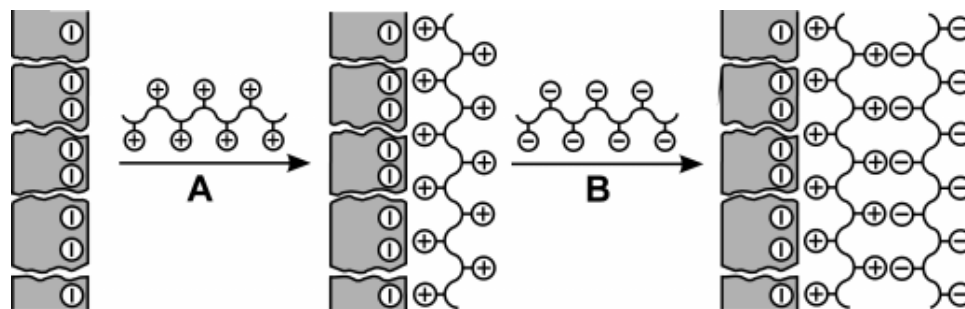


Figure 2.4 Scheme of Layer-by-Layer adsorption of polyelectrolytes [Tieke et al., 2001]

The conventional static Layer-by-Layer self-assembly is effective but time-consuming to prepare defect membrane. It has been reported that as many as 60 bilayers of polyelectrolytes were needed in order to produce membranes with sufficient selectivity [Van Ackern et al., 1998]. In order to decrease the fabrication time of the polyelectrolyte multilayers, a dynamic LbL deposition has been considered to reduce the number of bilayers required and improve the separation performance of the composite membranes.

Zhang et al.[2006] proposed a dynamic assembly method by alternatively depositing PAA/PEI onto a polyethersulfone (PES) ultrafiltration membrane under a pressure of 0.1 MPa. Only 4 polyelectrolyte bilayers were found to be sufficient to obtain a membrane with high separation performance by using the dynamic LbL deposition process. The separation factor of the polyelectrolyte composite membranes was 1207, and the permeation flux was $140\text{g}/(\text{m}^2\text{h})$ for the separation of ethanol from 95% ethanol/water mixtures at the feed temperature of 40°C .

Zhang et al. [2009] proposed dynamic deposition method by using an electric field to enhance separation performance of LbL-assembled polyelectrolyte membranes. The selectivity of the resulting membranes for 90% isopropanol/water mixtures was better than membranes prepared under static LbL assembly conditions. The membrane with four PEI/PAA bilayers showed a separation factor of 1075 and the permeation flux of $4.05\text{kg}/(\text{m}^2\text{h})$ at 70°C .

Yin et al. [2010] employed vibrations to enhance LbL assembly of PDDA and PSS on a modified polyamide reverse osmosis membrane. Compared to conventionally prepared composite membranes, the membranes so formed exhibited both high selectivity and high permeation flux. The enhancement of membrane performance was due to the more orderly deposited polymer chains and thus more dense and smooth surface of the membranes. The vibration method, therefore, was proved to be an effective way to improve the performance of multilayer membranes.

2.3.2 Materials for polyelectrolyte composite membranes

Substrates

When preparing polyelectrolyte composite membranes, the first step is to select a suitable substrate on which the polyelectrolyte multilayers will be assembled. In general, the substrates for LbL assembly should be porous ones. One advantage of using porous substrates is that the mass transport through the composite membranes is only slightly affected by the substrate itself. As a result, the separation properties of the membrane will be mainly determined by the ultrathin multilayers adsorbed on the substrates.

Tieke et al. [2001] studied the influence of substrates on the properties of polyelectrolyte composite membranes. The results showed that 1) All membranes with enough hydrophilicity could be used as substrates for adsorption of polyelectrolyte multilayer. 2) Low molecular weight polyelectrolytes were more easily adsorbed on the

substrate with a rough surface while high molecular weight polyelectrolytes were more easily adsorbed on pore-free membranes.

Xu et al. [2010] used commercial polyamide RO membrane as a substrate to produce polyelectrolyte bilayers for use as a pervaporation membrane. The results showed that 3-4 bilayers were sufficient for the membrane to yield a good permselectivity by using polyamide membranes as a substrate in comparison with conventionally used microporous polyacrylonitrile membranes. As many as 60-90 bilayers are often needed for polyelectrolyte to buildup on polyacrylonitrile substrate in order to be selective enough for pervaporation separation of solvents.

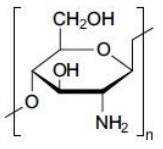
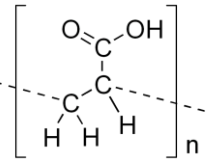
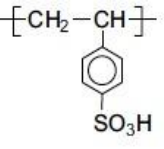
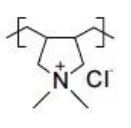
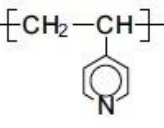
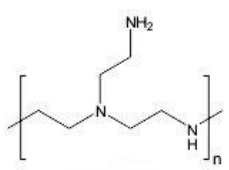
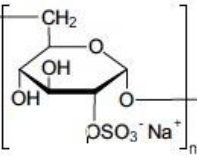
In the work of Malaisamy et al. [2005], PES ultrafiltration membranes were used as substrates for preparing polyelectrolyte composite membranes for nanofiltration. The results showed that the simple LbL adsorption of polyelectrolytes on the PES substrates with a MWCO of 50 kDa resulted in membranes with a high flux for selective nanofiltration of salts and sugars from aqueous solutions. In contrast, the LbL assemblies on the PES substrates with MWCOs of 300 and 500 kDa did not yield highly selective membranes, presumably because the polyelectrolyte films assembled were incapable of fully covering the large pores in these substrates.

Polyelectrolytes

A wide variety of polyelectrolytes can be used for LbL assembly, which allows tailoring of the thickness and structures of resulting composite membranes for various

separation applications. Table 2.2 is a partial list of polyelectrolytes used for preparation of separation layers. This literature review only introduces some of the most commonly used polyelectrolytes for preparation of LbL membrane.

Table 2.2 Polyelectrolytes used for LbL assembly of thin films [Tieke et al., 2001]

Compound	Abbreviation	Formula	Compound	Abbreviation	Formula
Chitosan	CS		poly(acrylic- acid)	PAA	
Poly(allylamine- hydrochloride)	PAH	$\left[\text{CH}_2 - \underset{\text{CH}_2 \text{NH}_3^+ \text{Cl}^-}{\text{CH}} \right]_n$	Poly(styrene- sulfonic acid)	PSS	
Poly(vinylamine)	PVAM	$\left[\text{CH}_2 - \underset{\text{NH}_2}{\text{CH}} \right]_n$	Poly(vinylsulfate- potassium salt)	PVS	$\left[\text{CH}_2 - \underset{\text{OSO}_3^- \text{K}^+}{\text{CH}} \right]_n$
Poly(dimethylallyl- ammoniumchlorid)	PDADMAC		Poly(4- vinylpyridine)	P4VP	
Branched Poly(ethyleneimine)	PEI		Dextransulfate Sodium salt	DEX	

Chitosan is a linear polymer produced by N-deacetylation of chitin, which can be extracted from the outer shells of crustaceans (e.g., crabs and shrimp) and cell walls of

fungi. Chitosan primarily composes of glucosamine. The amino groups in chitosan have a pKa value of 6.5, and they can be protonated in acidic to neutral solutions with a charge density dependent on pH-value (see Figure 2.5). The water solubility and bioadhesion of chitosan favor its binding to negatively charged membrane surfaces. Chitosan also has the advantages of favorable solvent stability, inexpensiveness, non-toxicity as well as great film-forming properties, which make it a good choice for use in membrane fabrication by LbL assembly.

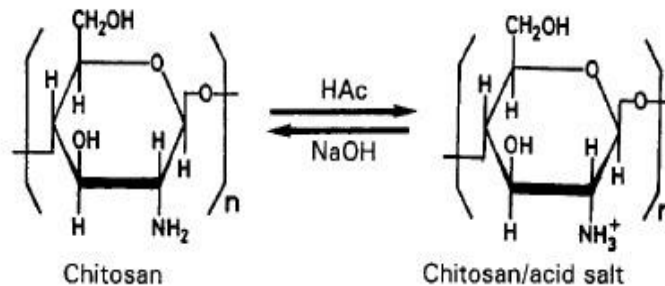


Figure 2.5 Dissolution of chitosan in dilute acetic acid [Feng and Huang, 1996]

Poly(acrylic acid) (PAA) is a water-soluble polymer. In a solution at neutral pH, the carboxyl groups on the side chains of PAA will lose their protons and become negatively charged. Thus, PAA is often used as an anionic polyelectrolyte in preparing LbL assembled membranes.

Polyethylenimine (PEI) is a cationic polymer with a high charge density. Branched PEI contains primary, secondary and tertiary amino groups, in contrast to linear PEI that contains all secondary amines. Both linear and branched PEI have a high thermal, solvent

and flame resistances and are favorite cationic polyelectrolytes for LbL assembly of polyelectrolyte bilayers.

2.3.3 LbL Assembly for membrane separation

LbL Assembly of oppositely charged polyelectrolytes has been proved to be a simple and promising method to prepare separation membranes. LbL assembled polyelectrolyte composite membranes are often used for pervaporation and gas separations. The LbL technique is also applicable to the preparation of NF and RO membranes for water treatment.

Krasemann and Tieke [1998] prepared polyelectrolyte composite membranes by alternating electrostatic adsorption of PAH and PSS on porous PAN/PET substrates and studied the pervaporation performance of the membranes. The separation factor of 70 and a permeation flux of 230 g/(m²h) were obtained at a water content in the feed (6.2 wt%). Annealing treatment of the membrane further improved the separation performance of the membrane at a annealing temperature above 60°C. The membrane selectivity was also increased when the number of PAH/PSS bilayers were increased.

Sullivan et al. [2005] reported a LbL-assembled membrane by alternating electrostatic deposition of PAH and poly(amic acid) that contains diaminobenzoic acid on a porous alumina substrate, followed by heat-induced imidization. These membranes exhibited water/alcohol selectivity of 1100 and 6100 for feed solutions containing 10 and 90% isopropanol respectively. The selectivities of these membranes for water/ethanol

separation decreased to 100 and 500 for 10 and 90% ethanol respectively, while the permeation fluxes were essentially the same.

Van Ackern et al. [1998] used composite membranes with layer pairs of PAH/PSS on PAN/PET substrates for gas separation. It was found that 60 bilayers of PAH/PSS reduced the gas flow to 0.1% of the initial value. The gas flow rates of oxygen, nitrogen and argon were nearly identical, while the gas flow rate of carbon dioxide was higher by a factor up to 2.4.

Krasemann and Tieke [2000] proposed to use self-assembled alternating multilayers of cationic and anionic polyelectrolytes on a PAN/PET substrate for ion separation. With 60 layer pairs of PAH/PSS, a separation factor for $\text{Na}^+/\text{Mg}^{2+}$ up to 112.5 and for $\text{Cl}^-/\text{SO}_4^{2-}$ up to 45.0 were obtained. Addition of salt to polyelectrolyte solutions led to improved ion separation ability of the membranes.

Ouyang et al. [2008] used PAH and PSS as cationic and anionic polyelectrolytes for LbL assembly on PES substrates to prepare NF membranes. A rejection of 40% of NaCl solution at a feed concentration of 1g/L was obtained. At a lower feed concentration of 0.1 g/L, the salt rejection was increased to 74%. The separation performance of the membranes for MgCl_2 was even better. The rejection for MgCl_2 was 93.5% and 93.6% while MgCl_2 concentration in the feed was 0.1g/L and 1g/L, respectively.

Malaisamy et al. [2011] prepared LbL assembled PDADMAC/PSS bilayers on a commercial polyamide nanofiltration membrane and measured the monovalent/anion

selectivity of these composite membranes. The rejection of the resulting membranes to Cl⁻ increased from 30 to 91% after 8-bilayer modification, and the flux decreased by 30%. Under identical operating conditions, the modified membranes showed higher selectivity and flux than the commercial BW30 RO membranes

2.4 Factors affecting the separation performance of LbL membranes

2.4.1 Number of deposited polyelectrolyte bilayers

The successive deposition of polyelectrolyte bilayers on a porous support will increase the thin film thickness and gradually seal the pores in the substrates. Consequently, the permeation flux of the membranes decreases as the selectivity increases. For example, increasing the number of assembled bilayers from 50 to 60 would decrease the permeation flux from 150 to 110 g/(m²h). Whereas, the water content in the permeate increased from 10 to 98 wt% [Krasemann and Tieke, 1998].

2.4.2 pH and ionic strength of polyelectrolyte solutions

Previous studies have shown that the pH and ionic strength of the polyelectrolyte solution affected the polar groups and chain conformation of the adsorbed polymers [Aravind et al., 2010; McAloney et al., 2001; Shiratori and Rubner, 2000; Steitz et al., 2001]. Thus, the thickness, surface roughness, and charge density of the polyelectrolyte multilayers are influenced by pH and ionic strength of the solutions used in LbL assembly.

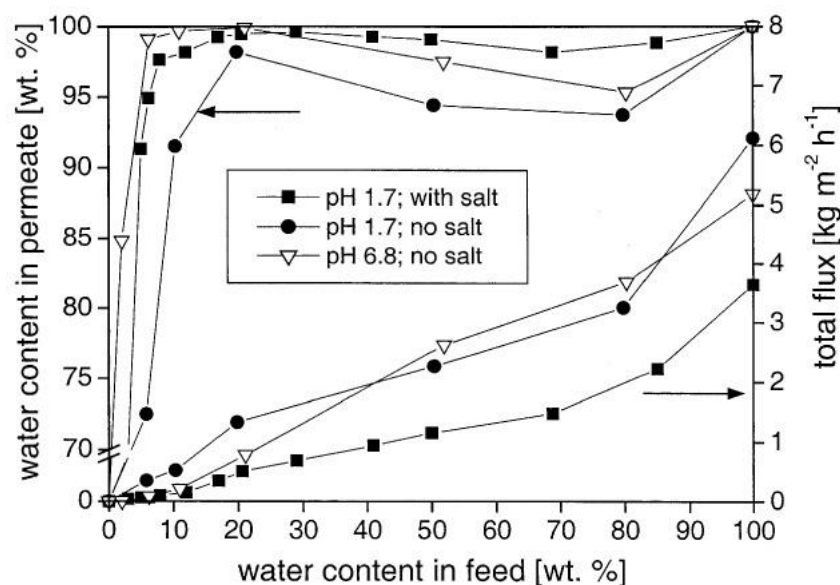


Figure 2.6 Separation characteristic of PVA/PVS membranes in ethanol/water feed mixture prepared at different pH, with or without addition of NaCl [Toutianoush and Tieke, 2002]

Toutianoush and Tieke [2002] studied the effects of pH and ionic strength of polyelectrolyte solutions on the separation characteristics of the resulting LbL-assembled membranes. As shown in Figure 2.6, the permeation flux was only affected by the salt present in the polyelectrolyte solutions. The presence of salt, especially at a higher pH, positively influenced the selectivity of the membranes. Membranes prepared at pH 1.7 with no salt present in the polyelectrolyte solution exhibited a lowest selectivity for the separation of ethanol/water mixtures.

2.4.3 Molecular weight of polyelectrolytes

The molecular weight of the polyelectrolyte is another important parameter that influences the separation characteristics of LbL membranes. Toutianoush and Tieke

[2002] studied the effects of molecular weight of PAA on the membrane performance base on PVA/PAA multiple layers. It is shown in Figure 2.7 that the permeation flux of the membrane formed with a low molecular weight PAA (5000) was only a quarter of the value found for the membrane formed with a high molecular weight PAA (250,000). Meanwhile, the membrane selectivity was the same for the two membranes when tested for ethanol/water separation.

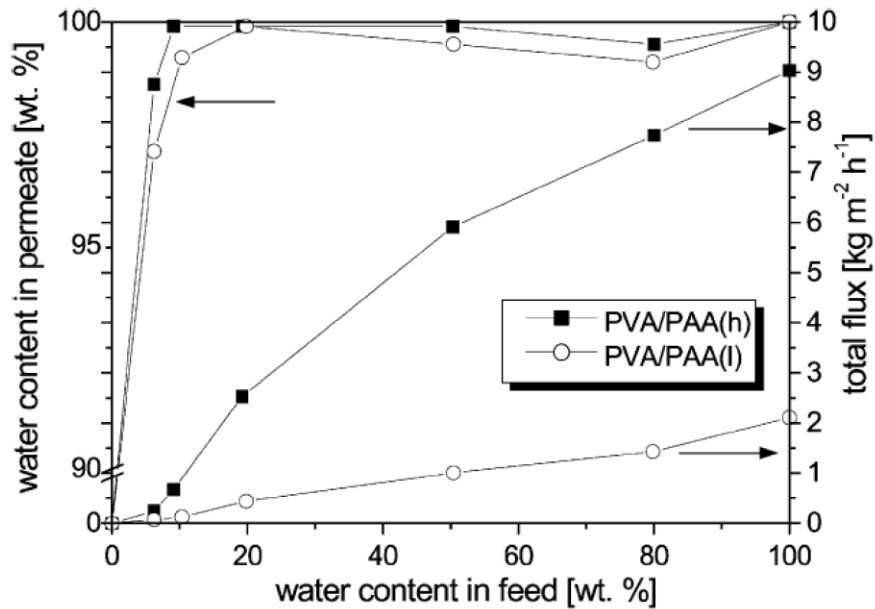


Figure 2.7 Dependence of separation performance on water content in ethanol/water mixture for PVA/PAA membranes with PAA of molecular weight 5000 or 250,000

[Toutianoush and Tieke, 2002]

2.5 Post-treatment procedures for optimizing membrane performance

2.5.1 Heat treatment

The permeation flux and separation performance of the membrane usually depends on the surface structure and morphology of the membrane, which are often affected by heat treatment. Figure 2.8 shows the effects of heat treatment on membrane performance for pervaporation separation of ethanol/water mixture with 6.2% water [Krasemann and Tieke, 1998].

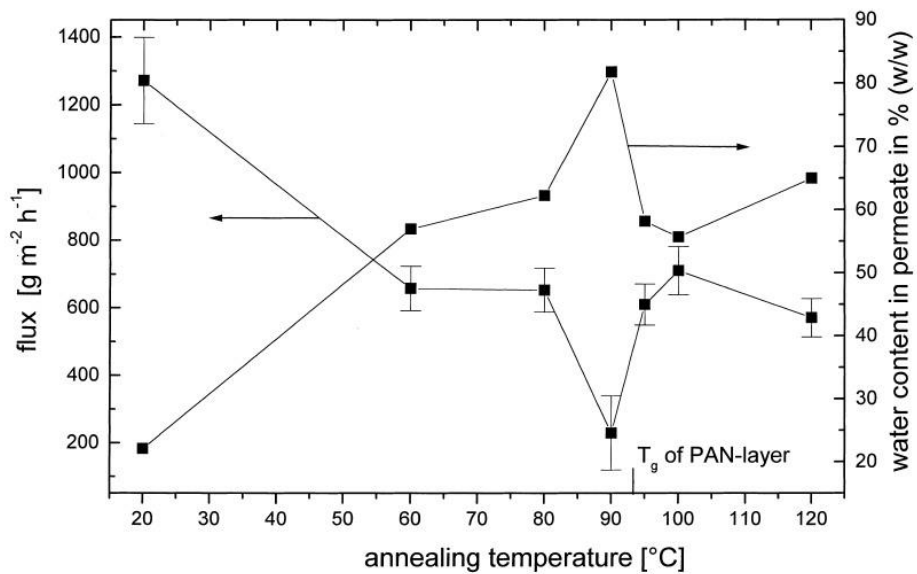


Figure 2.8 Effect of annealing temperature on flux and water content in the permeate for separation of ethanol/water mixture with 6.2% water [Krasemann and Tieke, 1998].

Composite membranes with 60 bilayers of PAH/PSS deposited on PAN/PET substrates were heated at different temperatures. The membranes heated at 60°C, or higher had a lower flux and higher water content in permeate than the non-heated

membranes. After annealing the membrane at 60 °C, the permeate water concentration increased from 20 to 60 wt%. The best pervaporation performance (water concentration of 80 wt% corresponding to a separation factor of 70) was obtained when the membrane was annealed at 90°C, a temperature slightly below the glass transition temperature of PAH.

2.5.2 Surface modification by crosslinking

Alternating deposition of polyelectrolytes can reduce the permeability of the membranes to some extent. However, the polyelectrolyte films are hydrophilic and will swell in water [Harris and Bruening, 2000; Lösche et al., 1998]. The swelling of the membrane occurs if the polymer-solvent interactions dominate over the polymer-polymer intermolecular forces in the membrane. When a hydrophilic membrane is operated in a solvent (eg., water, ethanol, and isopropanol), the hydrophilic solvent molecules can be incorporated into the hydrophilic polymer membranes due to their strong affinity, and thus leads to the swelling of the membranes.

Crosslinking has been proved to be an effective method to reduce membrane swelling and enhance membrane selectivity and stability. Crosslinking will bridge one polymer chain to another by covalent/ionic bonds to form a three-dimensional network on the membrane surface. Harris et al. [1999] studied possibility of crosslinking of PAH/PAA films through heat-induced amidation. The reaction process is shown in Figure 2.9.

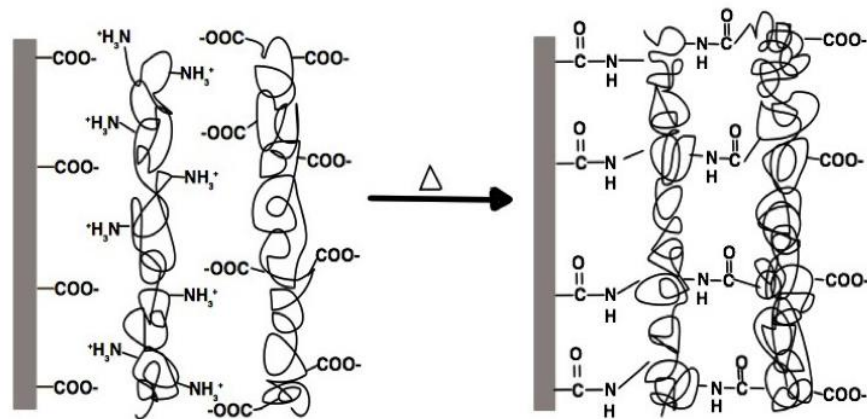


Figure 2.9 Schematic diagram of heat-induced cross-linking of PAH/PAA films via amidation [Harris et al., 1999]

Dai et al. [2000] used electrochemical impedance spectroscopy to study corrosion protection of aluminum, and it is shown that multilayers of PAH/PAA provided substantial protection to the aluminum surface against corrosion. After immersion in the 0.5 M NaCl solution for 4h, the resistance of aluminum coated with a crosslinked 9-bilayer PAA/PAH film was $70 \text{ M}\Omega \text{ cm}^2$ compared to the resistance of naked aluminum that was only $0.07 \text{ M}\Omega \text{ cm}^2$. The high resistance of the cross-linked PAA/PAH indicates a good corrosion protection. The crosslinked PAA/PAH functions as an ultrathin anticorrosion coating that may have advantages in maintaining substrate properties.

In some cases, crosslinking of polyelectrolytes requires the use of crosslinking agents. Du et al. [2007] crosslinked poly(N, N-dimethylaminoethyl methacrylate)/polysulfone (PDMAEMA/PSF) composite membranes by using p-xylylene dichloride (XDC) as a crosslinking agent. It is shown that the permselectivity of the membrane was affected by the concentration of the crosslinking agent, crosslinking time, PDMAMA concentration

and deposition time. The crosslinked composite membrane showed an ideal CO₂/N₂ separation factor of 50 at 23 °C and 0.41 MPa of CO₂ feed pressure. Zhang et al. [2013] crosslinked PEI and chitosan chains on LbL assembled membranes using glutaraldehyde as a crosslinking agent, and the stability and separation performance of the composite membranes for dehydration of ethanol and isopropanol were improved by the crosslinking of the outermost layer of PEI or chitosan.

In this study, both heat treatment and chemical crosslinking will be used to improve the stability and solute rejection of the NF membranes.

CHAPTER 3

Studies of LbL assembly of chitosan/PAA on PES substrates for salt rejection

3.1 Introduction

These days, quality regulations of drinking water are stringent and in some cases can only be met by membrane processes. Compared to conventional water treatment process which may require several different steps, membrane treatment is a simple one-step process for removal of undesirable components from water. NF as a commonly used membrane process is able to eliminate multivalent salts and large organic molecules ($MW > 300$) from liquid solutions, and it thus is widely used in drinking water treatments including turbidity and bacteria removal, groundwater softening and desalination of seawater [Mallevialle et al., 1996; Missimer and Watson, 1994].

In this study, the buildup of chitosan/PAA thin films on PES substrates was achieved by the LbL assembly technique. The effects of parameters involved in LbL assembly and the operating conditions in NF operation on the separation performance of the chitosan/PAA composite membranes were investigated. Heat treatment was used as a

post-treatment procedure to improve the stability and separation performance of the membranes. Stability test was also carried out to evaluate the stability of the chitosan/PAA composite membranes for long-term operation of the membrane in salt solutions.

3.2 Experimental

3.2.1 Materials

Microporous flat-sheet PES membranes (MWCO 10,000 Da) were supplied by Sepro Membranes Inc, and used as the substrates for LbL assembly of polyelectrolyte thin films.

Chitosan flakes (Flonac-N, Mw: 500,000, and 99% N-deacetylation) were supplied by Kyowa Technos Co. Ltd, Japan. PAA (Mw 250,000, in a 35 wt% aqueous solution) was purchased from Sigma-Aldrich. Chitosan and PAA were used in the LbL assembly as polycation and polyanion, respectively. Deionized water was utilized as a solvent to produce a dilute aqueous solution of PAA and to rinse the membranes during the LbL assembly process. Acetic acid supplied from Fisher Scientific was used to dissolve the chitosan flakes. Aqueous solutions of NaCl (EMD Chemical Inc), Na₂SO₄ (McArthur Chemical Co), MgCl₂ (J.T Baker Chemical Company) and MgSO₄ (BDH Chemicals Ltd) were used as feed solutions in the NF experiments.

3.2.2 Preparation of chitosan/PAA composite membranes

Chitosan was dissolved in 2wt% acetic acid solution and stirred for 24h to make a polycation solution. PAA was dissolved in deionized water and stirred for 24h to make a polyanion solution. PES substrate was soaked in deionized water overnight, and then the surface of the substrate was immersed in a 0.1wt% of NaOH solution for 7 min to clear away any preservative and dust. Then the PES substrate was rinsed with de-ionized water to remove residual NaOH on the membrane surface.

The PES substrate was then mounted in a cap device with the active PES surface side up and the nonwoven fabric side down. The aqueous solution of chitosan was poured into the cap device to contact with the surface of the PES substrate for 1 h. The excess chitosan solution on the substrate was removed by gently contacting the substrate surface with deionized water in the cap device for 1h. Then the PAA solution was charged into the cap device to contact with the chitosan-loaded PES substrate for 1h, during which period polyelectrolyte complex was produced on the substrate by electrostatic attraction between chitosan and PAA molecules. After the excess PAA molecules were removed from the membrane by immersing the membrane surface in deionized water for 1 h, the first electrostatically assembled chitosan/PAA bilayer was produced. Multiple chitosan/PAA bilayers were prepared by repeating the steps mentioned above. All the chitosan/PAA composite membranes were prepared by the LbL assembly at room temperature of 25°C. The LbL-assembly steps in a cap device are shown in Figure 3.1.

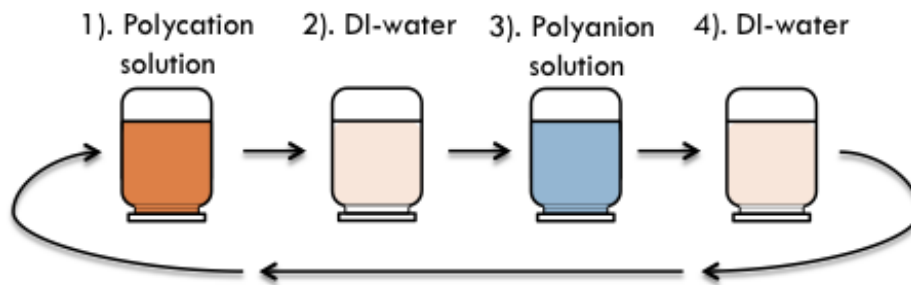


Figure 3.1 LbL-assembly steps in a cap device

3.2.3 Nanofiltration

The nanofiltration setup consisted of a dead-end filtration cell, a nitrogen cylinder, a pressure regulator, and a pressure gauge, as shown in Figure 3.2. The dead-end filtration cell, having an effective membrane area of 12.56 cm^2 , was made of stainless steel and installed with a magnetic bar. The membrane was mounted in the filtration cell, and the feed solution was filled into the membrane cell so that the active surface of the membrane contacted with the feed solution. The nitrogen cylinder yielded the desired transmembrane pressure for permeation, and the rotation speed of the magnetic stirrer produced was 1000 rpm. The liquid permeate was collected at the bottom of the filtration cell.

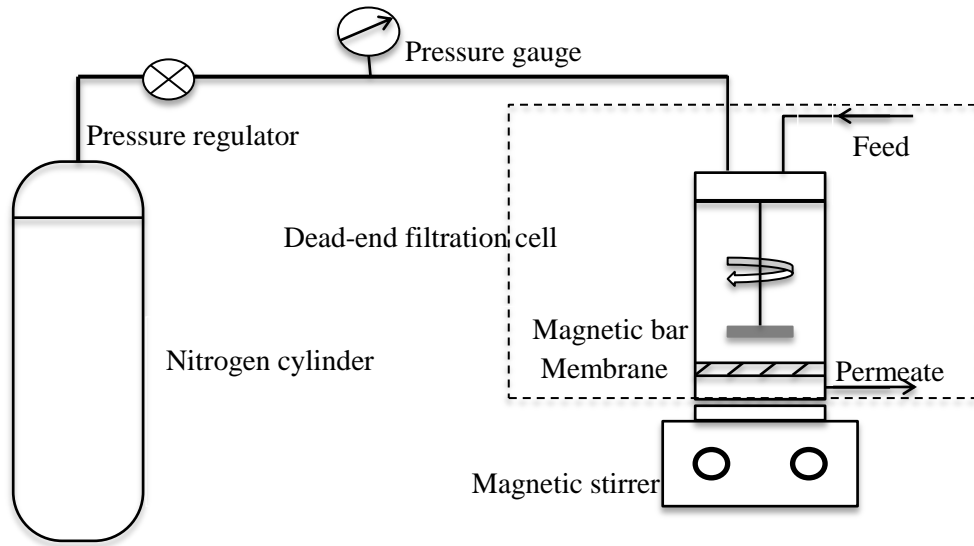


Figure 3.2 Schematic diagram of nanofiltration experiment

A conductivity meter was used to determine the concentrations of the salt solutes in the permeate and feed solutions. The salt rejection of the membrane was calculated by

$$R = \frac{c_f - c_p}{c_f} \quad (3-1)$$

where c_f and c_p are the salt concentrations in the feed and the permeate (ppm), respectively.

The volumetric flux of permeate ($L/(m^2h)$) was calculated from:

$$J = \frac{Q}{A \times \Delta t} \quad (3-2)$$

where Q is the volume of the permeate (L) collected over a period of time Δt (h), and A is the membrane area (m^2).

To evaluate the effects of LbL assembly conditions on the separation performance of the chitosan/PAA composite membranes, the permeation flux and salt rejection of the

membranes were measured by NF experiments with salt solutions of NaCl, Na₂SO₄, MgCl₂, and MgSO₄ at a feed concentration of 500 ppm and operating pressure of 0.7 MPa. To study the effects of operating conditions in NF experiments on the separation performance of the membranes, the NF experiments were first carried out at an operating pressure of 0.7 MPa and different feed concentrations (from 500 to 2000ppm), and then at a constant feed concentration of 500 ppm and varying operating pressures (from 0.1 to 0.9MPa). All NF experiments were performed at room temperature (25°C).

3.2.4 Heat treatment

To examine the effects of heat treatment on the separation performance of the chitosan/PAA composite membranes, the membrane was heat treated in an air circulating oven at temperatures in the range of 60 to 150 °C for 60 min, and then at a constant heating temperature of 150 °C with different heating times from 10 to 120 min.

3.2.5 Stability test of the polyelectrolyte composite membranes

The stability of a membrane is an important property of the membrane. It is measured by applying the membrane in salt solutions for a long-term NF operation.

The stability test of chitosan/PAA composite membranes for long-term operation in salt solutions includes 5 test cycles. In each test cycle, the membrane mounted in the filtration cell was subject to NF with Na₂SO₄ solution for 6 h during which period the separation performance (i.e., salt rejection and permeation flux) of the membrane for

Na₂SO₄ solution was measured. Subsequently, the MgSO₄ solution was used as the feed solution for NF test for 6 h, and the separation performance of the membrane for MgSO₄ rejection was characterized. The membrane was then tested for NF with MgCl₂ solution and NaCl solution, separately. This completed the first cycle of the stability test. The stability test of the membrane was carried out continuously by repeating the steps mentioned above until 5 test cycles were completed. All NF experiments were operated at an operating pressure of 0.7 MPa and feed solute concentration of 500 ppm. The stability of the membrane was then evaluated by comparing the variation in the separation performance of the membrane in the 5 test cycles.

3.3 Results and discussion

3.3.1 Effect of number of polyelectrolyte bilayers

A thin film composite membrane comprising of n chitosan/PAA bilayers from alternating deposition of chitosan and PAA solutions on a PES substrate is denoted as membrane [CS/PAA] _{n} . To investigate the effects of number of chitosan/PAA bilayers on the membrane performance, the composite membranes with different numbers (i.e., value of n) of chitosan/PAA bilayers were fabricated at a polyelectrolyte concentration of 1000 ppm and a deposition time of 60 min. The permeation flux and salt rejection of the resulting membranes are shown in Figure 3.3.

It can be seen that with an increase in the number of bilayers, the salt rejection increased and the permeation flux decreased gradually, and then both of which remained constant. This is easy to understand as the chitosan/PAA thin film was built up layer by layer on the surface of the PES substrate. At the first few assembly cycles, the LbL assembly of chitosan/PAA bilayers reduced the surface pore size of the PES substrate and increased the thickness of the polyelectrolyte thin film [Krasemann and Tieke, 1998], which resulted in a denser structure and higher mass transport residence of the thin film. Consequently, the salt rejection became higher and the permeation flux lower. When the LbL assembly reached a certain extent, however, the pore size on the membrane surface became sufficiently small, and adding more bilayers of chitosan/PAA on the PES substrate at this point would not play a significant role in sealing pores as before.

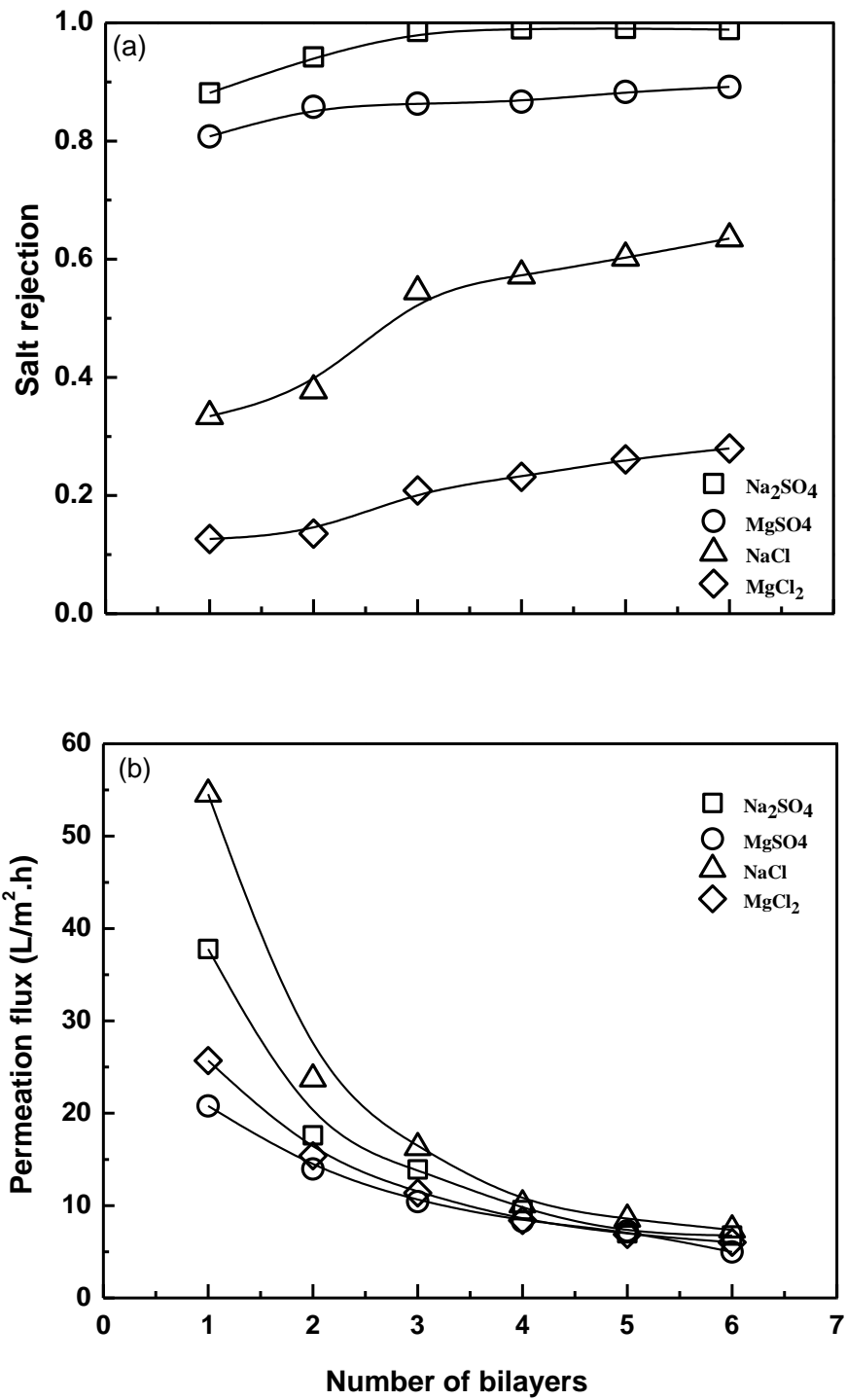


Figure 3.3 Effects of number of bilayers on (a) salt rejection and (b) permeation flux for the [CS/PAA]_n membranes (Operating pressure: 0.7 MPa; Salt concentration: 500 ppm)

The chitosan/PAA composite membranes showed different rejections to the solutes in an order of $\text{Na}_2\text{SO}_4 > \text{MgSO}_4 > \text{NaCl} > \text{MgCl}_2$. This sequence was the same as that of negatively charged membranes [Petersen, 1993; Schaep et al., 1998]. It demonstrates that the $[\text{CS/PAA}]_n$ membranes with PAA as an outermost layer had a negatively charged surface. It is well known that the separation mechanism of NF membranes involves sieving (steric) effect and Donnan (electrical) effect [Grignon and Scallan, 1980]. The Donnan effect describes that a charged membrane surface attracts oppositely charged ions to gather on or pass through the membrane while repulses similarly charged ions to retain in the solution. The higher the valence of the ions, the stronger the interaction force from the charged membrane surface. The sieving effect refers to a membrane that retains solutes having a particle size larger than the pore size of the membrane. The larger the particle size of the solutes, the higher the salt retention. Therefore, the negatively charged membrane surface strongly repulsed multivalent anion SO_4^{2-} and attracted multivalent cation Mg^{2+} , but exerted less force on monovalent anion Cl^- and monovalent cation Na^+ . It led to the highest salt rejection of Na_2SO_4 and lowest salt rejection of MgCl_2 . In addition, Mg^{2+} and SO_4^{2-} have particle sizes larger than Cl^- and Na^+ . This explains the higher salt rejection of MgSO_4 than that of NaCl by the membrane.

The order of the permeation fluxes of the membrane for different salt solutions was $\text{NaCl} > \text{Na}_2\text{SO}_4 > \text{MgCl}_2 > \text{MgSO}_4$. Interestingly it was the same as the order of diffusion coefficients of these salts in aqueous solutions at 25 °C (shown in Table 3.1). It appears

that the salt with larger diffusion coefficient in aqueous solutions had the faster mass transport through the membrane.

Table 3.1 Diffusion Coefficient D_i of salts in water at 25°C [Schaep et al., 1998]

Salts	$D_i(10^{-9} \text{ m}^2/\text{s})$
NaCl	1.61
MgCl ₂	1.25
Na ₂ SO ₄	1.23
MgSO ₄	0.85

3.3.2 Effect of polyelectrolyte deposition time

The adsorption of polyelectrolytes on an oppositely charged substrate is a process during which polyelectrolytes in the bulk solution diffuse to the vicinity of substrate surface. Due to strong attractive force between the substrate surface and the polyelectrolytes, the polyelectrolytes are adsorbed onto the substrate surface, forming a polyelectrolyte complex. Since it takes time for the polyelectrolyte adsorption to reach equilibrium, the deposition time of polyelectrolyte is an important factor in thin film formation and affects the separation performance of the polyelectrolyte composite membrane formed.

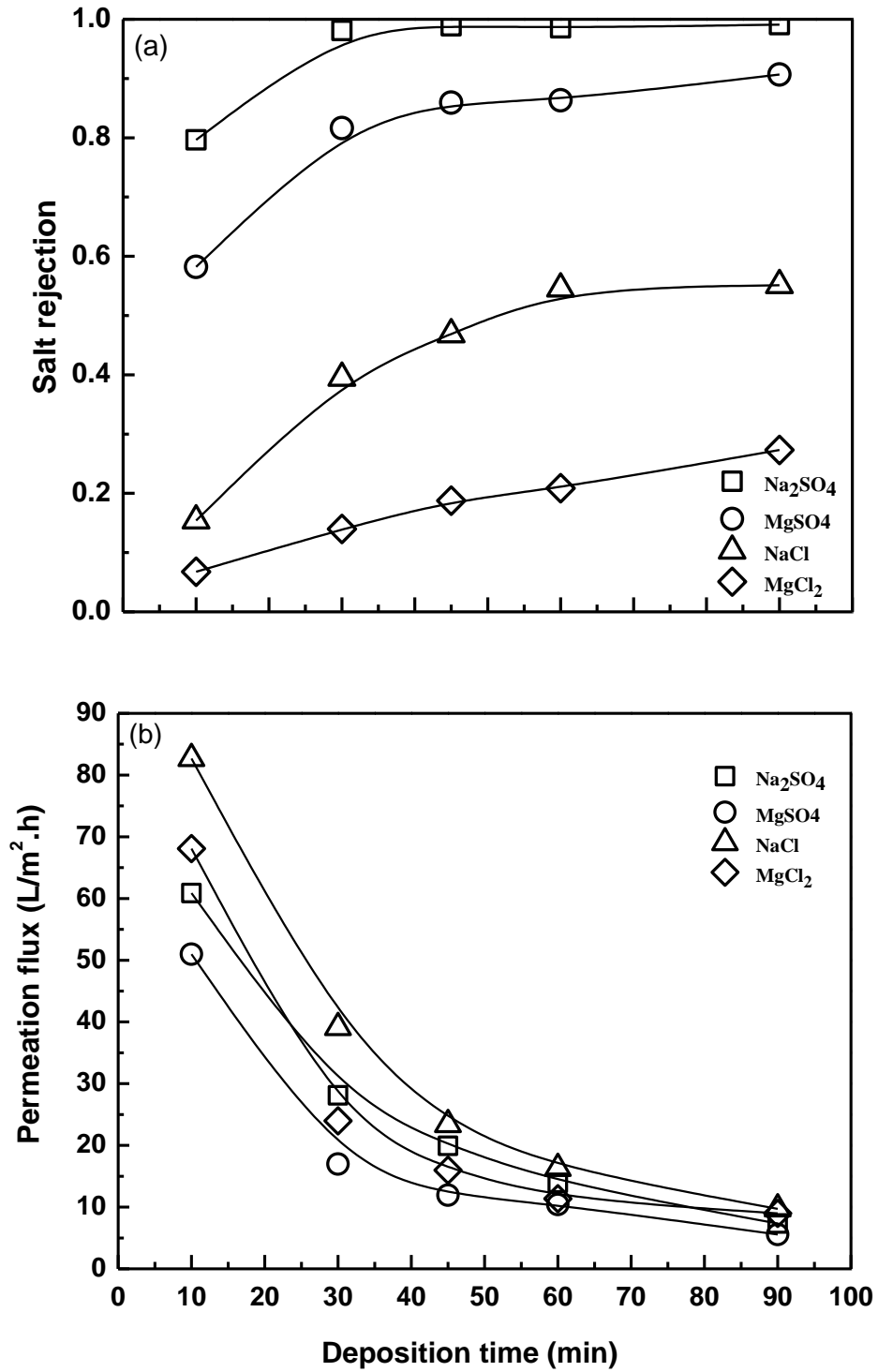


Figure 3.4 Effects of polyelectrolyte deposition time on (a) salt rejection and (b) permeation flux of the resulting polyelectrolyte membranes (Operating pressure: 0.7 MPa; Salt concentration: 500 ppm)

To investigate the effects of polyelectrolyte deposition time on the membrane performance, [CS/PAA]₄ membranes with 4 bilayers were fabricated at a polyelectrolyte concentration of 1000 ppm and different deposition times from 10 to 90 min. The permeation flux and salt rejection of the resulting membranes are shown in Figure 3.4.

It can be seen that the permeation flux decreased and the salt rejection increased with an increase in the polyelectrolyte deposition time from 10 to 60 min. The polyelectrolyte molecules adsorbed on the membrane surface were increased with the deposition time, which led to a denser and thicker polyelectrolyte thin film. Consequently, a higher salt rejection and lower permeation flux of the membrane resulted. However, beyond 60 min of deposition, a further increase in the deposition time do not have significant influence on the separation performance of the membrane. It is understandable because when the adsorption of polyelectrolytes on the membrane surface reached equilibrium, no more polyelectrolytes could be adsorbed on the substrate surface with an increase in the deposition time.

3.3.3 Effects of concentration of polyelectrolyte solution

Polyelectrolyte concentration in the deposition solutions plays an important role in the adsorption of polyelectrolytes on a substrate, and thus influences the structure and charge property of the polyelectrolyte composite membrane [Ng et al., 2013]. To investigate the effects of the polyelectrolyte concentration on the membrane performance, the [CS/PAA]₄ membranes were prepared at a deposition time of 60 min and at

polyelectrolyte concentrations from 500 to 2000 ppm. The salt rejection and permeation flux of the resulting membranes were presented in Figure 3.5.

It is shown that the salt rejection of the membrane for the four salt solutions all increased with an increase in the polyelectrolyte concentration from 500 to 1000ppm. An increase in the polyelectrolyte concentration led to more polyelectrolyte macromolecules deposited on the substrate, and thus a thicker and denser chitosan/PAA thin film was produced. Interestingly, above 1000 ppm in the polyelectrolyte concentration, Na_2SO_4 rejection decreased slightly and MgCl_2 increased, which appears to suggest that the negatively charged membrane surface become increasingly important.

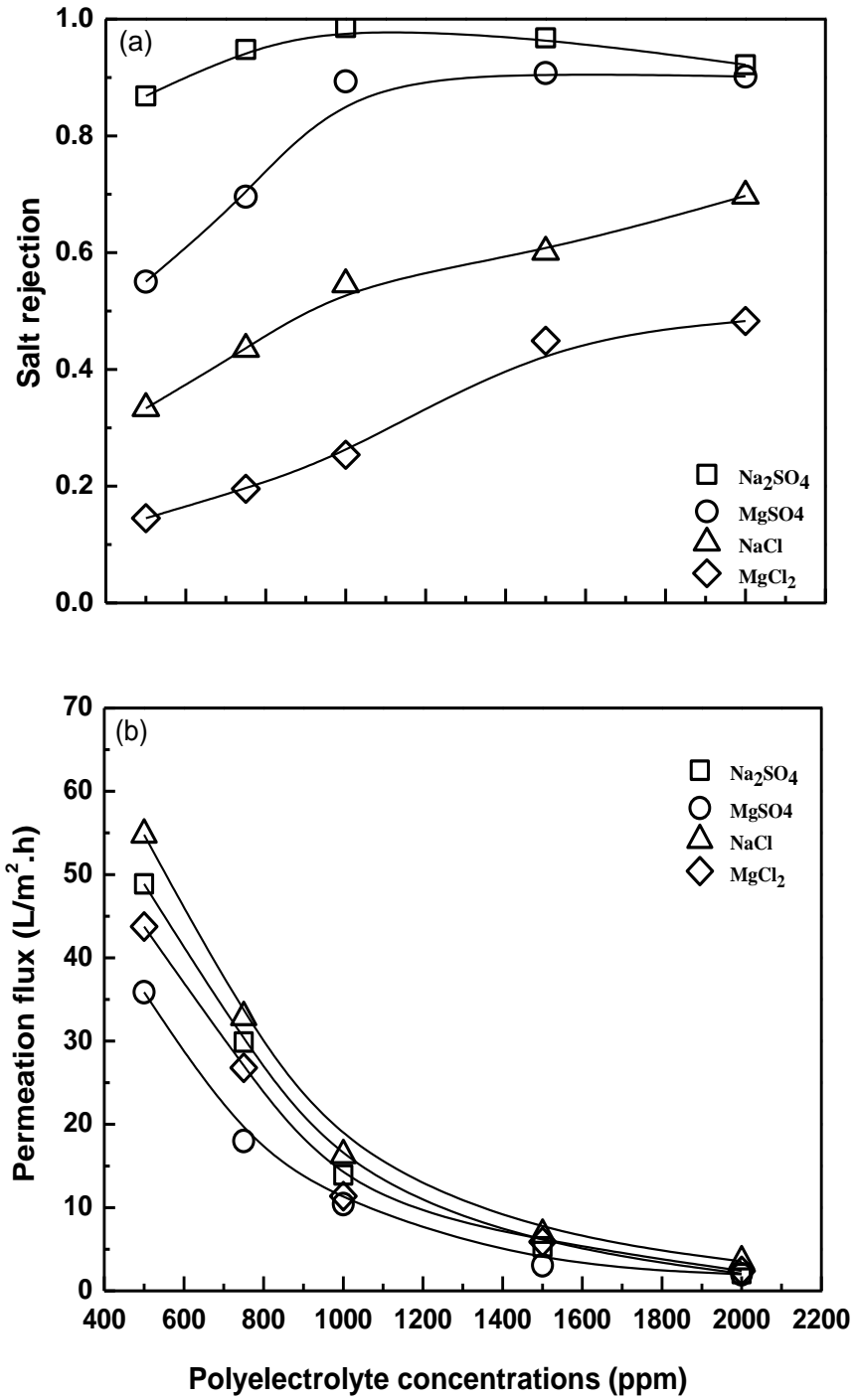


Figure 3.5 Effects of polyelectrolyte concentration on (a) salt rejection and (b) permeation flux of the [CS/PAA]₄ membranes (Operating pressure: 0.7 MPa; Salt concentration: 500 ppm)

The water permeation flux of the membrane for the four salt solutions all decreased with an increase in the polyelectrolyte concentration from 500 to 2000 ppm. The effects of the polyelectrolyte concentration on permeation flux of a membrane can be explained from the following aspects [Xu et al., 2011]: 1). In dilute solutions, polyelectrolyte chains are well stretched and dispersed, and there are sufficient binding sites on the membrane surface for the polyelectrolyte chains to deposit on. At this stage, a loose thin film is formed, and the permeation flux has little variation. 2) With an increase in the polyelectrolyte concentration, less stretched polyelectrolyte chains are yielded due to charge balance of the counter-ions. This leads to a lower sealing effect of polyelectrolytes on the membrane pores. Consequently, the mass transport resistance of thin film decreases, and the permeation flux increases. 3). However, when the polyelectrolyte concentration is sufficiently high, a further increase in the polyelectrolyte concentration leads to aggregation and entanglement of polyelectrolytes, thereby yielding a more compact polyelectrolyte layer with a lower permeation flux. In this study, the permeation flux decreased with an increase in the polyelectrolyte concentration because a considerably high polyelectrolyte concentration was used.

3.3.4 Effects of the outermost layer of the membrane

The electrostatic LbL assembly of oppositely charged polyelectrolytes is achieved when the adsorption of one monolayer can be overcompensated and charge reversed by the adsorption of a next layer [Decher et al., 1998]. Therefore, the charge of polyelectrolyte of the outermost layer determines the surface charge of the membrane. That means, positively or negatively charged surface can be fabricated by controlling the number of the deposition cycles (odd or even cycles) [Conlon and McClellan, 1989; Schönhoff, 2003].

In this work, $[\text{CS}/\text{PAA}]_n\text{CS}$ membrane refers to a thin film composite membrane comprising of n chitosan/PAA bilayers and a chitosan layer as the outermost layer from alternating deposition of chitosan and PAA solutions on a PES substrate. The number of bilayers of a $[\text{CS}/\text{PAA}]_n\text{CS}$ membrane can be considered to be $n+0.5$. For example, The number of bilayers of the $[\text{CS}/\text{PAA}]_2\text{CS}$ membrane is $2+0.5 = 2.5$. The outermost chitosan layer determines the sign of surface charge of $[\text{CS}/\text{PAA}]_n\text{CS}$ membranes, which means a positively charged surface of $[\text{CS}/\text{PAA}]_n\text{CS}$ membranes.

In this study, the $[\text{CS}/\text{PAA}]_n\text{CS}$ membranes with different number of chitosan/PAA bilayers were prepared at a polyelectrolyte concentration of 1000 ppm and a deposition time of 60 min. The salt rejection and permeation flux of the resulting membranes are shown in Figure 3.6.

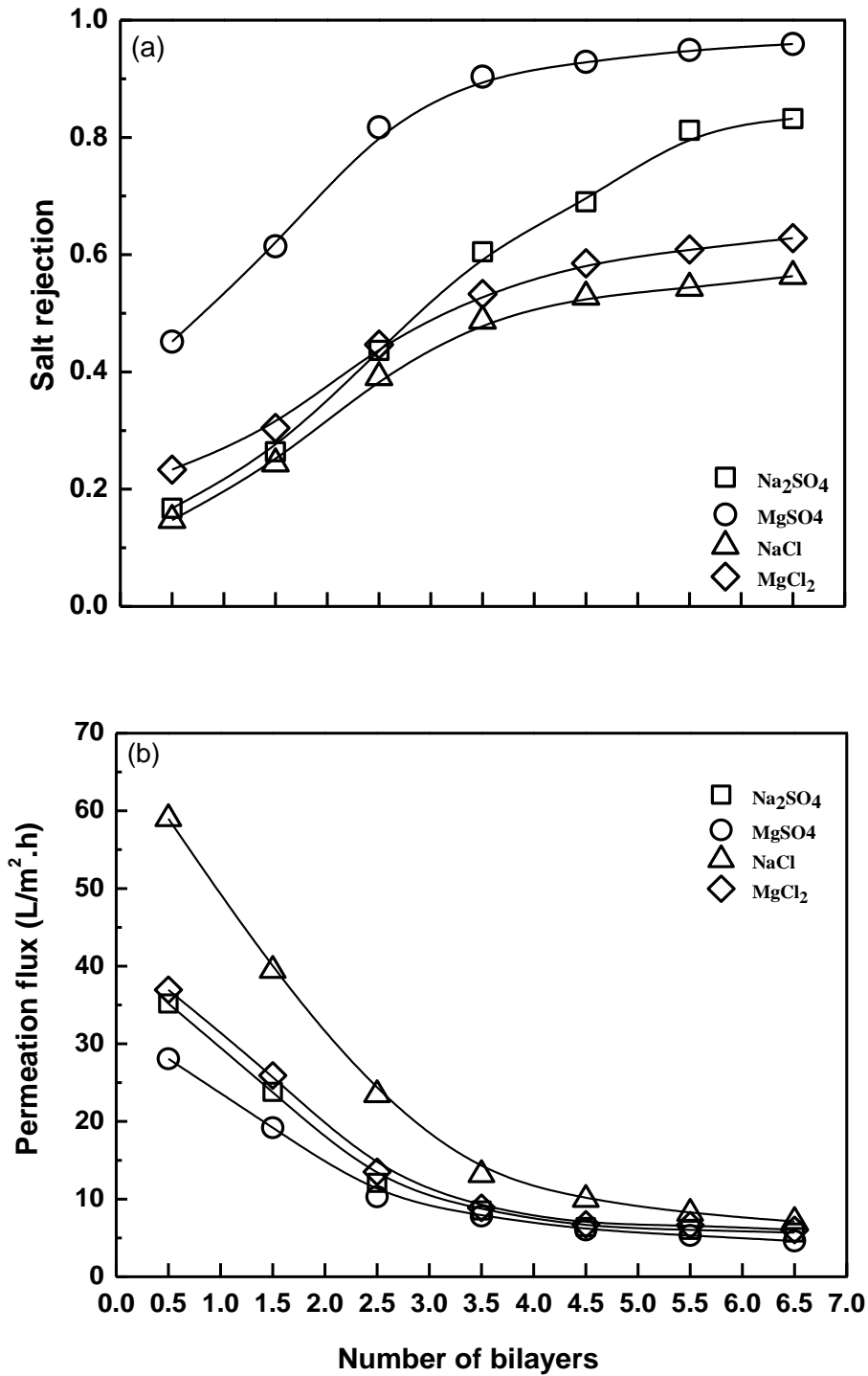


Figure 3.6 Effects of number of bilayers on (a) salt rejection and (b) permeation flux for [CS/PAA]_nCS membranes (Operating pressure: 0.7 MPa; Salt concentration: 500 ppm)

It can be seen that the salt rejections of this series of positively charged [CS/PAA]_nCS membranes were different from those of the negatively charged [CS/PAA]_n membranes (i.e., Na₂SO₄ > MgSO₄ > NaCl > MgCl₂, shown in Figure 3.3). It indicates that the surface charge of a polyelectrolyte composite membrane played a significant role in the separation performance of the membrane. In addition, the salt rejections of the [CS/PAA]_nCS membranes were not the same as those of strongly positively charged membranes, in which the separation mechanism is dominated by the Donnan effect (i.e., MgCl₂ > NaCl > MgSO₄ > Na₂SO₄) [Schaep et al., 1998].

As shown in Figure 3.6, while the number of polyelectrolyte bilayers was 2.5 or more, the salt rejections of the [CS/PAA]_nCS membranes were in the order of MgSO₄ > Na₂SO₄ > MgCl₂ > NaCl. This sequence was similar to that of membranes with a neutral surface [Schaep et al., 1998]. It indicates that the positive surface charge of the [CS/PAA]_nCS membranes was weak, and thus the Donnan effect of the membranes was insignificant. For membranes with 2.5 chitosan/PAA bilayers or less, the pores of the substrate were still large. In this case, the separation performance of the [CS/PAA]_nCS membranes was influenced by both the Donnan and sieving effects. With an increase in the number of bilayers, the pores of the substrate were gradually sealed, and therefore the sieving effect was increasingly more important than the Donnan effect on the separation performance of the membrane. Beyond 2.5 chitosan/PAA bilayers, the sieving effect dominated over the Donnan effect on the separation performance of the membranes.

The permeation flux of the membranes for different salt solutions decreased as per order of $\text{NaCl} > \text{Na}_2\text{SO}_4 > \text{MgCl}_2 > \text{MgSO}_4$. This was in the same order as the diffusivity of these salts in aqueous solutions at 25 °C (shown in Table 3.1).

3.3.5 Effects of heat treatment temperature

Heat treatment affects the morphology and porosity of the polyelectrolyte composite membranes, and thus influences the separation performance of the membranes. To study the effects of heating temperature on the membrane performance, the $[\text{CS}/\text{PAA}]_4$ membranes fabricated at a polyelectrolyte concentration of 1000 ppm and a deposition time of 60 min were heated for 90 min at temperatures varying from 60 to 150°C. The permeation flux and salt rejection of the resulting membranes are presented in Figure 3.7.

It is shown that the salt rejection increased and the permeation flux decreased with an increase in the heat treatment temperature. At a high heat treatment temperature, polyelectrolyte chains have a high mobility. In addition, with an increase in heat treatment temperature, more water molecules were released from the polyelectrolyte thin film, which tended to produce smaller pore sizes. Therefore, the heat treatment of the membrane led to a more compact structure.

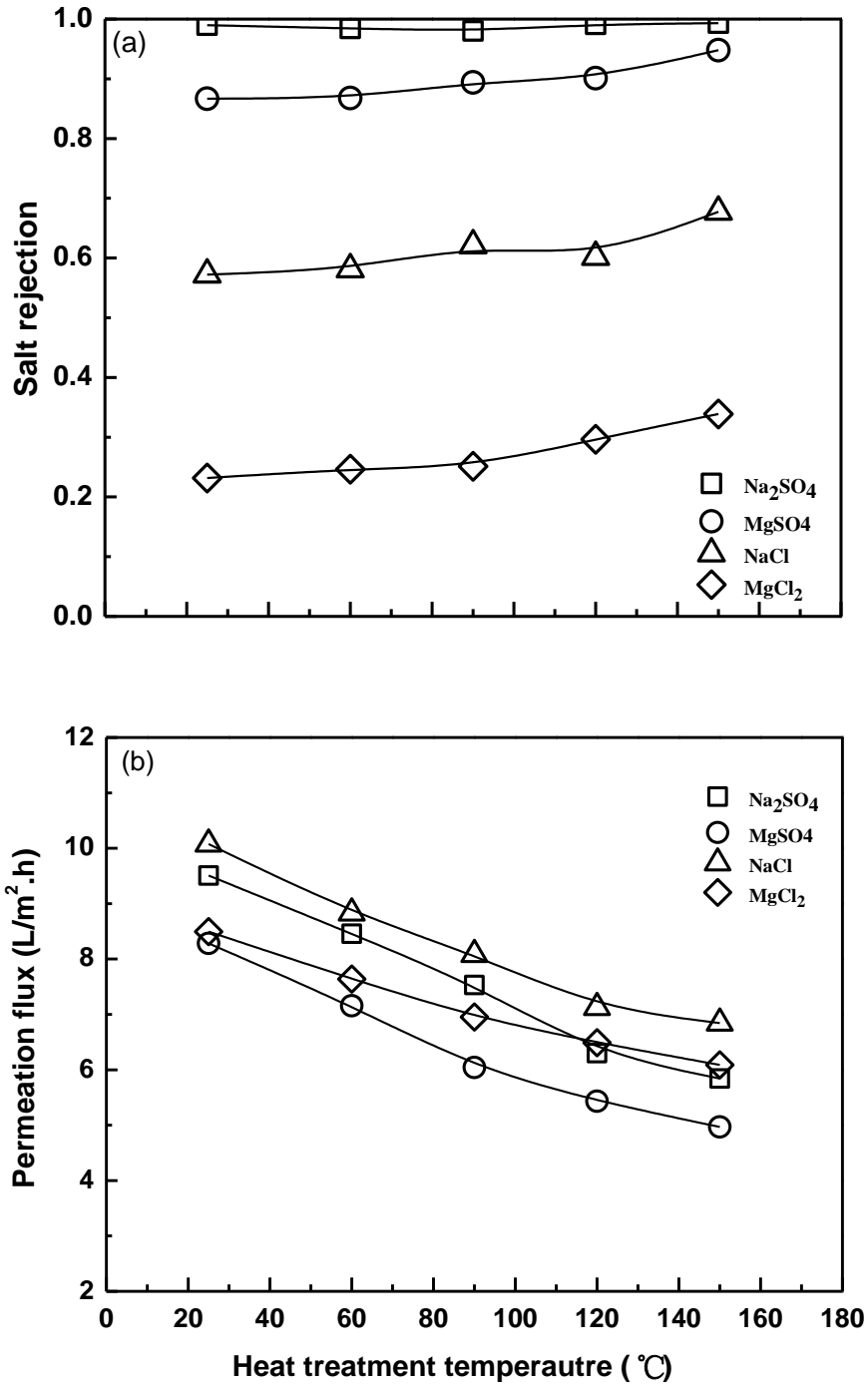


Figure 3.7 Effects of heat treatment temperature on (a) salt rejection and (b) permeation flux for the [CS/PAA]₄ membrane (Polyelectrolyte concentration: 1000 ppm; Deposition time: 60 min; Heat treatment time: 90 min; Operating pressure: 0.7 MPa; Salt concentration: 500 ppm)

Moreover, when the membrane was heated at 90 °C or higher, the yellow coloring of the membrane surface was intensified. This phenomenon was similar to what proposed by some previous studies, in which the yellow coloring of the membrane was attributed to a slight crosslinking between the amino groups in chitosan and the carboxylic groups in PAA [Ghiorghita et al., 2014; Lim and Wan, 1995]. Thus, crosslinking of chitosan and PAA on the membrane surface may be another reason for the enhanced salt rejection and reduced permeation flux by heat treatment of the membranes.

3.3.6 Effects of heat treatment time

As mentioned above, heat treatment of chitosan/PAA composite membranes enhances the mobility of the polyelectrolytes and releases water from the polyelectrolyte thin film. It may also result in crosslinking of the polyelectrolytes on the membrane surface. In order to evaluate the effects of heat treatment time on the membrane performance, the [CS/PAA]₄ membranes fabricated at a polyelectrolyte concentration of 1000 ppm and a deposition time of 60 min were heat-treated at a temperature of 150°C for a period of 10 to 120 min. Figure 3.8 shows the salt rejection and permeation flux of the resulting membranes.

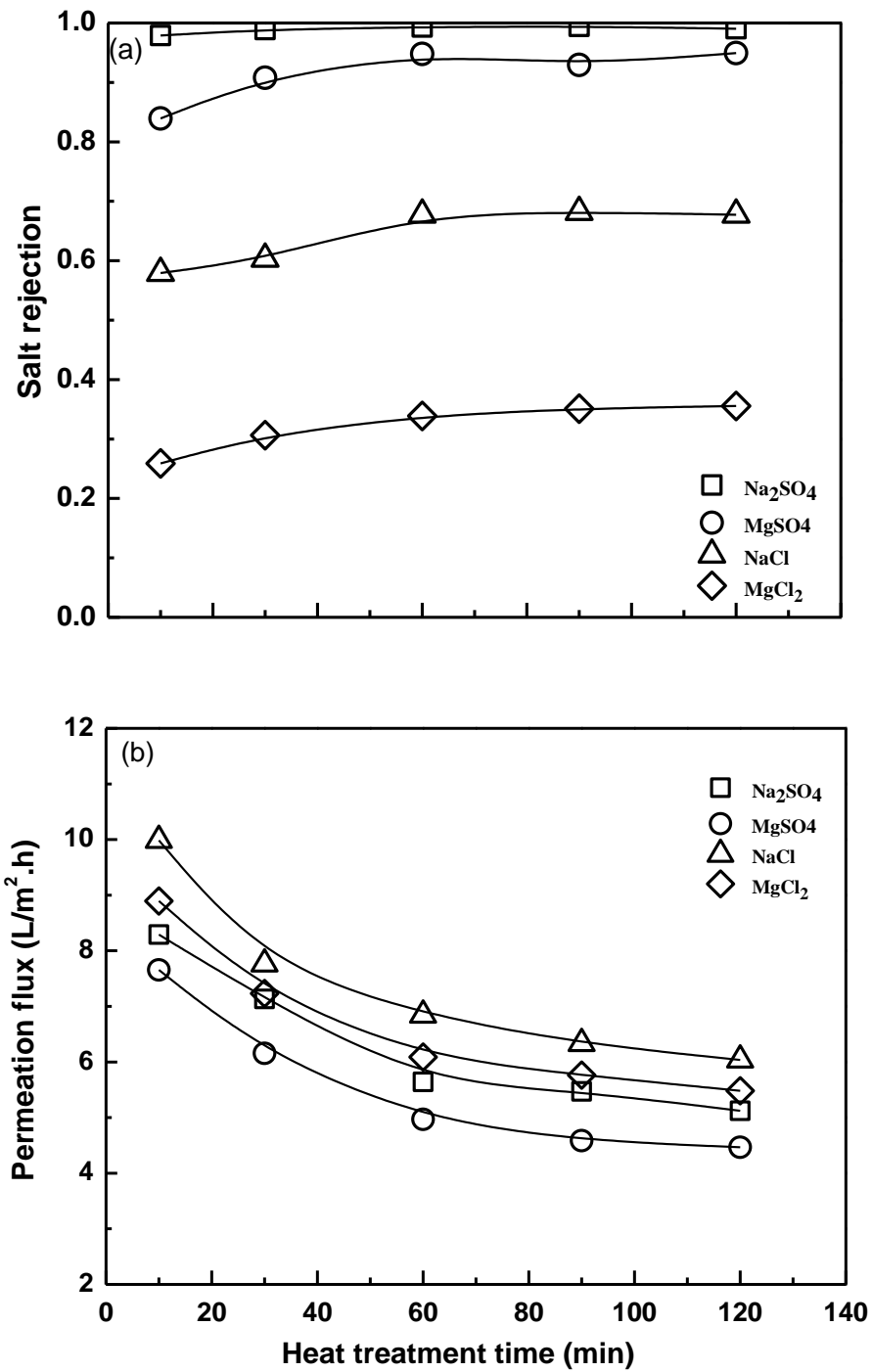


Figure 3.8 Effects of heat treatment time on (a) salt rejection and (b) permeation flux for the [CS/PAA]₄ membrane (Polyelectrolyte concentration: 1000 ppm; Deposition time: 60 min; Heat treatment temperature: 150°C; Operating pressure: 0.7 MPa; Salt concentration: 500 ppm)

It is shown that the permeation flux decreased and the salt rejection increased with an increase in heat treatment time from 10 to 60 min and then remained constant. Due to an increase in heat treatment time, more water was initially released from the polyelectrolyte thin film, and thus a smaller pore size and denser structure of the polyelectrolyte thin films were obtained. However, when the heat treatment time was sufficiently long, the water in the polyelectrolyte thin film would be released completely. A further increase in heat treatment time would have little impact on the structure of the polyelectrolyte thin films. This explains the salt rejection and permeation flux that remained essentially constant when the heat treatment time was beyond 60 min.

3.3.7 Effects of operating pressure in nanofiltration

The operating pressure in NF affects the mass transport rate through the membrane. To study the effects of operating pressure on the separation performance of the membrane, NF experiments were carried out using a [CS/PAA]₄ membrane at a feed concentration of 500 ppm. The separation performance of the [CS/PAA]₄ membrane without heat treatment and the heat-treated [CS/PAA]₄ membrane is presented in Figures 3.9 and 3.10, respectively. Both membranes were fabricated with a polyelectrolyte concentration of 1000 ppm and deposition time of 60 min.

It can be seen that no matter whether the [CS/PAA]₄ membrane was heat-treated or not, an increase in operating pressure increased the permeation flux linearly, whereas the

salt rejection increased gradually and then remained constant. This can be explained by the solution-diffusion model [Hussain and Al-Rawajfeh, 2009]:

$$F = A(\Delta P - \beta \Delta \pi) \quad (3-3)$$

where F is the water flux, A is the water permeation coefficient, ΔP is the operating pressure difference, β is the polarization factor, and $\Delta \pi$ is the osmosis pressure difference between the two sides of the membrane.

$$F_s = B(\beta C_1 - C_2) \quad (3-4)$$

where F_s is the salt flux, B is the salt permeation coefficient, C_1 and C_2 are the salt concentrations in the feed and permeate side on the membrane, respectively.

Equation (3-3) indicates that when the feed concentration is low enough where β can be neglected, the water flux F increases linearly with an increase in ΔP . Equation (3-4) shows that the salt flux has no direct relation to ΔP but is a function of salt concentration on both sides of the membrane. Therefore, an increase in operating pressure increases the water flux while the salt flux does not change significantly. It results in a decrease in C_2 and an increase in salt rejection. However, a decrease in C_2 will lead to an increase in the concentration differences between the feed side and permeate side of the membrane. It results in an increase in the salt flux and a decrease in salt rejection. These two opposite effects lead to an increase in salt rejection as operating pressure increases.

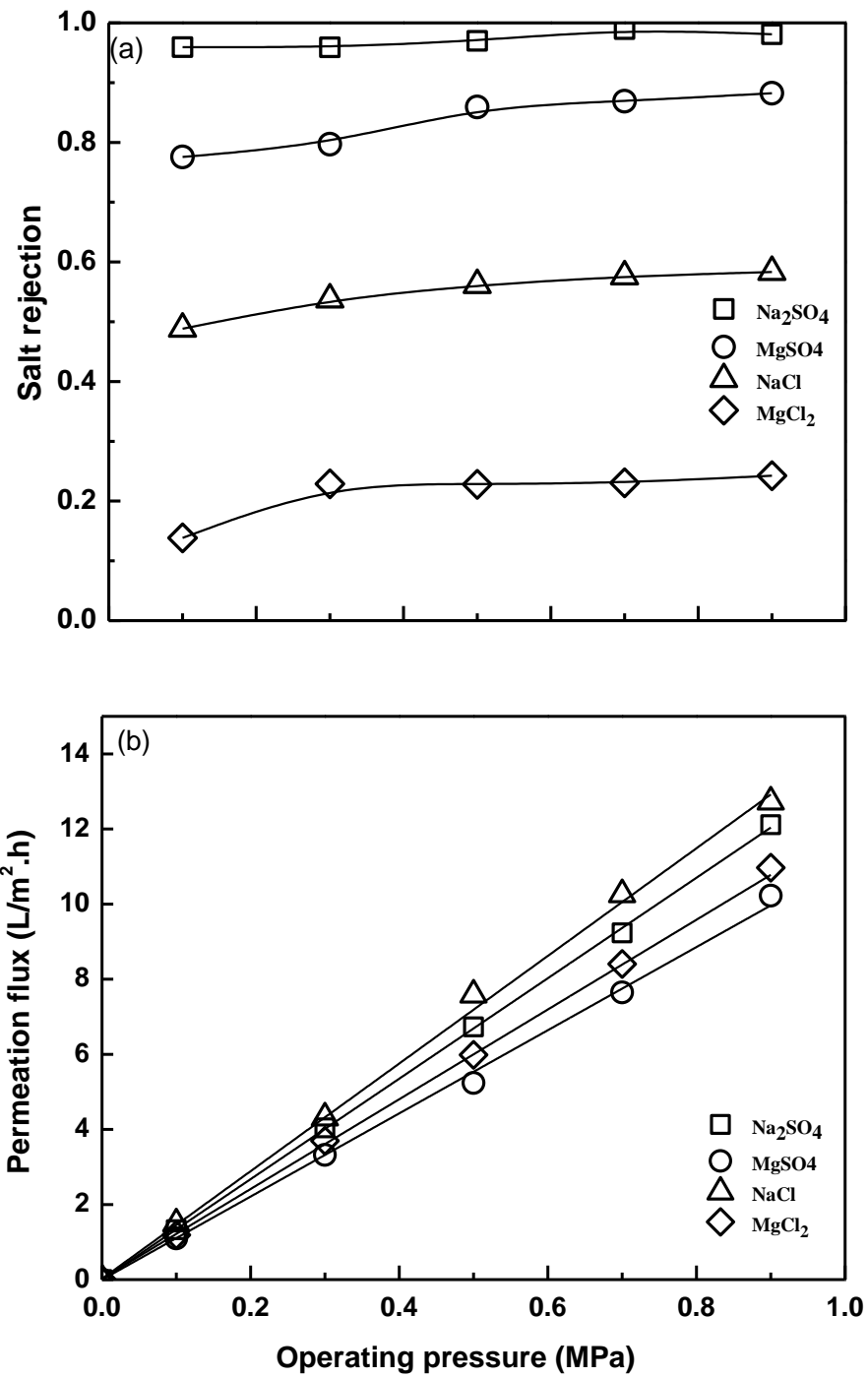


Figure 3.9 Effect of operating pressure on (a) salt rejection and (b) permeation flux for the [CS/PAA]₄ membrane without heat treatment (Polyelectrolyte concentration : 1000 ppm; Deposition time : 60 min)

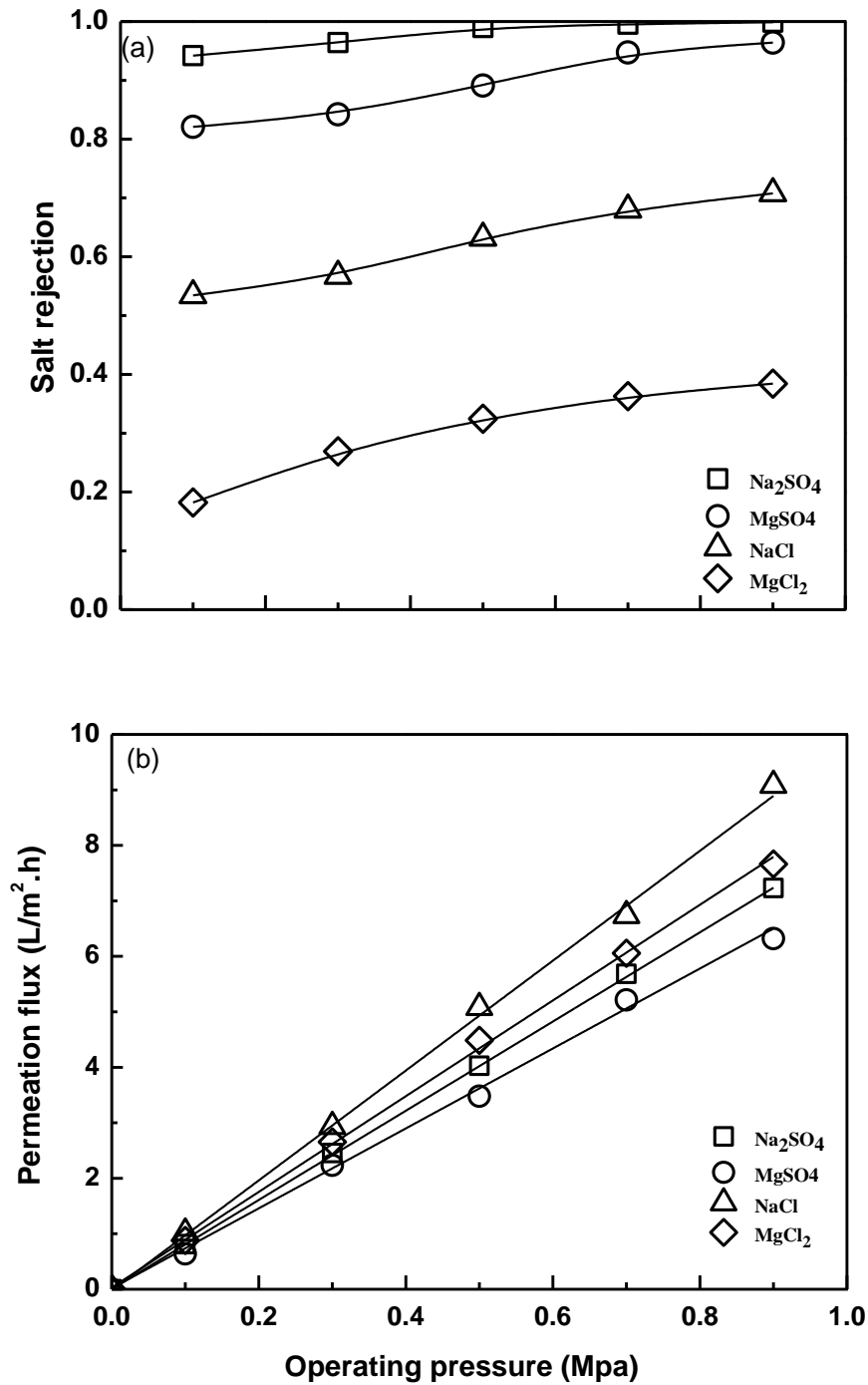


Figure 3.10 Effects of operating pressure on (a) salt rejection and (b) permeation flux for the heat-treated [CS/PAA]₄ membrane (Polyelectrolyte concentration : 1000 ppm; Deposition time : 60 min; Heat treatment temperature: 150°C; Heat treatment time: 60 min)

In addition, it is shown that with an increase in operating pressure, the heat-treated membrane had a more significant increase in salt rejection than the membrane without heat treatment. An increase in operating pressure increases water flux significantly, whereas salt passage through the membrane also increases but to a lesser extent. Heat-treated membranes with a higher degree of crystallinity have a better ability to prevent salts passing through or depositing on the membrane surface than membranes without heat treatment. Therefore, an increase in operating pressure will increase the salt rejection of the heat-treated membrane more significantly than the membrane without heat treatment.

3.3.8 Effects of feed salt concentration in nanofiltration

The salts in the feed solution may interact with polyelectrolytes. It is expected that the feed concentration affects the charge property of chitosan/PAA composite membranes and thus influences the separation performance of the membranes. To investigate the effects of feed salt concentration on the membrane performance, NF experiments were carried out using [CS/PAA]₄ membranes at an operating pressure of 0.7 MPa and feed concentrations from 500 to 2000 ppm. The separation performance of the [CS/PAA]₄ membrane without heat treatment and the heat-treated [CS/PAA]₄ membrane is presented in Figures 3.11 and 3.12, respectively.

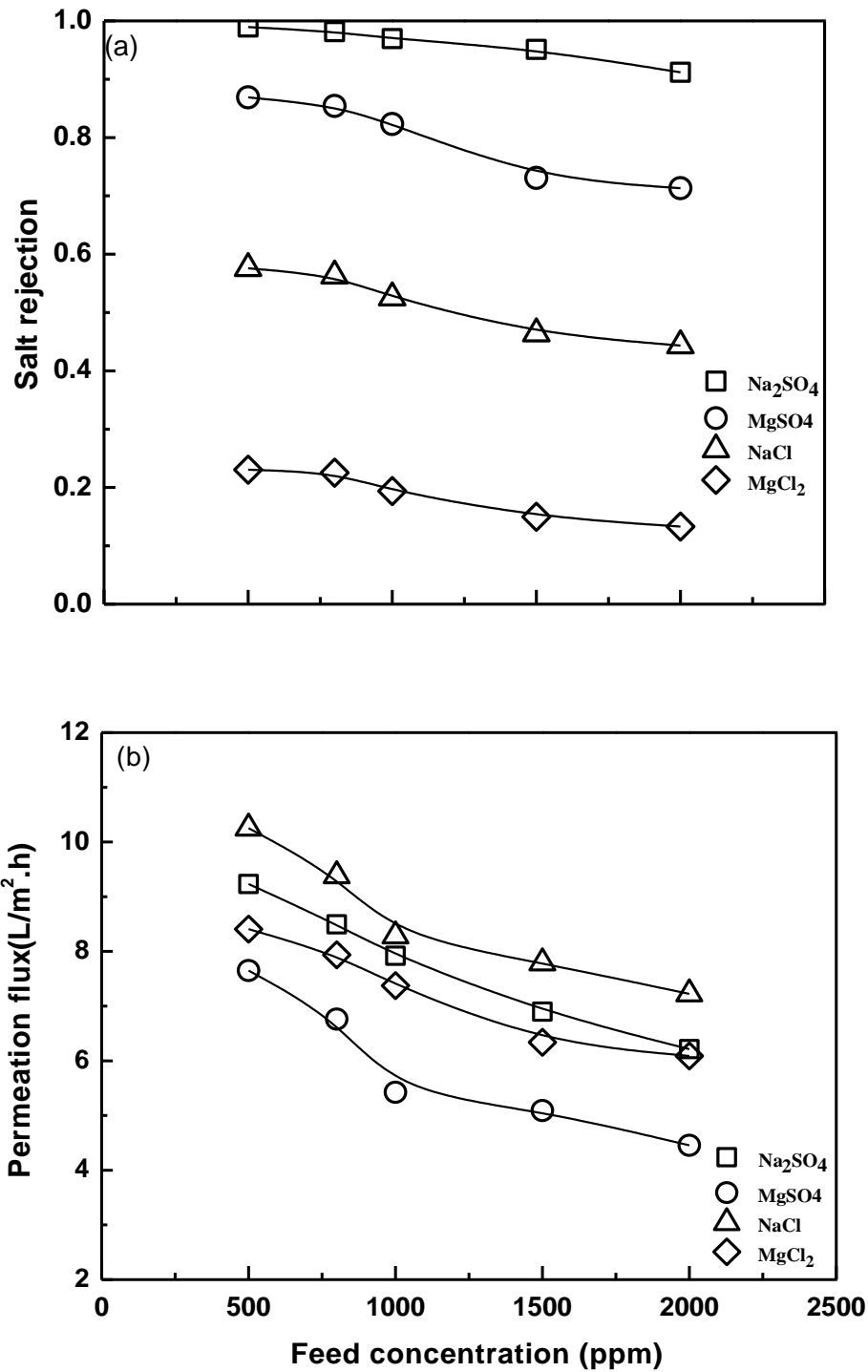


Figure 3.11 Effects of feed salt concentration on (a) salt rejection and (b) permeation flux for the [CS/PAA]₄ membrane without heat treatment (Polyelectrolyte concentration : 1000 ppm; Deposition time : 60 min)

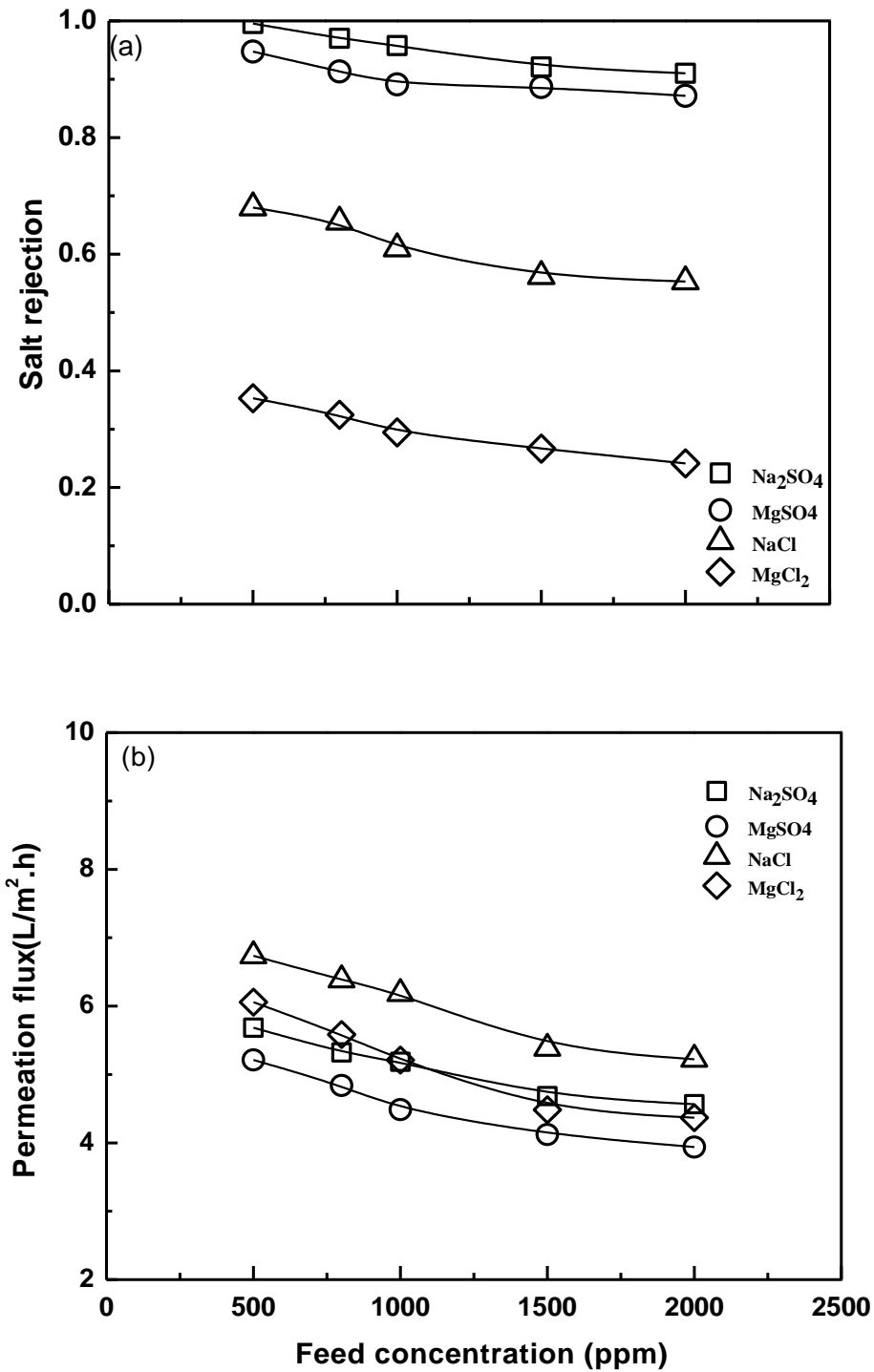


Figure 3.12 Effects of feed concentration on (a) salt rejection and (b) permeation flux for the heat-treated [CS/PAA]₄ membrane (Polyelectrolyte concentration : 1000 ppm; Deposition time : 60 min; Heat treatment temperature: 150°C; Heat treatment time: 60 min)

It is shown that, whether the [CS/PAA]₄ membrane was prepared with or without heat treatment, the salt rejection and permeation flux of the membranes decreased with an increase in the feed concentration. This may be explained by the Donnan equilibrium theory [Petersen, 1993]. Salt rejection mainly results from electrostatic repulsion between membrane surface and ions in the feed. With an increase in feed salt concentration, the shield effect of surface cations on the negatively charged membrane became stronger. This tends to result in a decline in the surface charge density as well as a weaker repulsion of the membrane to anions in the feed. A decrease in permeation flux can be explained by the concentration polarization near the membrane surface. Concentration polarization in NF refers to the concentration gradient of salts formed between the membrane surface and bulk solution along with the process of salt filtration. It leads to a decrease in permeation flux [Aravind et al., 2010].

Moreover, an increase in salt concentration had less influence on separation performance of the heat-treated membrane than that of the membrane without heat treatment. The heat-treated polyelectrolyte composite membrane had a stronger polymer - polymer interaction and thus a higher capability of preventing salts from passing through or depositing on the membrane than the membrane without heat treatment.

3.3.9 Stability of chitosan/PAA composite membrane without heat treatment

The stability test of a [CS/PAA]₄ membrane without heat treatment was carried out at an operating pressure of 0.7 MPa and feed concentration of 500 ppm. The permeation

flux and salt rejection of the membrane in 5 cycles of NF experiments are presented in Figure 3.13.

As shown in Figure 3.13, the salt rejection decreased and the permeation flux increased remarkably from the 3rd to 5th cycle. It indicates that the stability of the [CS/PAA]₄ membrane is a potential problem. It is well known that the performance decline in a NF membrane results from two factors: membrane swelling and membrane fouling [Luo and Wan, 2011]. Membrane swelling refers to the dissolution of the polymers in water, which results in an increase in the permeation flux and a decrease in the selectivity of the membrane. Membrane fouling is caused by solutes in the feed solutions deposited on the membrane, which leads to a decrease in both the selectivity and the permeation flux of the membrane. In this study, the membrane swelling seems to be a primary reason for the performance decline of the membrane because an increase in permeation flux and a decrease in salt rejection took place during the tests.

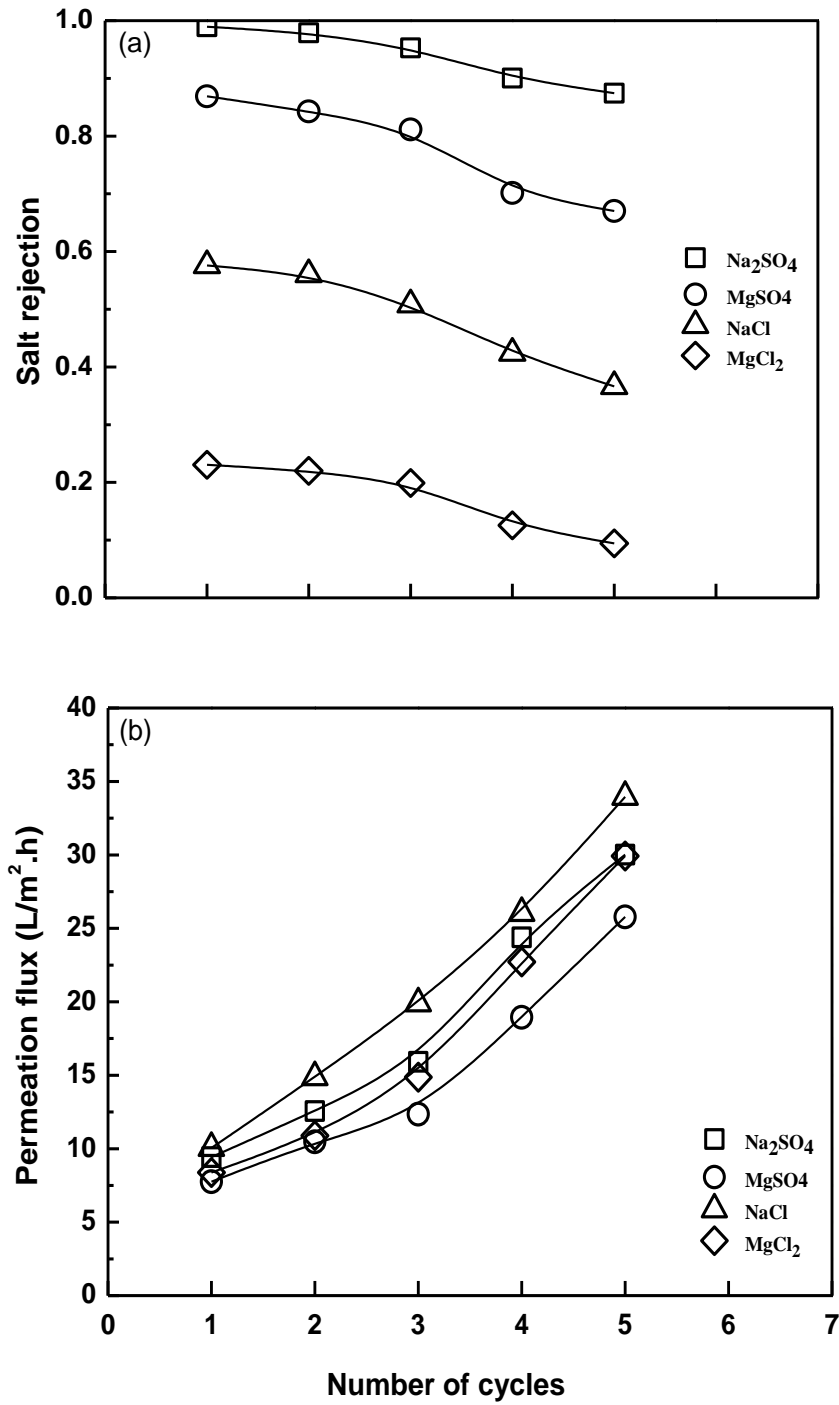


Figure 3.13 Stability of the [CS/PAA]₄ membrane without heat treatment, (a) salt rejection and (b) permeation flux (Polyelectrolyte concentration : 1000 ppm; Deposition time : 60 min; Operating pressure: 0.7 MPa; Salt concentration: 500 ppm)

Several studies proved that the presence of salts resulted in swelling of the polyelectrolyte composite membranes. Sukhorukov et al. [1996] proposed that when the salt concentration in polyelectrolyte composite membranes reached a significant point, the swelling of the membranes took place. Wang et al. [2002] found that the presence of salts reduced the thickness of the hydration layer on the pore walls and slightly broadened the path of solutes through the membrane. Consequently, the solutes permeate through the membrane more easily. In this study, the continuous NF experiments of salt rejection led to an increased salt concentration in the membrane. Membrane swelling then took place, which resulted in a decline in the performance of the membrane. In order to prevent or minimize the swelling of chitosan/PAA composite membranes, proper post-treatments should be used to make the membrane stable over a prolonged period of time.

3.3.10 Stability of heat-treated CS/PAA composite membrane

Heat treatment has been proved to be an effective way to improve the separation performance of polyelectrolyte composite membranes. To evaluate the influence of heat treatment on membrane stability, the stability testing of a heat-treated [CS/PAA]₄ membrane was tested at an operating pressure of 0.7 MPa and a feed concentration of 500 ppm for 5 cycles of nanofiltration. The permeation flux and salt rejection of the membrane are shown in Figure 3.14.

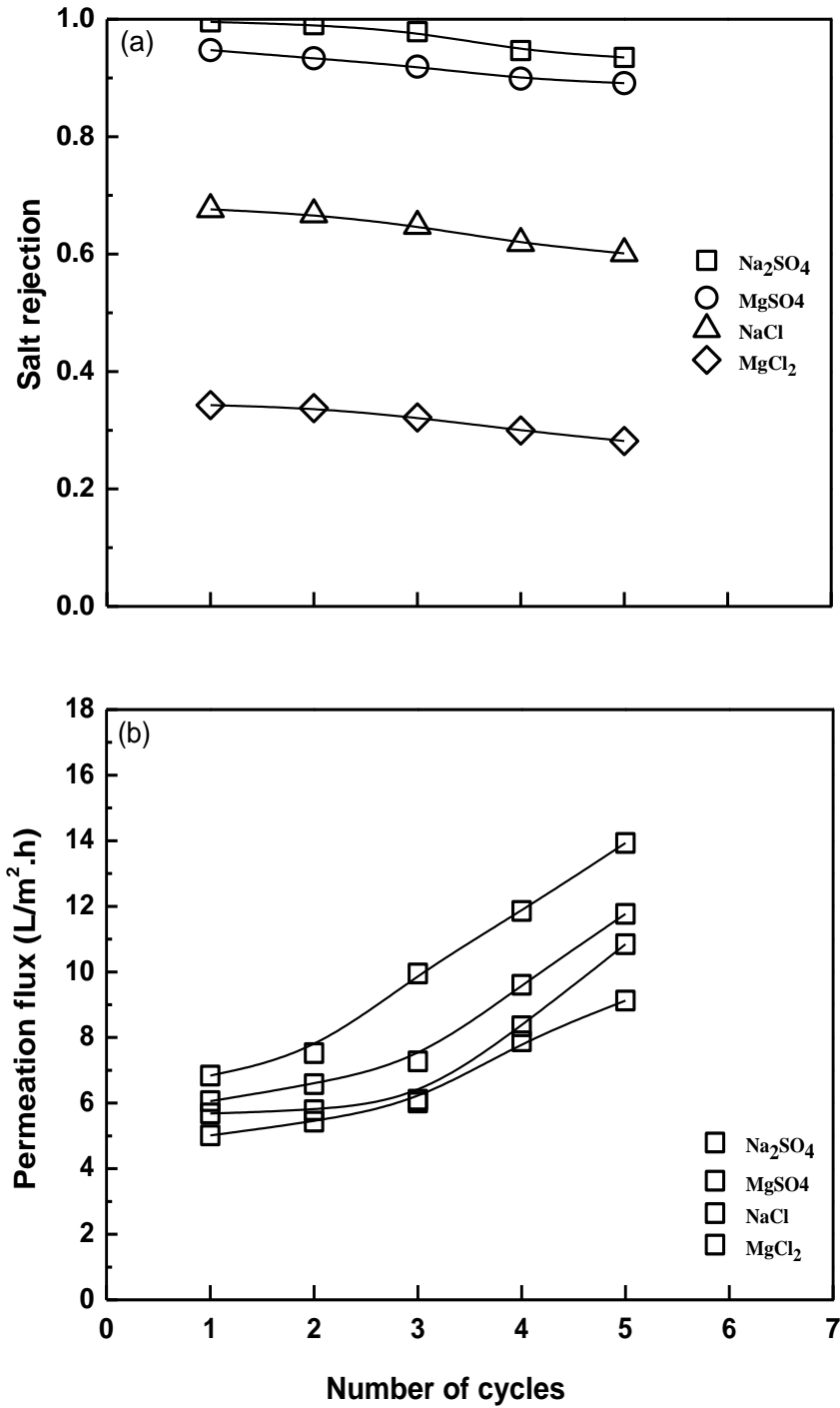


Figure 3.14 Stability of the heat-treated [CS/PAA]₄ membrane, (a) salt rejection and (b) permeation flux (Polyelectrolyte concentration : 1000 ppm; Deposition time : 60 min; Heat treatment temperature: 150°C; Heat treatment time: 60 min; Operating pressure: 0.7 MPa; Salt concentration: 500 ppm)

It can be seen that the stability of the [CS/PAA]₄ membrane was improved by the heat treatment. The separation performance of the heat-treated membrane had less variance in 5 cycles of NF experiments than that of the membrane without heat treatment. Heat treatment can effectively constrain membrane swelling and thus enhance the stability of the membrane. Heat treatment can increase crystallinity and crosslinks the polyelectrolyte networks, and lead to a more stable membrane structure.

3.4 Conclusions

In this chapter, the LbL assembly technique was used to produce chitosan/PAA composite membranes. The effects of parameters involved in LbL assembly and the operating conditions in NF on the separation performance of the membranes were investigated. Heat treatment was used as a post-treatment procedure to improve the membrane performance. The following conclusions can be drawn:

- (1) The LbL assembly of chitosan/PAA bilayers on PES substrate was effective to prepare NF membranes with good separation performance. An increase in number of chitosan/PAA bilayers led to an increase in salt rejection and a reduction in permeation flux. With an increase in polyelectrolyte deposition time, the salt rejection increased and permeation flux decreased, and then both of them maintained constant when the polyelectrolyte deposition time was sufficiently long. An increase in the polyelectrolyte concentration of the deposition solutions also improved the salt rejection at an expense of reduced permeation flux up to a

polyelectrolyte concentration of 1000 ppm; a further increase in polyelectrolyte concentration beyond 1000 ppm resulted in a decrease in Na_2SO_4 rejection and an increase in MgCl_2 rejection. In addition, when the chitosan/PAA bilayers was deposited with an additional chitosan layer to form $[\text{CS}/\text{PAA}]_n\text{CS}$ membranes where the outermost layer was chitosan, the surface charge of the membrane was reversed from negative charges to positive charges.

- (2) The operating conditions in NF influenced the separation performance of the chitosan/PAA composite membranes. An increase in operating pressure led to a linear increase in the permeation flux and a gradual increase in the salt rejection. An increase in salt concentration in the feed resulted in a reduction in both the salt rejection and permeation flux.
- (3) Heat treatment was used as a post-treatment procedure to improve the separation performance and stability of the composite membranes. The salt rejection of the membrane increased and the permeation flux decreased by the heat treatment. The stability of the composite membranes was also enhanced by heat treatment.

CHAPTER 4

Studies of chemical crosslinking on performance of chitosan/PAA composite membranes

4.1 Introduction

Several modification techniques can be used to improve the separation performance and stability of polyelectrolyte composite membranes, one of which is chemical crosslinking of polyelectrolyte chains with a crosslinking agent. The membrane swelling in aqueous solutions generally results in a degradation in the separation performance as the membrane is used in water and wastewater treatment. Chemical crosslinking is often used to constrain membrane swelling.

Glutaraldehyde is a commonly used crosslinking agent for surface modification of chitosan-based membranes. In this chapter, the chitosan/PAA composite membranes were chemically crosslinked by glutaraldehyde. The separation performance and stability of the crosslinked membranes were studied.

4.2 Experimental

4.2.1 Materials and membrane preparation

The materials and LbL assembly process used in the preparation of chitosan/PAA composite membranes were the same as mentioned in chapter 3. Glutaraldehyde (aqueous solution, 25 wt%) purchased from Sigma-Aldrich was used as a crosslinking agent. [CS/PAA]₄CS membranes with chitosan as an outermost layer were prepared by LbL assembly. The membrane preparation conditions were polyelectrolyte concentration of 1000 ppm and deposition time of 60 min.

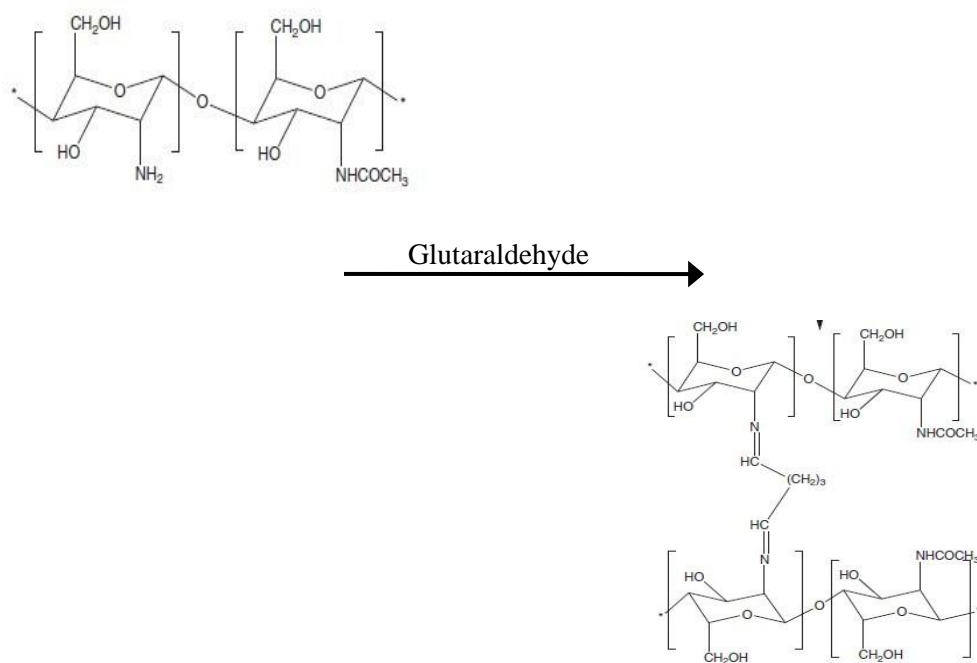


Figure 4.1 Structure of crosslinked chitosan molecular

4.2.2 Crosslinking of chitosan/PAA composite membranes

Surface crosslinking reaction was carried out by immersing the active surface of [CS/PAA]₄CS membranes in the glutaraldehyde solutions. The crosslinking reaction between chitosan and glutaraldehyde is shown in Figure 4.1.

4.2.3 Experimental Design

Crosslinking of chitosan/PAA composite membranes with glutaraldehyde is a chemical reaction. In this study, a 2³ factorial experimental design was used to study the effects of crosslinking on the separation performance of the membranes according to Yate's analysis [Yates, 1978]. Three major factors (i.e., independent variables) were investigated: crosslinking temperature (A), crosslinking time (B), and glutaraldehyde concentration (C). The values and levels of the independent variables are shown in Table 4.1; the two levels were chosen based on preliminary test results.

Table 4.1 Variables investigated and their levels in the experimental design

Variables	Level	
	-1	+1
(A) Crosslinking temperature (°C)	25	85
(B) Crosslinking time (min)	30	150
(C) Glutaraldehyde concentration (wt%)	0.2	2.0

4.2.4 Stability test of crosslinked chitosan/PAA composite membrane

The procedure of the stability test of the crosslinked chitosan/PAA membranes is the same as that described in Chapter 3. In the NF experiments, the operating pressure was 0.7 MPa and the feed salt concentration was 500 ppm.

Table 4.2 Design arrangement and experimental results

Ex	A	B	C	Salt rejection				Permeation flux (L/(m ² h))			
				Na ₂ SO ₄	MgSO ₄	NaCl	MgCl ₂	Na ₂ SO ₄	MgSO ₄	NaCl	MgCl ₂
1	-1	-1	-1	0.9720	0.8901	0.5829	0.2632	7.6698	6.5390	10.181	7.1025
2	+1	-1	-1	0.9799	0.9553	0.6693	0.3578	6.0823	4.7123	7.5086	5.3098
3	-1	+1	-1	0.9727	0.9056	0.5931	0.2833	7.3246	6.0498	9.5423	6.7207
4	+1	+1	-1	0.9801	0.9671	0.6710	0.3795	5.8239	4.4687	7.1445	5.0411
5	-1	-1	+1	0.9812	0.9625	0.6657	0.3851	5.7505	4.0684	6.7987	5.1408
6	+1	-1	+1	0.9969	0.9880	0.7092	0.3988	5.4198	3.8615	6.4202	4.9086
7	-1	+1	+1	0.9864	0.9718	0.6913	0.3843	5.6554	4.0135	6.5989	5.0134
8	+1	+1	+1	0.9998	0.9870	0.7232	0.4083	5.3367	3.8921	6.3103	4.8231

A: Crosslinking temperature (°C), B: Crosslinking time (min), C: Glutaraldehyde concentration (wt%)

4.3 Results and discussion

4.3.1 Pareto charts for the factorial design

Two responses measured were the permeation flux (F) and salt rejection (R). The experimental design of $N = 2^3 = 8$ experimental units and the NF results are presented in

Table 4.2. To analyze the experimental design in Table 4.2, the MINITAB Software 17.0 was utilized. MINITAB is a comprehensive data analysis, graphics, and database management software. It can provide the widest selection of predictive modeling and the most comprehensive array of data analysis. The effects of the three main factors (i.e., A, B, and C) and their interactions (i.e., AB, BC, AC, and ABC) on the separation performance of the crosslinked [CS/PAA]₄CS membranes were studied. The Pareto charts were used to evaluate how each effect and interaction influenced the membrane performance.

The Pareto charts representing the absolute effects of crosslinking factors and interactions on the salt rejection of the membranes for the four model solute salts are shown in Figure 4.2. The red dotted line in the Pareto chart is a reference line, any effect that extends beyond which is statistically significant. It is shown in Figure 4.2 that the Pareto charts for all the four model solutes followed a similar pattern and that the glutaraldehyde concentration (C) was the most significant factor on the salt rejection. On the other hand, the effects of both glutaraldehyde concentration (C) and crosslinking temperature (A) were significant on salt rejection of the membrane within the range of the operating levels. Crosslinking time (B) and all the interactions (AB, BC, AC, and ABC) were less significant than glutaraldehyde concentration (C) and crosslinking temperature (A). However, the importance of crosslinking time (B) and the interactions (AB, BC, AC, and ABC) cannot be neglected. The statistical insignificance of three effects does not mean that these factors are unimportant, and it just implies less influence on the response.

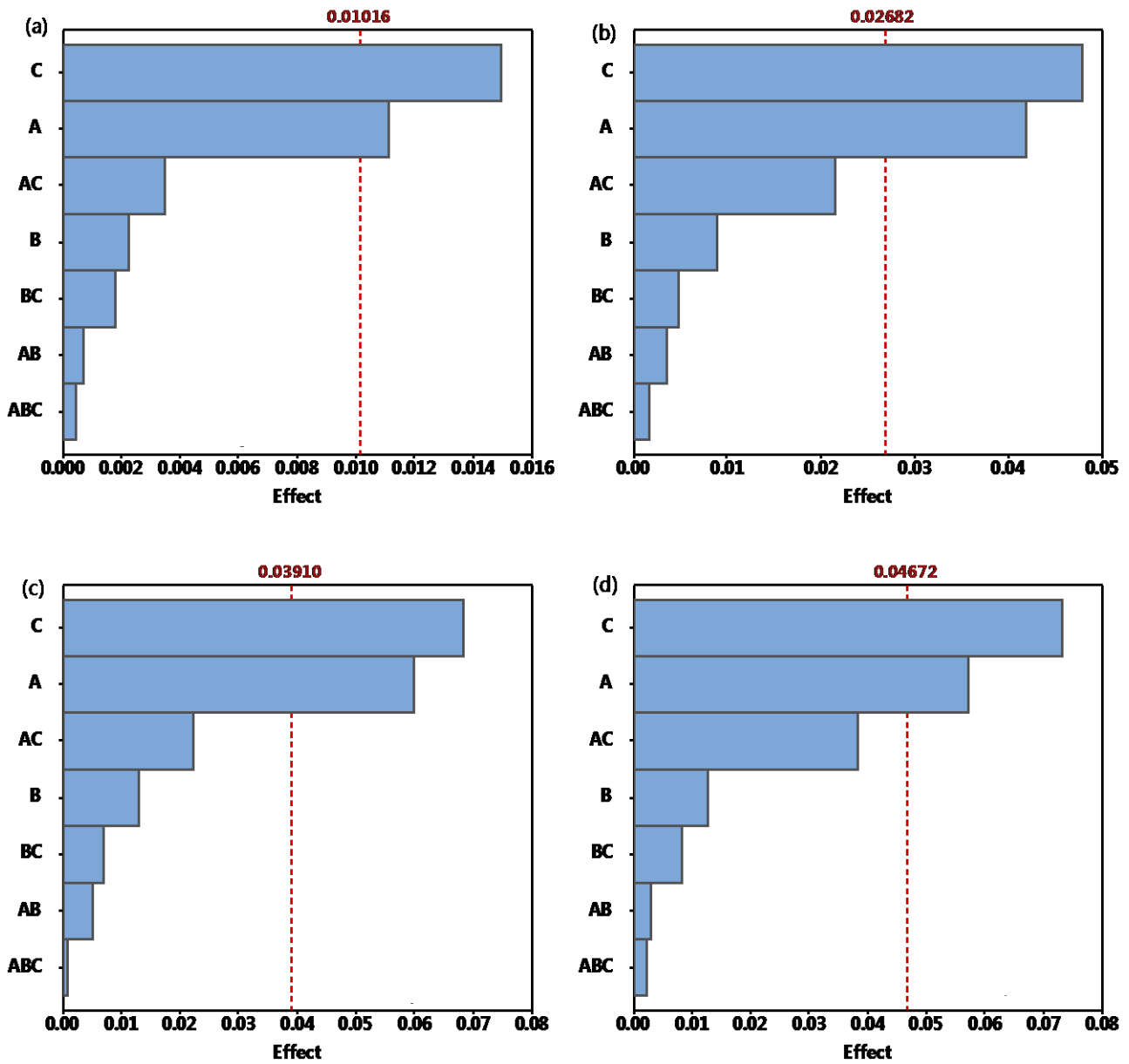


Figure 4.2 Pareto charts of the crosslinking effects on salt rejection for (a) Na₂SO₄, (b) MgSO₄, (c), NaCl and (d) MgCl₂. (A) Crosslinking temperature; (B) Crosslinking time; and (C) Glutaraldehyde concentration.

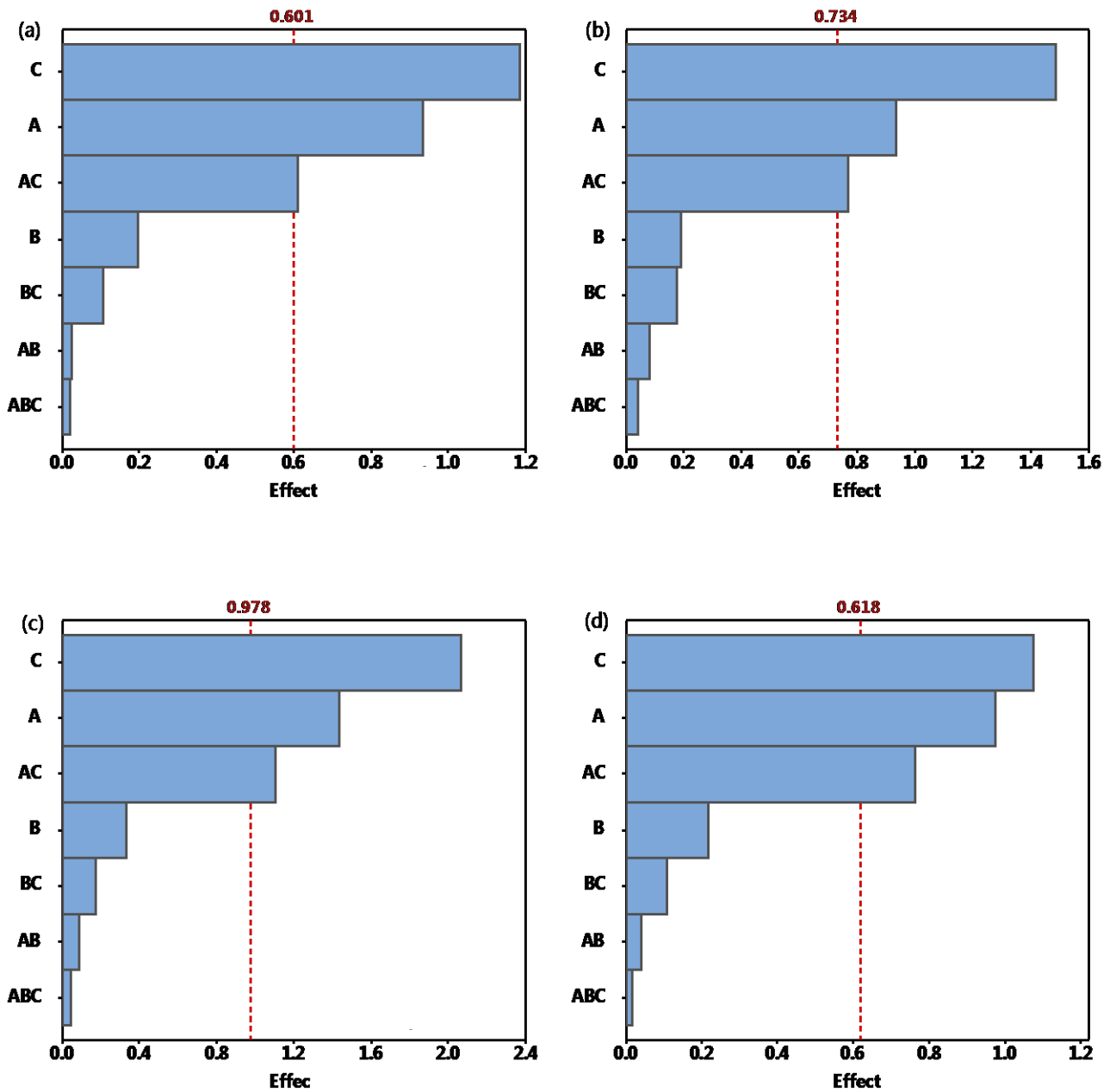


Figure 4.3 Pareto charts of the crosslinking effects on permeation flux for (a) Na₂SO₄, (b) MgSO₄, (c), NaCl and (d) MgCl₂. (A) Crosslinking temperature; (B) Crosslinking time; and (C) Glutaraldehyde concentration.

The Pareto charts reflecting the effects of crosslinking factors and interactions on permeation flux of the membranes for four salts are shown in Figure 4.3. It can be seen that the glutaraldehyde concentration (C) was the most significant factor. The effects of glutaraldehyde concentration (C), crosslinking temperature (A), and their interaction (AC) are important on the permeation flux of the crosslinked membranes within the range of the operating levels. Crosslinking time (B) and its interactions (AB, BC, and ABC) are less important than the other factors (C, A and AC). In addition, the 3-way interaction ABC is the least significant effect on both the permeation flux and salt rejection of the membranes.

4.3.2 Analysis of variance

An analysis of variance (ANOVA) was conducted for a further evaluation of the crosslinking effects on the membrane performance. In ANOVA, the total sum of squares (SST) expresses the total variation that can be attributed to various factors. It equals the regression sum of squares (SSR) plus the error sum of squares (SSE). The hypothesis tests (e.g., *F*-test and *t*-test) use statistics to determine if a given hypothesis is true. The *F*-test can test the hypothesis and reject the hypothesis at the significance level α when $F > F_{\alpha}$. The *p*-value is calculated as the lowest α to determine if we can reject the null hypothesis (a hypothesis of “no difference”) for a given set of observations, and a *p*-value of less than 0.05 is usually considered to be “statistically significant”. The coefficient of determination

R^2 ($R^2=1- (SSE/SST)$) is a measure of the proportion of variability explained by the fitted model; If the model is perfect, $R^2 =1$.

From the experimental data of permeation flux and salt rejection in Table 4.2, based on a linear regression model, the p -values and coded coefficients of three major factors (A, B and C) and their 2-way interactions (AB, AC and BC) were estimated. The R^2 was also evaluated. These data are presented in Tables 4.3 and 4.4. It can be seen that R^2 -values for all the four salts are greater than 0.990, indicating that the model can explain more than 99.0 % of the variations in the observed data. The p -values for the models in Tables 4.3 and 4.4 are all less than 0.05, which indicates that the models are adequate at the 95% confidence level.

Table 4.3 The *p*-values and coded coefficients from ANOVA for salt rejection

Source	Na ₂ SO ₄		MgSO ₄		NaCl		MgCl ₂	
	<i>p</i> -Value	Coef	<i>p</i> -Value	Coef	<i>p</i> -Value	Coef	<i>p</i> -Value	Coef
Model	0.044	0.9836	0.046	0.9534	0.015	0.6632	0.040	0.3575
A	0.026	0.0056	0.025	0.0209	0.008	0.0299	0.024	0.0286
B	0.126	0.0011	0.117	0.0045	0.038	0.0064	0.109	0.0063
C	0.019	0.0075	0.022	0.0239	0.007	0.0341	0.019	0.0366
AB	0.364	-0.0004	0.280	-0.0018	0.097	-0.0025	0.402	0.0015
AC	0.083	0.0017	0.049	-0.0108	0.022	-0.0111	0.036	-0.0191
BC	0.156	0.0009	0.213	-0.0024	0.071	-0.0035	0.164	-0.0041
	$R^2=0.9961$		$R^2=0.9959$		$R^2=0.9995$		$R^2=0.9968$	

Table 4.4 The *p*-values and coded coefficients from ANOVA for permeation flux

Source	Na ₂ SO ₄		MgSO ₄		NaCl		MgCl ₂	
	<i>p</i> -Value	Coef	<i>p</i> -Value	Coef	<i>p</i> -Value	Coef	<i>p</i> -Value	Coef
Model	0.021	6.1329	0.039	4.7007	0.031	7.5631	0.020	5.5075
A	0.013	-0.4672	0.027	-0.4670	0.020	-0.7172	0.012	-0.4869
B	0.061	-0.0977	0.133	-0.0946	0.089	-0.1641	0.052	-0.1079
C	0.010	-0.5923	0.017	-0.7418	0.014	-1.0310	0.011	-0.5360
AB	0.413	0.0124	0.287	0.0414	0.299	0.0456	0.274	0.0194
AC	0.020	0.3049	0.033	0.3849	0.027	0.5504	0.015	0.3812
BC	0.111	0.0532	0.141	0.0886	0.166	0.0866	0.103	0.0547
	$R^2=0.9991$		$R^2=0.9970$		$R^2=0.9981$		$R^2=0.9992$	

Coef= coded coefficients

Using the coded coefficients from ANOVA, the linear models for the relationship between the response (i.e., salt rejection R and permeation flux F) and the crosslinking variables are:

For Na₂SO₄ rejection:

$$F = 6.1329 - 0.4672A - 0.0977B - 0.5923C + 0.0124AB + 0.3049AC + 0.0532BC$$

$$R = 0.9834 + 0.0056A + 0.0011B + 0.0075C - 0.0004AB + 0.0017AC + 0.0009BC$$

For MgSO₄ rejection:

$$F = 4.7007 - 0.4670A - 0.0946B - 0.7418C + 0.0414AB + 0.3849AC + 0.0886BC$$

$$R = 0.9534 + 0.0209A + 0.0045B + 0.0239C - 0.0018AB - 0.0108AC - 0.0024BC$$

For NaCl rejection:

$$F = 7.5631 - 0.7172A - 0.1641B - 1.0310C + 0.0456AB + 0.5504AC + 0.0866BC$$

$$R = 0.6632 + 0.0299A + 0.0064B + 0.0341C - 0.0025AB - 0.0111AC - 0.0035BC$$

For MgCl₂ rejection:

$$F = 5.5075 - 0.4869A - 0.1079B - 0.5360C + 0.0194AB + 0.3812AC + 0.0547BC$$

$$R = 0.3575 + 0.0286A + 0.0063B + 0.0366C + 0.0015AB - 0.0191AC - 0.0041BC$$

The unit for F is L/(m²h). It is worth noting that these models did not take into account the 3-way interaction (i.e., ABC) and quadratic effects (i.e., A², B² and C²). Therefore, they can only give a general idea of how the crosslinking parameters influenced the separation performance of the membranes. To further understand the effects of the three crosslinking factors on the separation performance of the membranes,

experiments were also carried out by varying one crosslinking factor and fixing the other two factors (i.e., one variable at a time).

4.3.3 Effect of concentration of glutaraldehyde solution

Membrane crosslinking, which reduces the mobility of polymeric chains, will result in a decrease in the free volume of the membrane. Thus, the stability and selectivity of the membrane will generally be improved [Huang et al., 2000]. Glutaraldehyde is a commonly used crosslinking agent for chitosan-based membranes. However, the glutaraldehyde concentration used in crosslinking reaction should not be too high, otherwise the resulting membrane will be too rigid and brittle [Krajewska et al., 1989]. To evaluate the effects of glutaraldehyde concentration on the membrane performance, the [CS/PAA]₄CS membranes were crosslinked with glutaraldehyde solutions at room temperature (25 °C) at different glutaraldehyde concentrations (0.2 to 2.0 wt%) for 60 min. Figure 4.4 shows the permeation flux and salt rejection of the resulting membranes.

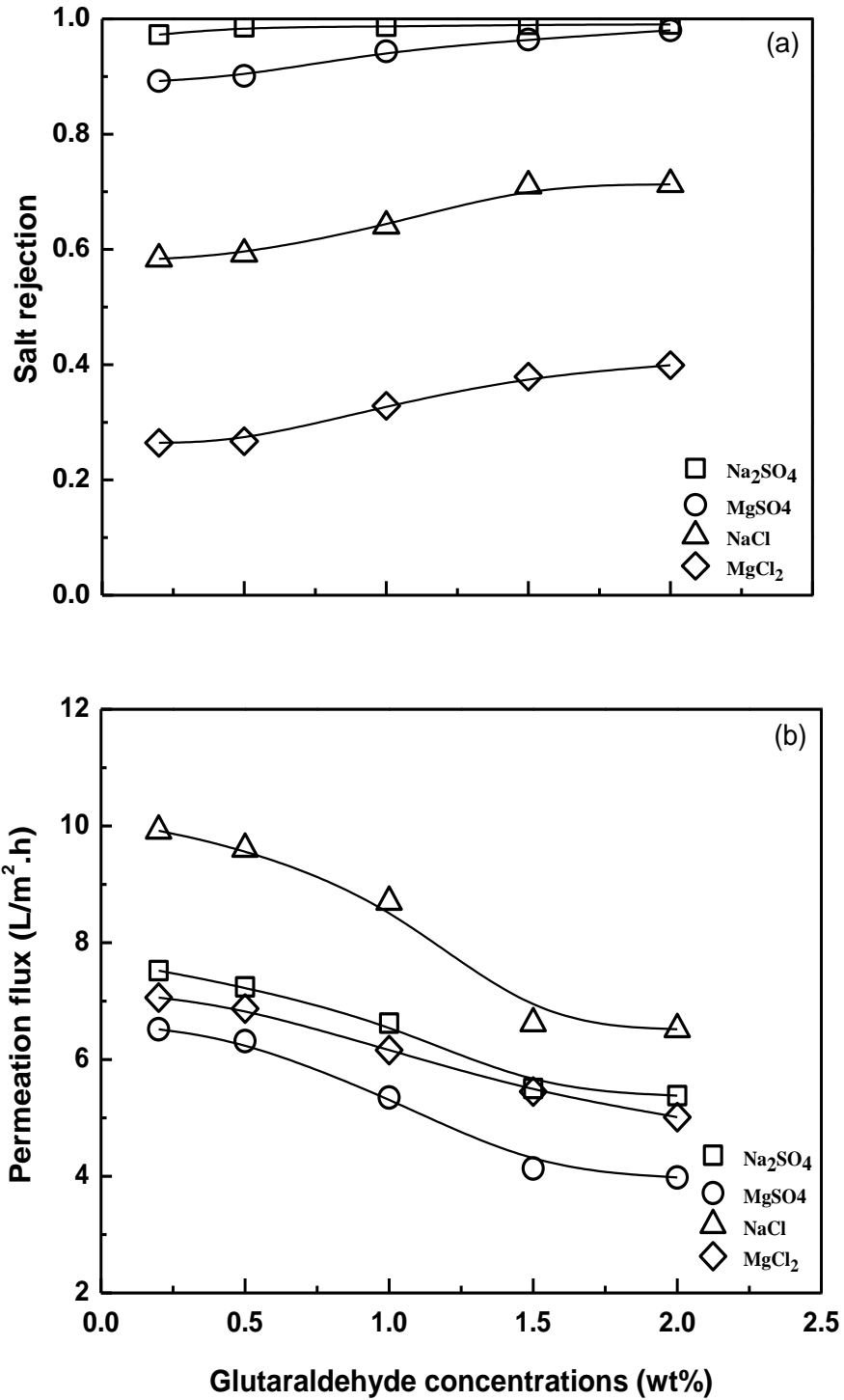


Figure 4.4 Effects of glutaraldehyde concentrations on (a) salt rejection and (b) permeation flux (Operating pressure: 0.7 MPa; Salt concentration: 500 ppm)

It can be seen with an increase in glutaraldehyde concentration, the permeation flux decreased and salt rejection increased until the glutaraldehyde concentration was above 1.5 wt%, and thereafter there were little changes in either flux or salt rejection. An increase in glutaraldehyde concentration helps the glutaraldehyde molecules to penetrate into pores of the membrane and increase the degree of crosslinking in chitosan/PAA composite membranes. Beyond a glutaraldehyde concentration of 1.5%, however, the chitosan chains in chitosan/PAA thin films were substantially crosslinked with glutaraldehyde molecules, and a further increase in glutaraldehyde concentration would have little influence on the separation performance of the membrane.

It is interesting that the [CS/PAA]₄CS membranes crosslinked with glutaraldehyde had a salt rejection in the order of Na₂SO₄ > MgSO₄ > NaCl > MgCl₂. This sequence was different from that of the uncrosslinked [CS/PAA]₄CS membranes. A possible explanation is that the positively charged amino groups in chitosan were gradually crosslinked with glutaraldehyde, and as a result the positive surface charge was compromised by the chemical crosslinking. The beneath negatively charged PAA layer then became increasingly important to the surface charge property and the separation performance of the crosslinked [CS/PAA]₄CS composite membranes.

4.3.4 Effect of crosslinking temperature

The crosslinking reaction between chitosan and glutaraldehyde can be accelerated by using a higher temperature. At a higher temperature, glutaraldehyde molecules are more dynamic and will penetrate more deeply into chitosan/PAA thin films, which resulted in a faster reaction and more crosslinks formed in the membrane. In order to investigate the effects of crosslinking temperature on the membrane performance, [CS/PAA]₄CS membranes were crosslinked at different temperatures ranging from 25 to 85 °C and a glutaraldehyde concentration of 1.0 wt% for 60 min. The salt rejection and permeation flux of the resulting membranes are presented in Figure 4.5.

It is shown that the salt rejection increased and the permeation flux decreased significantly when the crosslinking temperature increased from 25 to 70°C. It is believed that at a glutaraldehyde concentration of 1.0 wt% and crosslinking time of 60 min, the outermost layer of chitosan in the thin film was crosslinked by glutaraldehyde significantly when the crosslinking temperature reached 70°C. A further increase in the temperature beyond 70°C had little influence on separation performance of the membrane.

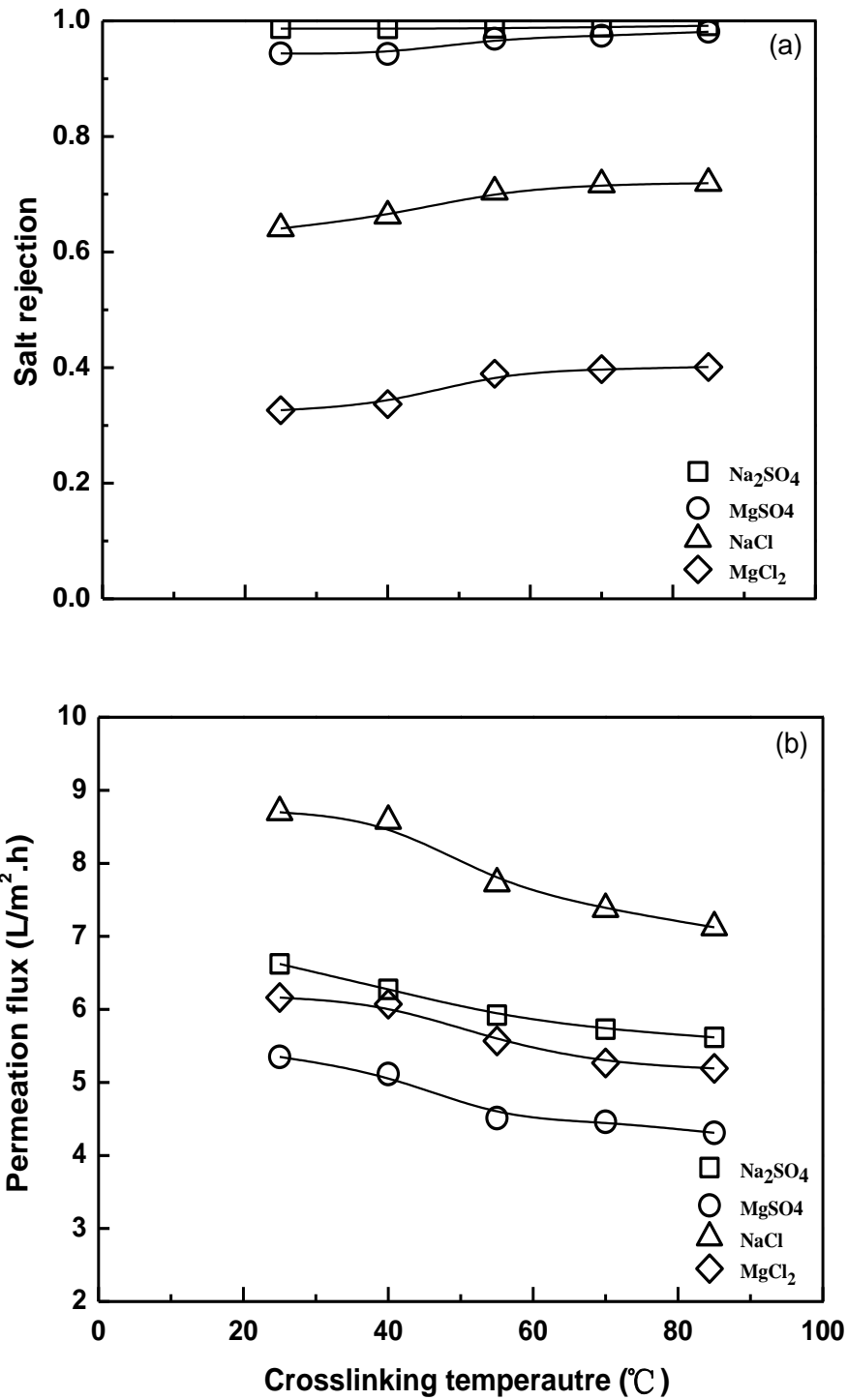


Figure 4.5 Effects of crosslinking temperature on (a) salt rejection and (b) permeation flux (Operating pressure: 0.7 MPa; Salt concentration: 500 ppm)

4.3.5 Effect of crosslinking time

Crosslinking time is another factor that affects the degree of crosslinking of the membrane. A longer crosslinking time allows chitosan molecules on the membrane to react with glutaraldehyde more completely and thus leads to a higher degree of crosslinking of the membrane [Hyder et al., 2009]. The crosslinking reactions between the [CS/PAA]₄CS membranes and 1.0 wt% of glutaraldehyde solutions were carried out at a room temperature (25°C) for different periods of crosslinking time (30 to 150 min). The permeation flux and salt rejection of the resulting membranes are shown in Figure 4.6.

It can be seen that the effect of crosslinking time on membrane performance was not significant at a crosslinking temperature of 25°C and glutaraldehyde concentration of 1.0 wt%. This is consistent with the result obtained from the 2³ factorial design, where the membrane performance was not affected by the crosslinking time significantly within the operating conditions (shown in Figure 4.2 and 4.3).

Therefore, a crosslinking reaction of 30 min seems to be enough to fabricate the crosslinked chitosan/PAA composite membranes with a good salt rejection and reasonable permeation flux.

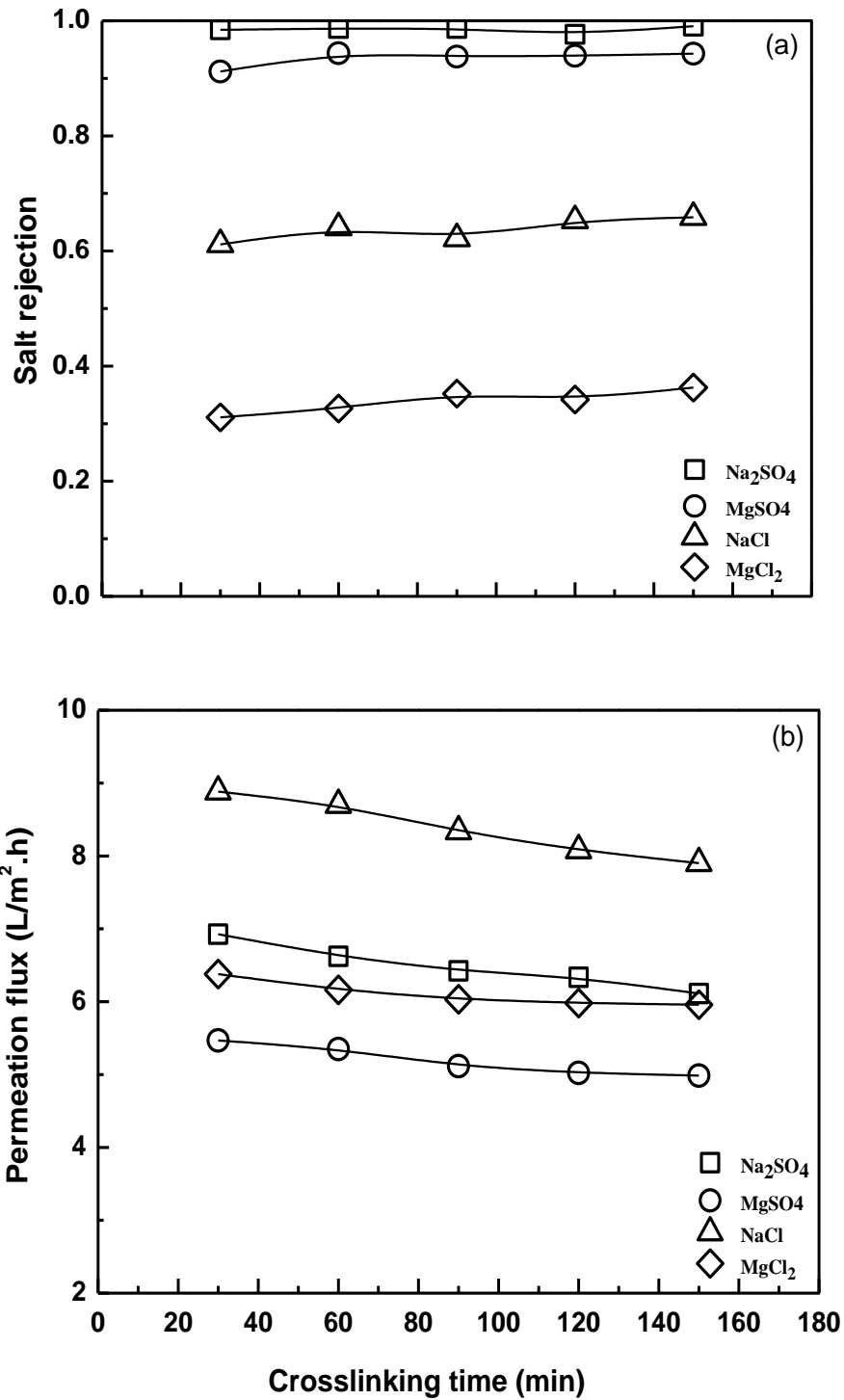


Figure 4.6 Effects of crosslinking time on (a) salt rejection and (b) permeation flux (Operating pressure: 0.7 MPa; Salt concentration: 500 ppm)

4.3.6 Effect of operating pressure in nanofiltration

To investigate the effects of operating pressure on the separation performance of crosslinked chitosan/PAA composite membranes, NF experiments were carried out using a crosslinked [CS/PAA]₄ membrane for salt rejection at a feed concentration of 500 ppm and at different pressures from 0.1 to 0.9 MPa. The permeation flux and salt rejection of the membrane are presented in Figure 4.7.

An increase in operating pressure increased both the permeation flux and the salt rejection. As mentioned before, the mass transport through a NF membrane is mainly based on the solution-diffusion mechanism. When the feed salt concentration is as low as 500 ppm, the osmotic pressure on the membrane surface is not significant. Therefore, an increase in operating pressure resulted in almost a linear increase in permeation flux and a gradual increase in salt rejection.

In addition, with an increase in operating pressure, the enhancement in salt rejection and permeation flux of the uncrosslinked membrane (shown in Figure 3.9) were less significant than that of the crosslinked membrane. This is because surface crosslinking of the membranes with glutaraldehyde produced more hydrophobic and rigid membrane surface [Beppu et al., 2007], which led to a higher resistance to salts transport through the membrane.

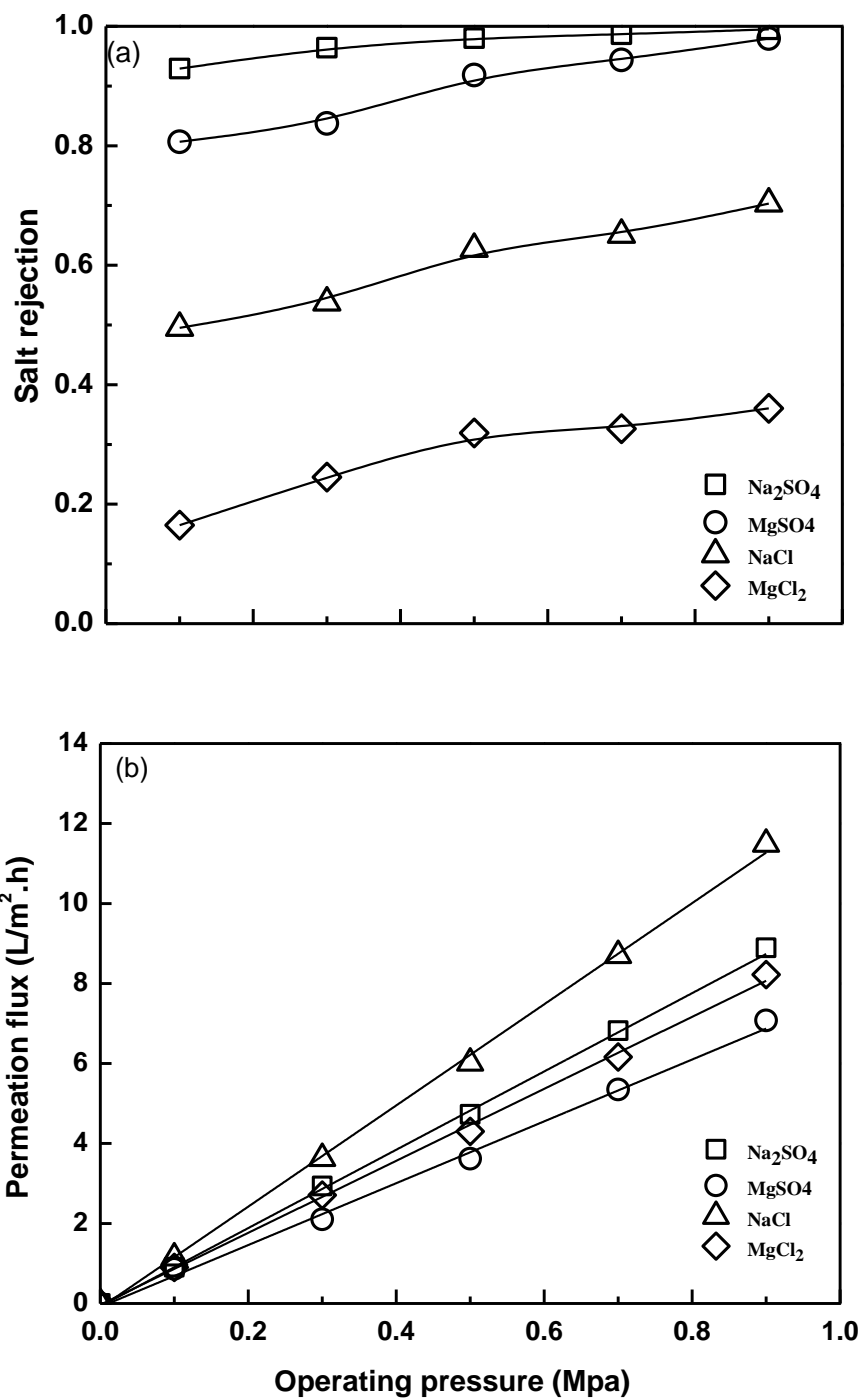


Figure 4.7 Effects of operating pressure on (a) salt rejection and (b) permeation flux for the crosslinked [CS/PAA]₄CS membrane (Polyelectrolyte concentration : 1000 ppm; Deposition time : 60 min; Crosslinking temperature: 25°C; Crosslinking time: 60 min; Glutaraldehyde concentration: 1.0 wt%)

4.3.7 Effect of feed salt concentration in nanofiltration

To investigate the effects of feed salt concentration on separation performance of crosslinked chitosan/PAA composite membranes, NF experiments were carried out using a crosslinked [CS/PAA]₄ membrane for salt rejection at an operating pressure of 0.7 MPa and different feed salt concentrations from 500 to 2000 ppm. The permeation flux and salt rejection of the membrane are shown in Figure 4.8.

Both the salt rejection and permeation flux decreased slightly with an increase in feed salt concentration. Compared to the uncrosslinked membrane (shown in Figure 3.11), the salt rejection and permeation flux of the crosslinked membrane decreased less significantly.

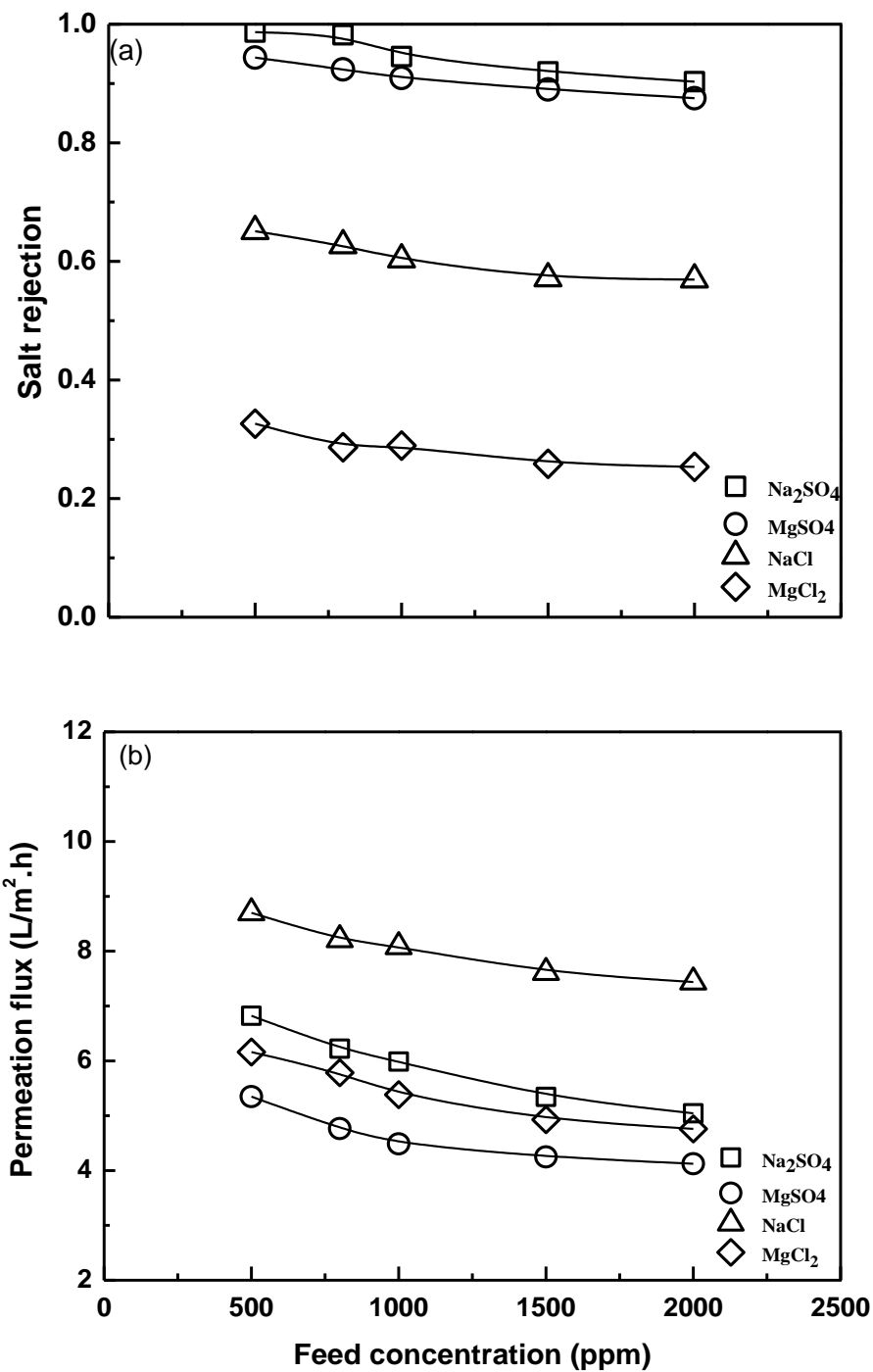


Figure 4.8 Effects of feed salt concentration on (a) salt rejection and (b) permeation flux for the crosslinked [CS/PAA]₄CS membrane (Polyelectrolyte concentration : 1000 ppm ; Deposition time : 60 min; Crosslinking temperature: 25°C; Crosslinking time: 60 min; Glutaraldehyde concentration: 1.0 wt%)

4.3.8 Stability of crosslinked chitosan/PAA composite membrane

The stability test of the crosslinked [CS/PAA]₄CS membrane was carried out. The [CS/PAA]₄CS membrane was crosslinked with 1.0 wt% of glutaraldehyde solution at a temperature of 25 °C for 60 min. The salt rejection and permeation flux of the membrane in 5 cycles of NF experiments are presented in the Figure 4.9.

It is shown that the membrane performance maintained constant during the NF tests. The improved membrane stability is attributed to crosslinks produced using glutaraldehyde as the crosslinking agent. The polyelectrolytes in an uncrosslinked chitosan/PAA composite membrane were mainly held together by electrostatic attractions. Crosslinking of the membrane with glutaraldehyde produced a three-dimensional networks linked chemically, which makes the polyelectrolyte membrane stable in the salt solutions. Therefore, membrane swelling is constrained by the crosslinking. Surface crosslinking of membranes is frequently used to improve the stability and the separation performance of the membranes [Homberg et al., 1998; Yeom and Lee, 1998].

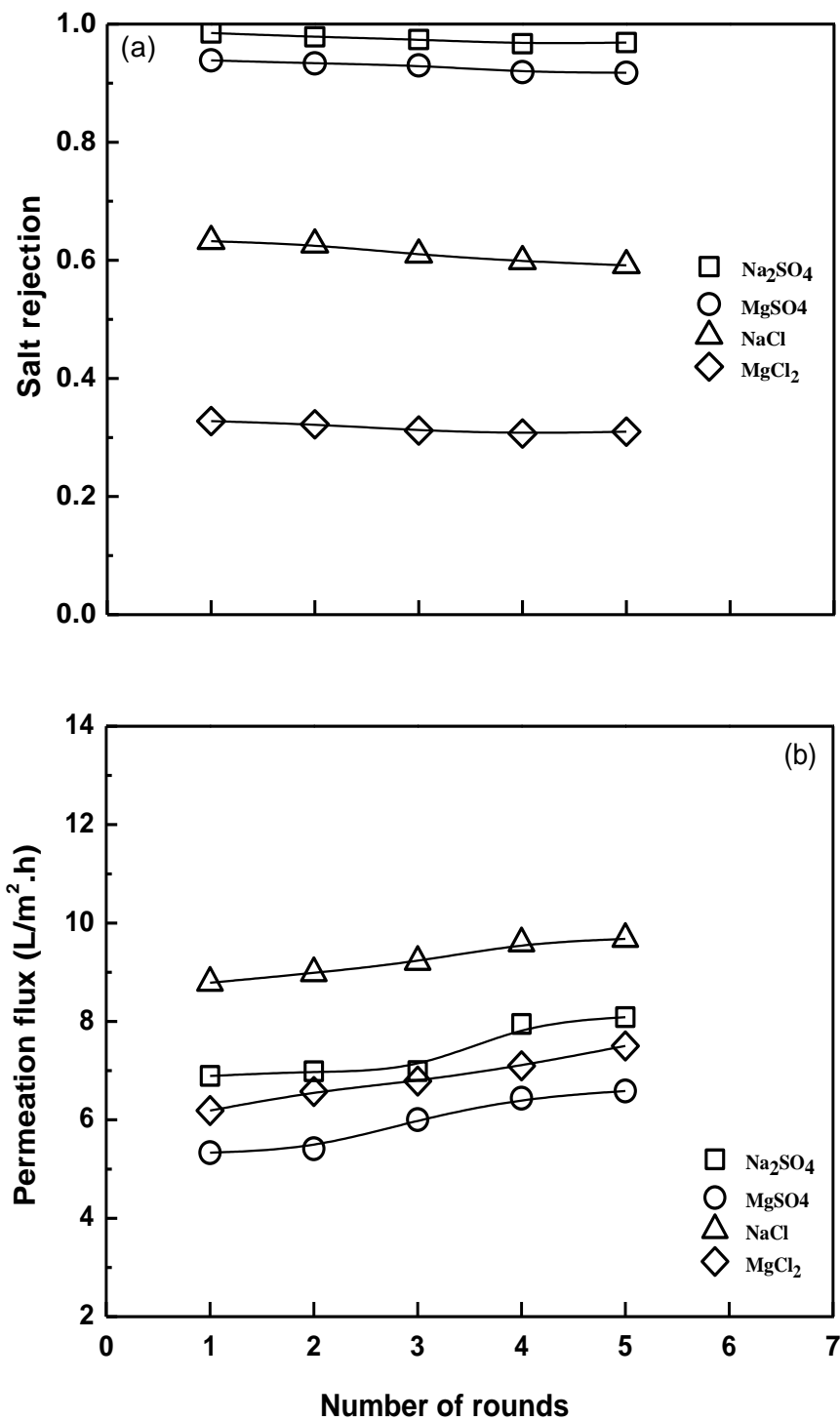


Figure 4.9 Stability of the crosslinked [CS/PAA]₄CS membrane, (a) salt rejection and (b) permeation flux (Operating pressure: 0.7 MPa; Salt concentration: 500 ppm; Crosslinking temperature: 25°C; Crosslinking time: 60 min; Glutaraldehyde concentration: 1.0 wt%)

4.4 Conclusions

In this chapter, surface crosslinking of chitosan/PAA composite membranes with glutaraldehyde was carried out to enhance the separation performance and stability of the membranes. A 2^3 factorial design was used to investigate the effects of factors involved in the crosslinking procedure (i.e., crosslinking temperature, crosslinking time, and glutaraldehyde concentration) and their interactions on the separation performance of the membranes. Experiments were also conducted with “one variable at a time” to better understand the various factors. The stability of the crosslinked membranes was confirmed with experiments. The following conclusions can be drawn:

- (1) Within the range of operating conditions, glutaraldehyde concentration (C) was the most significant factor to the membrane performance. The glutaraldehyde concentration (C), crosslinking temperature (A), and the interaction (AC) are more significant than other effects (B, AB, BC, and ABC). In addition, the 3-way interaction (ABC) was the least important factor to the separation performance of the membranes.
- (2) The factorial design results were analyzed with ANOVA. The *p*-values and coded coefficients were obtained and used to evaluate the significance of each factor and the interaction effect in crosslinking reaction. Linear models for the relationship between separation performance and crosslinking conditions were also derived from ANOVA.

- (3) An increase in glutaraldehyde concentration led to an increase in salt rejection and a decrease in permeation flux up to a concentration of 1.5 wt%, beyond which concentration both the permeation flux and the salt rejection did not change significantly with an increase in glutaraldehyde concentration. The crosslinked membrane showed a salt rejection in the order of $\text{Na}_2\text{SO}_4 > \text{MgSO}_4 > \text{NaCl} > \text{MgCl}_2$.
- (4) The separation performance of the crosslinked membrane was improved by increasing the crosslinking temperature from 25 to 70°C; A further increase in the crosslinking temperature did not affect the membrane performance significantly. The stability of the chitosan/PAA composite membranes was improved by crosslinking with glutaraldehyde.

CHAPTER 5

General conclusions and Recommendations

5.1 General conclusions

The following conclusions can be drawn from this thesis work:

- (1) The LbL self-assembly of chitosan/PAA thin films on PES substrates was used to fabricate NF membranes with good separation performance. An increase in the number of polyelectrolyte bilayers led to an increase in salt rejection and a decrease in permeation flux of the membranes. A polyelectrolyte deposition time of 60 min was adequate for adsorption of polyelectrolytes on the membrane surface. The polyelectrolyte concentration in the deposition solutions also affected the membrane performance, and a polyelectrolyte concentration of 1000 ppm was shown to be appropriate for the membrane fabrication. $[\text{CS}/\text{PAA}]_n\text{CS}$ membranes with chitosan as the outermost layer had different salt rejections compared to $[\text{CS}/\text{PAA}]_n$ membranes that had PAA as the outermost layer.
- (2) The operating conditions in NF (i.e., operating pressure and feed concentration) also affected the separation performance of the chitosan/PAA composite

membranes. An increase in operating pressure increased the permeation flux linearly, while the salt rejection gradually increased. With an increase in the feed salt concentration, however, both the salt rejection and permeation flux decreased.

(3) The performance of the chitosan/PAA composite membranes declined over time for a prolonged period of nanofiltration with the feed solutions. The membranes were thus subjected to heat treatment in order to improve the stability and selectivity of the membranes.

(4) Chemical crosslinking of the membranes using glutaraldehyde effectively improved the membrane stability. A factorial design was used to evaluate the effects of crosslinking conditions on the membrane performance. The separation performance of the membranes can be optimized by properly controlling the crosslinking conditions (e.g., crosslinking agent concentration and crosslinking time and temperature).

5.2 Recommendations

The results of this study showed that polyelectrolyte thin films were not very stable for nanofiltration of salt solutions over long-term operation. Both heat treatment and chemical crosslinking of the membrane improved the membrane stability. In order to enhance the stability and optimize the separation performance of the membranes, future research is recommended to (1) study the effects of membrane preparation conditions in LbL assembly on membrane performance systematically, (2) investigate the surface

modification techniques for the LbL-assembled membranes. This will help improve and optimize the membrane performance. In addition, the chitosan/PAA composite membranes should be tested for nanofiltration of fluids relevant to treatment of industrial wastewater.

5.2.1 Preparation conditions in LbL assembly

Although some of the preparation conditions in LbL assembly have been investigated in this study (chapter 3), there are other parameters involved in the membrane fabrication that may affect the separation performance of the LbL-assembled polyelectrolyte composite membranes.

The molecular weight of the polyelectrolytes affects the formation of polyelectrolyte thin films. The polyelectrolytes with smaller molecular weights can penetrate pores of the substrate more easily, which is undesirable in LbL assembly of polyelectrolyte composite membranes. In addition, the molecular weight of polyelectrolytes influences the molecular affinity. For instance, Chen et al. [2002], who prepared a series of membranes using chitosan of different molecular weights and tested for separation of bovine serum protein, showed that membranes prepared from chitosan with high molecular weights had a low permeability and a high affinity.

The charge density ρ_c of polyelectrolyte bilayer is also important. A higher charge density of polyelectrolytes will result in a denser network of thin films and thus a better selectivity and a lower permeability [Schönhoff, 2003].

The pH condition of polyelectrolyte solutions affects the degree of ionization, and thus it will affect the separation performance of the polyelectrolyte membranes [Ouyang et al., 2008]. Neither a low nor a high pH of polyelectrolyte solution is preferred because a low pH leads to a high protonation of the polar groups of polyelectrolytes while a high pH results in an opposite situation. An optimum pH with a favorable degree of ionization can be estimated from [Krasemann et al., 2001]:

$$pH_{opt} = \frac{pK_a(\text{polyanion}) + pK_a(\text{polycation})}{2} \quad (6-1)$$

The cationic and anionic polyelectrolytes will partially ionize at a pH above or below pH_{opt} .

Adsorption of polyelectrolytes on the substrate is an exothermal process, and a low-temperature is desirable from the polyelectrolyte adsorption standpoint. However, a high temperature will speed up the diffusion of polyelectrolyte in the solution. Therefore, there may be an optimum temperature for polyelectrolyte deposition, which may be investigated in the future work.

In addition, the commonly used LbL assembly technique is based on the static deposition. Some recent studies used dynamic deposition to improve the efficiency of membrane formation by using an electric-field or external pressure during the polyelectrolyte depositions. The use of electric field in LbL assembly helps orientate the polyelectrolyte chains more quickly [Zhang et al., 2008], and the use of external pressure helps the polyelectrolytes to aggregate on the membrane surface, which leads to a more

uniform and integrated skin layer [Zhang et al., 2006]. Therefore, dynamic deposition in membrane preparation may be used to improve the separation performance of the membrane.

5.2.2 Modification of LbL-assembled membranes

Crosslinking of polyelectrolyte composite membrane leads to a more rigid and compact membrane structure, which enhances separation performance of the membranes. Besides glutaraldehyde, some other crosslinking agents may also be used for surface modification of the chitosan/PAA composite membranes. Nam et al. [1999] employed sulfuric acid as a crosslinking agent to modify chitosan membranes for pervaporation applications, and Devi et al. [2005] utilized toluene diisocyanate (TDI) to crosslink chitosan membranes for dehydration of isopropanol/water mixtures. Therefore, modification of chitosan/PAA composite membranes using different crosslinking agents can also be considered in the future study.

5.2.3 Membrane separation in a complex system

This work focused on the development of chitosan/PAA composite membranes and they were tested with simple salt solutions. It is recommended to test these membrane for nanofiltration of complex effluents that are relevant to practical applications.

Stanton et al. [2003], who fabricated the PSS/PAH thin films on porous alumina substrates and tested the membranes with a solution of a mixed salt of CaCl_2 and Na_2SO_4 ,

showed that the surface charge property of the membrane influenced the rejection of CaCl_2 and Na_2SO_4 differently. The selectivity of SO_4^{2-} in a mixed solution was higher than that measured in a single salt solution, which indicates that the membrane performance is affected by the interactions between the solutes, thereby influencing the membrane performance for rejection of a mixed solutes in water purification.

Aravind et al. [2010] used chitosan/PSS composite membranes to treat wastewater from paper mill and textile effluents. The membranes were able to remove color and COD from the wastewater. The COD values of the effluents were reduced by 70 - 88%. A neutral or a low pH condition led to a high removal of the color and COD.

In summary, all the aspects mentioned above are recommended for further studies in the future work in order to improve the performance of polyelectrolyte composite membranes prepared by LbL assembly and to establish a baseline for treatment of industrial wastewater with specific compositions relevant to practical applications.

References

Abu Seman, M. N., M. Khayet, N. Hilal, Nanofiltration thin-film composite polyester polyethersulfone-based membranes prepared by interfacial polymerization, *Journal of Membrane Science*. 348(2010)109-116.

Al-Zoubi, H., N. Hilal, N. A. Darwish, A. W. Mohammad, Rejection and modelling of sulphate and potassium salts by nanofiltration membranes: neural network and Spiegler-Kedem model, *Desalination*. 206(2007)42-60.

Anjali Devi, D., B. Smitha, S. Sridhar, T. M. Aminabhavi, Pervaporation separation of isopropanol/water mixtures through crosslinked chitosan membranes, *Journal of Membrane Science*. 262(2005)91-99.

Aravind, U. K., B. George, M. S. Baburaj, S. Thomas, A. P. Thomas, C. T. Aravindakumar, Treatment of industrial effluents using polyelectrolyte membranes, *Desalination*. 252(2010)27-32.

Beppu, M. M., R. S. Vieira, C. G. Aimoli, C. C. Santana, Crosslinking of chitosan membranes using glutaraldehyde: Effect on ion permeability and water absorption, *Journal of Membrane Science*. 301(2007)126-130.

Bergman, R., *Reverse Osmosis and Nanofiltration*, American Water Works Association, 2007.

Bessarabov, D., Z. Twardowski, Industrial application of nanofiltration - new perspectives, *Membrane Technology*. 9(2002)6-9.

Bonekamp, B. C., R. Kreiter, J. F. Vente, Sol-gel approaches in the synthesis of membrane materials for nanofiltration and pervaporation, *Sol-Gel Methods for Materials Processing*, Springer, 2008, pp. 47-65.

Buron, C. C., C. Filiatre, F. Membrey, C. Bainier, L. Buisson, D. Charraut, et al., Surface morphology and thickness of a multilayer film composed of strong and weak polyelectrolytes: Effect of the number of adsorbed layers, concentration and type of salts, *Thin Solid Films*. 517(2009)2611-2617.

Cadotte, J. E., R. S. King, R. J. Majerle, R. J. Petersen, Interfacial synthesis in the

preparation of reverse osmosis membranes, *Journal of Macromolecular Science, Part A: Chemistry*. 15(1981)727-755.

Chakraborty, S., M. K. Purkait, S. DasGupta, S. De, J. K. Basu, Nanofiltration of textile plant effluent for color removal and reduction in COD, *Separation and Purification Technology*. 31(2003)141-151.

Chen, X., L. Zheng, Z. Wang, C. Lee, H. J. Park, Molecular affinity and permeability of different molecular weight chitosan membranes, *Journal of Agricultural and Food Chemistry*. 50(2002)5915-5918.

Childress, A. E., M. Elimelech, Relating nanofiltration membrane performance to membrane charge (electrokinetic) characteristics, *Environmental Science & Technology*. 34(2000)3710-3716.

Cisneros- Zevallos, L., J. M. Krochta, Dependence of coating thickness on viscosity of coating solution applied to fruits and vegetables by dipping method, *Journal of Food Science*. 68(2003)503-510.

Conlon, W. J., S. A. McClellan, Membrane softening: a treatment process comes of age, *Journal of the American Water Works Association*. 81(1989)47-51.

Cui, Z., Y. Xiang, J. Si, M. Yang, Q. Zhang, T. Zhang, Ionic interactions between sulfuric acid and chitosan membranes, *Carbohydrate Polymers*. 73(2008)111-116.

Dai, J., D. M. Sullivan, M. L. Bruening, Ultrathin, layered polyamide and polyimide coatings on aluminum, *Industrial & Engineering Chemistry Research*. 39(2000)3528-3535.

Daufin, G., J. P. Escudier, H. Carrere, S. Berot, L. Fillaudeau, M. Decloux, Recent and emerging applications of membrane processes in the food and dairy industry, *Food and Bioproducts Processing*. 79(2001)89-102.

Decher, G., J. D. Hong, Buildup of ultrathin multilayer films by a self- assembly process, 1. Consecutive adsorption of anionic and cationic bipolar amphiphiles on charged surfaces, *Makromolekulare Chemie Macromolecular Symposia*. 46(1991)321-327.

Decher, G., Molecular multilayer films: The quest for order, orientation, and optical properties, *Photonic and Optoelectronic Polymers*. 672(1997)445-459.

Decher, G., M. Eckle, J. Schmitt, B. Struth, Layer-by-layer assembled multicomposite films, *Current Opinion in Colloid & Interface Science*. 3(1998)32-39.

Decher, G., J. B. Schlenoff, *Multilayer Thin Films: Sequential Assembly of Nanocomposite Materials*, Wiley, 2006.

Devi, D. A., B. Smitha, S. Sridhar, T. M. Aminabhavi, Pervaporation separation of isopropanol/water mixtures through crosslinked chitosan membranes, *Journal of Membrane Science*. 262(2005)91-99.

Dresner, L., Some remarks on the integration of the extended Nernst-Planck equations in the hyperfiltration of multicomponent solutions, *Desalination*. 10(1972)27-46.

Du, R. H., A. Chakma, X. Feng, Interfacially formed poly(N,N-dimethylaminoethyl methacrylate)/polysulfone composite membranes for CO₂/N₂ separation, *Journal of Membrane Science*. 290(2007)19-28.

Feng, X., R. Y. M. Huang, Pervaporation with chitosan membranes .1. Separation of water from ethylene glycol by a chitosan/polysulfone composite membrane, *Journal of Membrane Science*. 116(1996)67-76.

Fred, W. B., *Textbook of Polymer Science*, Wiley, 1984.

Ghazali, M., M. Nawawi, R. Y. M. Huang, Pervaporation dehydration of isopropanol with chitosan membranes, *Journal of Membrane Science*. 124(1997)53-62.

Ghiorghita, C. A., F. Bucatariu, G. Hitruc, M. Mihai, E. S. Dragan, Polyelectrolyte multilayers composed of chitosan and poly(acrylic-acid), *Materiale Plastice*. 51(2014)323-327.

Ghizellaoui, S., A. Chibani, S. Ghizellaoui, Use of nanofiltration for partial softening of very hard water, *Desalination*. 179(2005)315-322.

Grignon, J., A. M. Scallan, Effect of pH and neutral salts upon the swelling of cellulose gels, *Journal of Applied Polymer Science*. 25(1980)2829-2843.

Hagmeyer, G., R. Gimbel, Modelling the salt rejection of nanofiltration membranes for ternary ion mixtures and for single salts at different pH values, *Desalination*. 117(1998)247-256.

Hall, T., J. Hart, B. Croll, R. Gregory, Laboratory- scale investigations of algal toxin removal by water treatment, *Water and Environment Journal*. 14(2000)143-149.

Harris, J. J., P. M. DeRose, M. L. Bruening, Synthesis of passivating, nylon-like coatings through cross-linking of ultrathin polyelectrolyte films, *Journal of the American Chemical Society*. 121(1999)1978-1979.

Harris, J. J., M. L. Bruening, Electrochemical and in situ ellipsometric investigation of the permeability and stability of layered polyelectrolyte films, *Langmuir*. 16(2000)2006-2013.

Hayes, T. B., P. Case, S. Chui, D. Chung, C. Haeffele, K. Haston, et al., Pesticide mixtures, endocrine disruption, and amphibian declines: are we underestimating the impact?, *Environmental Health Perspectives*. 114(2006)40.

Hitzfeld, B. C., S. J. Höger, D. R. Dietrich, Cyanobacterial toxins: removal during drinking water treatment, and human risk assessment, *Environmental Health Perspectives*. 108(2000)113.

Homberg, S., J. H. Näsman, F. Sundholm, Synthesis and properties of sulfonated and crosslinked poly[(vinylidene-fluoride)- graft- styrene] membranes, *Polymers for Advanced Technologies*. 9(1998)121-127.

Hong, S. U., O. Y. Lu, M. L. Bruening, Recovery of phosphate using multilayer polyelectrolyte nanofiltration membranes, *Journal of Membrane Science*. 327(2009)2-5.

Hu, S., X. Ren, M. Bachman, C. E. Sims, G. P. Li, N. Allbritton, Surface modification of poly(dimethylsiloxane) microfluidic devices by ultraviolet polymer grafting, *Analytical Chemistry*. 74(2002)4117-4123.

Huang, R. H., G. H. Chen, M. K. Sun, Y. M. Hu, C. J. Gao, Studies on nanofiltration membrane formed by diisocyanate cross-linking of quaternized chitosan on poly(acrylonitrile) (PAN) support, *Journal of Membrane Science*. 286(2006)237-244.

Huang, R. Y. M., R. Pal, G. Y. Moon, Pervaporation dehydration of aqueous ethanol and isopropanol mixtures through alginate/chitosan two ply composite membranes supported by poly(vinylidene fluoride) porous membrane, *Journal of Membrane Science*. 167(2000)275-289.

Hussain, A. A., A. E. Al-Rawajfeh, Recent patents of nanofiltration applications in oil processing, desalination, wastewater and food industries, *Recent Patents on Chemical Engineering*. 2(2009)51-66.

Hyder, M. N., R. Y. M. Huang, P. Chen, Composite poly(vinyl-alcohol)-polysulfone membranes crosslinked by trimesoyl chloride: Characterization and dehydration of ethylene glycol-water mixtures, *Journal of Membrane Science*. 326(2009)363-371.

Jeanet, R., J. L. Maubois, P. Boyaval, Semicontinuous production of lactic acid in a bioreactor coupled with nanofiltration membranes, *Enzyme and Microbial Technology*. 19(1996)614-619.

Jegal, J., K. H. Lee, Chitosan membranes crosslinked with sulfosuccinic acid for the pervaporation separation of water/alcohol mixtures, *Journal of Applied Polymer Science*. 71(1999)671-675.

Jin, W., A. Toutianoush, B. Tieke, Use of polyelectrolyte layer-by-layer assemblies as nanofiltration and reverse osmosis membranes, *Langmuir*. 19(2003)2550-2553.

Ju, H., B. D. McCloskey, A. C. Sagle, Y. H. Wu, V. A. Kusuma, B. D. Freeman, Crosslinked poly(ethylene oxide) fouling resistant coating materials for oil/water separation, *Journal of Membrane Science*. 307(2008)260-267.

Kelly, J., P. Kelly, Desalination of acid casein whey by nanofiltration, *International Dairy Journal*. 5(1995)291-303.

Kim, I. C., J. Jegal, K. H. Lee, Effect of aqueous and organic solutions on the performance of polyamide thin-film-composite nanofiltration membranes, *Journal of Polymer Science Part B: Polymer Physics*. 40(2002)2151-2163.

Koyuncu, I., Reactive dye removal in dye/salt mixtures by nanofiltration membranes containing vinylsulphone dyes: Effects of feed concentration and cross flow velocity, *Desalination*. 143(2002)243-253.

Krajewska, B., M. Leszko, W. Zaborska, Development of urease-chitosan membrane, *Polimery w Medycynie*. 20(1989)31-41.

Krasemann, L., B. Tieke, Ultrathin self-assembled polyelectrolyte membranes for pervaporation, *Journal of Membrane Science*. 150(1998)23-30.

Krasemann, L., B. Tieke, Composite membranes with ultrathin separation layer prepared by self-assembly of polyelectrolytes, *Materials Science and Engineering: C*. 8-9(1999)513-518.

Krasemann, L., B. Tieke, Selective ion transport across self-assembled alternating multilayers of cationic and anionic polyelectrolytes, *Langmuir*. 16(2000)287-290.

Krasemann, L., A. Toutianoush, B. Tieke, Self-assembled polyelectrolyte multilayer membranes with highly improved pervaporation separation of ethanol/water mixtures, *Journal of Membrane Science*. 181(2001)221-228.

Le Gouellec, Y. A., M. Elimelech, Calcium sulfate (gypsum) scaling in nanofiltration of agricultural drainage water, *Journal of Membrane Science*. 205(2002)279-291.

Li, Y. Y., T. Nomura, A. Sakoda, M. Suzuki, Fabrication of carbon coated ceramic

membranes by pyrolysis of methane using a modified chemical vapor deposition apparatus, *Journal of Membrane Science*. 197(2002)23-35.

Lim, L. Y., L. S. C. Wan, Heat-treatment of chitosan films, *Drug Development and Industrial Pharmacy*. 21(1995)839-846.

Lösche, M., J. Schmitt, G. Decher, W. G. Bouwman, K. Kjaer, Detailed structure of molecularly thin polyelectrolyte multilayer films on solid substrates as revealed by neutron reflectometry, *Macromolecules*. 31(1998)8893-8906.

Lu, O. Y., R. Malaisamy, M. L. Bruening, Multilayer polyelectrolyte films as nanofiltration membranes for separating monovalent and divalent cations, *Journal of Membrane Science*. 310(2008)76-84.

Luo, J., Y. Wan, Effect of highly concentrated salt on retention of organic solutes by nanofiltration polymeric membranes, *Journal of Membrane Science*. 372(2011)145-153.

Malaisamy, R., M. L. Bruening, High-flux nanofiltration membranes prepared by adsorption of multilayer polyelectrolyte membranes on polymeric supports, *Langmuir*. 21(2005)10587-10592.

Malaisamy, R., A. Talla-Nwafo, K. L. Jones, Polyelectrolyte modification of nanofiltration membrane for selective removal of monovalent anions, *Separation and Purification Technology*. 77(2011)367-374.

Mallevalle, J., P. E. Odendaal, M. R. Wiesner, *Water Treatment Membrane Processes*, American Water Works Association, 1996.

McAloney, R. A., M. Sinyor, V. Dudnik, M. C. Goh, Atomic force microscopy studies of salt effects on polyelectrolyte multilayer film morphology, *Langmuir*. 17(2001)6655-6663.

Meier-Haack, J., W. Lenk, D. Lehmann, K. Lunchwitz, Pervaporation separation of water/alcohol mixtures using composite membranes based on polyelectrolyte multilayer assemblies, *Journal of Membrane Science*. 184(2001)233-243.

Missimer, T. M., I. Watson, *Water Supply Development for Membrane Water Treatment Facilities*, Lewis Publishers, 1994.

Moore, A., C. P. Waring, Mechanistic Effects of a triazine pesticide on reproductive endocrine function in mature male atlantic salmon (*salmo salar*L.) parr, *Pesticide Biochemistry and Physiology*. 62(1998)41-50.

Mulder, J., *Basic Principles of Membrane Technology*, Springer Netherlands, 1996.

Nam, S. Y., Y. M. Lee, Pervaporation separation of methanol/methyl t-butyl ether through chitosan composite membrane modified with surfactants, *Journal of Membrane Science*. 157(1999)63-71.

Ng, L. Y., A. W. Mohammad, C. Y. Ng, A review on nanofiltration membrane fabrication and modification using polyelectrolytes: Effective ways to develop membrane selective barriers and rejection capability, *Advances in Colloid and Interface Science*. 197(2013)85-107.

Nghiem, L. D., A. I. Schafer, M. Elimelech, Removal of natural hormones by nanofiltration membranes: Measurement, modeling, and mechanisms, *Environmental Science & Technology*. 38(2004)1888-1896.

Ouyang, L., R. Malaisamy, M. L. Bruening, Multilayer polyelectrolyte films as nanofiltration membranes for separating monovalent and divalent cations, *Journal of Membrane Science*. 310(2008)76-84.

Patel, T. M., K. Nath, Modeling of permeate flux and mass transfer resistances in the reclamation of molasses wastewater by a novel gas-sparged nanofiltration, *Korean Journal of Chemical Engineering*. 31(2014)1865-1876.

Peeters, J. M. M., J. P. Boom, M. H. V. Mulder, H. Strathmann, Retention measurements of nanofiltration membranes with electrolyte solutions, *Journal of Membrane Science*. 145(1998)199-209.

Petersen, R. J., Composite reverse osmosis and nanofiltration membranes, *Journal of Membrane Science*. 83(1993)81-150.

Pieracci, J., J. V. Crivello, G. Belfort, Photochemical modification of 10kDa polyethersulfone ultrafiltration membranes for reduction of biofouling, *Journal of Membrane Science*. 156(1999)223-240.

Quinn, J. F., F. Caruso, Facile tailoring of film morphology and release properties using layer-by-layer assembly of thermoresponsive materials, *Langmuir*. 20(2004)20-22.

Rautenbach, R., A. Groschl, Separation potential of nanofiltration membranes, *Desalination*. 77(1990)73-84.

Ray, T. K., A modified method for the isolation of the plasma membrane from rat liver, *Biochimica et Biophysica Acta (BBA)-Biomembranes*. 196(1970)1-9.

Rektor, A., G. Vatai, Membrane filtration of Mozzarella whey, *Desalination*. 162(2004)279-286.

Robinson, J. P., E. S. Tarleton, K. Ebert, C. R. Millington, A. Nijmeijer, Influence of cross-linking and process parameters on the separation performance of poly(dimethylsiloxane) nanofiltration membranes, *Industrial & Engineering Chemistry Research*. 44(2005)3238-3248.

Rosa, M. J., M. N. de Pinho, The role of ultrafiltration and nanofiltration on the minimisation of the environmental impact of bleached pulp effluents, *Journal of Membrane Science*. 102(1995)155-161.

Schaep, J., B. Van der Bruggen, S. Uytterhoeven, R. Croux, C. Vandecasteele, D. Wilms, Removal of hardness from groundwater by nanofiltration, *Desalination*. 119(1998)295-301.

Schaep, J., B. Van der Bruggen, C. Vandecasteele, D. Wilms, Influence of ion size and charge in nanofiltration, *Separation and Purification Technology*. 14(1998)155-162.

Schäfer, A. I., A. G. Fane, T. D. Waite, *Nanofiltration: Principles and Applications*, Elsevier Advanced Technology, 2005.

Schlögl, R., Membrane permeation in systems far from equilibrium, *Berichte der Bunsengesellschaft für Physikalische Chemie*. 70(1966)400-414.

Schönhoff, M., Self-assembled polyelectrolyte multilayers, *Current Opinion in Colloid & Interface Science*. 8(2003)86-95.

Shiratori, S. S., M. F. Rubner, pH-dependent thickness behavior of sequentially adsorbed layers of weak polyelectrolytes, *Macromolecules*. 33(2000)4213-4219.

Smith, D. P., V. Falls, A. D. Levine, B. MacLeod, M. Simpson, T. L. Champlin, Nanofiltration to augment conventional treatment for removal of algal toxins, taste and odor compounds, and natural organic matter, In: *Proceedings of the Water Quality Technology Conference*, Seattle, Washington, 2002, pp. 10-14.

Son, S. H., J. Jegal, Preparation and characterization of polyamide reverse- osmosis membranes with good chlorine tolerance, *Journal of Applied Polymer Science*. 120(2011)1245-1252.

Stanton, B. W., J. J. Harris, M. D. Miller, M. L. Bruening, Ultrathin, multilayered polyelectrolyte films as nanofiltration membranes, *Langmuir*. 19(2003)7038-7042.

Steitz, R., W. Jaeger, R. v. Klitzing, Influence of charge density and ionic strength on the multilayer formation of strong polyelectrolytes, *Langmuir*. 17(2001)4471-4474.

Su, B. W., T. T. Wang, Z. W. Wang, X. L. Gao, C. J. Gao, Preparation and performance of dynamic layer-by-layer PDADMAC/PSS nanofiltration membrane, *Journal of Membrane Science*. 423(2012)324-331.

Sukhorukov, G. B., J. Schmitt, G. Decher, Reversible swelling of polyanion/polycation multilayer films in solutions of different ionic strength, *Berichte der Bunsengesellschaft für Physikalische Chemie*. 100(1996)948-953.

Sullivan, D. M., M. L. Bruening, Ultrathin, cross-linked polyimide pervaporation membranes prepared from polyelectrolyte multilayers, *Journal of Membrane Science*. 248(2005)161-170.

Tang, C., V. Chen, Nanofiltration of textile wastewater for water reuse, *Desalination*. 143(2002)11-20.

Tang, C. Y., Y. N. Kwon, J. O. Leckie, Effect of membrane chemistry and coating layer on physicochemical properties of thin film composite polyamide RO and NF membranes: I. FTIR and XPS characterization of polyamide and coating layer chemistry, *Desalination*. 242(2009)149-167.

Tieke, B., F. Van Ackern, L. Krasemann, A. Toutianoush, Ultrathin self-assembled polyelectrolyte multilayer membranes, *The European Physical Journal E*. 5(2001)29-39.

Tieke, B., A. Toutianoush, W. Q. Jin, Selective transport of ions and molecules across layer-by-layer assembled membranes of polyelectrolytes, p-sulfonato-calix[n]arenes and Prussian Blue-type complex salts, *Advances in Colloid and Interface Science*. 116(2005)121-131.

Toutianoush, A., L. Krasemann, B. Tieke, Polyelectrolyte multilayer membranes for pervaporation separation of alcohol/water mixtures, *Colloids and Surfaces A: Physicochemical and Engineering Aspects*. 198(2002)881-889.

Toutianoush, A., B. Tieke, Pervaporation separation of alcohol/water mixtures using self-assembled polyelectrolyte multilayer membranes of high charge density, *Materials Science and Engineering: C*. 22(2002)459-463.

Tsuru, T., H. Takezoe, M. Asaeda, Ion separation by porous silica- zirconia nanofiltration membranes, *AIChE Journal*. 44(1998)765-768.

Tsuru, T., T. Sudoh, T. Yoshioka, M. Asaeda, Nanofiltration in non-aqueous solutions by

porous silica–zirconia membranes, *Journal of Membrane Science*. 185(2001)253-261.

Uragami, T., H. Kinoshita, H. Okuno, Characteristics of permeation and separation of aqueous alcoholic solutions with chitosan derivative membranes, *Die Angewandte Makromolekulare Chemie*. 209(1993)41-53.

Valadez-Blanco, R., F. C. Ferreira, R. F. Jorge, A. G. Livingston, A membrane bioreactor for biotransformations of hydrophobic molecules using organic solvent nanofiltration (OSN) membranes, *Journal of Membrane Science*. 317(2008)50-64.

Van Ackern, F., L. Krasemann, B. Tieke, Ultrathin membranes for gas separation and pervaporation prepared upon electrostatic self-assembly of polyelectrolytes, *Thin Solid Films*. 327(1998)762-766.

Van der Bruggen, B., K. Everaert, D. Wilms, C. Vandecasteele, Application of nanofiltration for removal of pesticides, nitrate and hardness from ground water: rejection properties and economic evaluation, *Journal of Membrane Science*. 193(2001)239-248.

Van Gestel, T., C. Vandecasteele, A. Buekenhoudt, C. Dotremont, J. Luyten, R. Leysen, Salt retention in nanofiltration with multilayer ceramic TiO₂ membranes, *Journal of Membrane Science*. 209(2002)379-389.

Vanderhorst, H. C., J. M. K. Timmer, T. Robbertsen, J. Leenders, Use of nanofiltration for concentration and demineralization in the dairy industry: Model for mass transport, *Journal of Membrane Science*. 104(1995)205-218.

Wan, Y., K. A. M. Creber, B. Peppley, V. T. Bui, Ionic conductivity and related properties of crosslinked chitosan membranes, *Journal of Applied Polymer Science*. 89(2003)306-317.

Wang, X. L., C. Zhang, P. Ouyang, The possibility of separating saccharides from a NaCl solution by using nanofiltration in diafiltration mode, *Journal of Membrane Science*. 204(2002)271-281.

Wu, D., Y. Huang, S. Yu, D. Lawless, X. Feng, Thin film composite nanofiltration membranes assembled layer-by-layer via interfacial polymerization from polyethylenimine and trimesoyl chloride, *Journal of Membrane Science*. 472(2014)141-153.

Xu, J., C. Gao, X. Feng, Thin-film-composite membranes comprising of self-assembled polyelectrolytes for separation of water from ethylene glycol by pervaporation, *Journal of Membrane Science*. 352(2010)197-204.

Xu, J., X. Feng, C. Gao, Surface modification of thin-film-composite polyamide membranes for improved reverse osmosis performance, *Journal of Membrane Science*. 370(2011)116-123.

Yates, F., *The Design and Analysis of Factorial Experiments*, Imperial Bureau of Soil Science, 1978.

Yeom, C. K., K. H. Lee, Characterization of sodium alginate membrane crosslinked with glutaraldehyde in pervaporation separation, *Journal of Applied Polymer Science*. 67(1998)209-219.

Yin, M., J. Qian, Q. An, Q. Zhao, Z. Gui, J. Li, Polyelectrolyte layer-by-layer self-assembly at vibration condition and the pervaporation performance of assembly multilayer films in dehydration of isopropanol, *Journal of Membrane Science*. 358(2010)43-50.

Zaidi, A., H. Buisson, S. Sourirajan, H. Wood, Ultra-and nano-filtration in advanced effluent treatment schemes for pollution control in the pulp and paper industry, *Water Science & Technology*. 25(1992)263-276.

Zeng, X., E. Ruckenstein, Cross-linked macroporous chitosan anion-exchange membranes for protein separations, *Journal of Membrane Science*. 148(1998)195-205.

Zhang, G., W. Gu, S. Ji, Z. Liu, Y. Peng, Z. Wang, Preparation of polyelectrolyte multilayer membranes by dynamic layer-by-layer process for pervaporation separation of alcohol/water mixtures, *Journal of Membrane Science*. 280(2006)727-733.

Zhang, L., L. Wang, G. Zhang, X. Wang, Fouling of nanofiltration membrane by effluent organic matter: characterization using different organic fractions in wastewater, *Journal of Environmental Sciences*. 21(2009)49-53.

Zhang, P., J. Qian, Y. Yang, Q. An, X. Liu, Z. Gui, Polyelectrolyte layer-by-layer self-assembly enhanced by electric field and their multilayer membranes for separating isopropanol–water mixtures, *Journal of Membrane Science*. 320(2008)73-77.

Zhang, P., J. Qian, Q. An, X. Liu, Q. Zhao, H. Jin, Surface morphology and pervaporation performance of electric field enhanced multilayer membranes, *Journal of Membrane Science*. 328(2009)141-147.

Zhang, Y., J. W. Rhim, X. Feng, Improving the stability of layer-by-layer self-assembled membranes for dehydration of alcohol and diol, *Journal of Membrane Science*. 444(2013)22-31.

Zhou, W. M., F. Fu, M. Tagaya, T. Kobayashi, Electrostatic layer-by-layer polymer membranes for heavy metal ion desalination, Transactions on Gigaku. 1(2012)1-10.

Zhu, Z., X. Feng, A. Penlidis, Self-assembled nano-structured polyelectrolyte composite membranes for pervaporation, Materials Science and Engineering: C. 26(2006)1-8.

Zhu, Z., X. Feng, A. Penlidis, Layer-by-layer self-assembled polyelectrolyte membranes for solvent dehydration by pervaporation, Materials Science and Engineering: C. 27(2007)612-619.

Appendix A

A-1. Sample calculations of the permeation flux and salt rejection

Sample calculations for NF of Na₂SO₄ solution at 25°C where 14.632 g of permeate was collected over 1 h with a membrane area of 12.56 cm². The electrical conductivity of permeate and feed was 9.8 μs/cm and 817 μs/cm, respectively.

Total permeation flux

$$J = \frac{Q}{A \times \Delta t} = \frac{14.632/1000/1}{1 \times (12.56/10000)} = 11.650 \text{ L}/(\text{m}^2 \text{ h})$$

J = permeation flux, L/(m² h);

Q = amount of the permeate, L;

A = area of membrane, m²;

Δt = operating time, h

Salt rejection

Figure A-1 shows the relationship between salt concentration and electrical conductivity of the salt solutions prepared under laboratory conditions. It is shown that the linear model fits the data well. Therefore, the collected conductivity data of permeate and feed can be converted to the concentration data, and the salt rejection is calculated as follow:

$$R = \frac{c_f - c_p}{c_f} = \frac{k_f - k_p}{k_f} = \frac{817 - 9.8}{817} = 0.9880$$

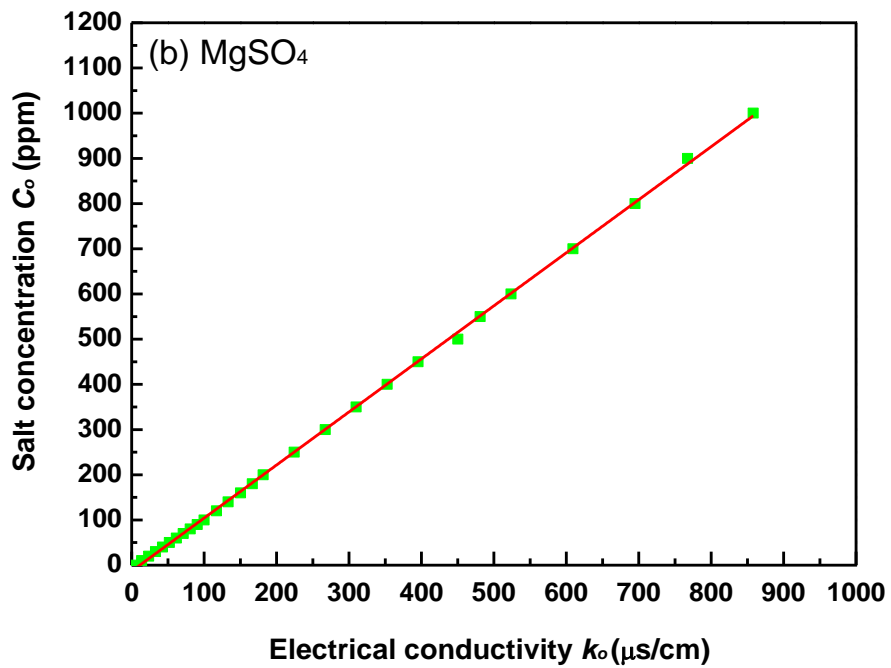
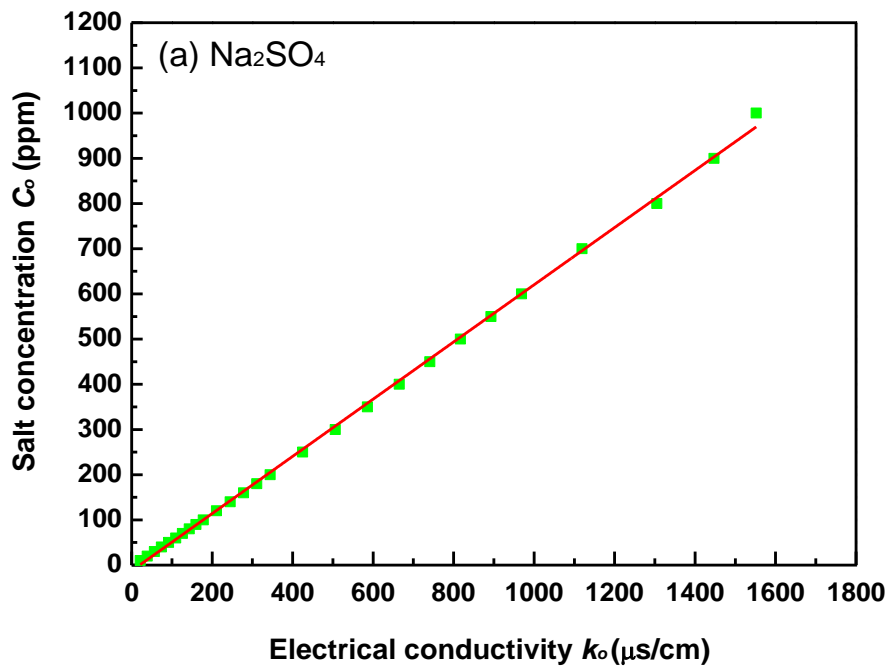
R = rejection rate;

c_f = salt concentration of the feed, ppm;

c_p = salt concentration of the permeate, ppm;

k_f = electrical conductivity of the feed, $\mu\text{s}/\text{cm}$;

k_p = electrical conductivity of the permeate, $\mu\text{s}/\text{cm}$



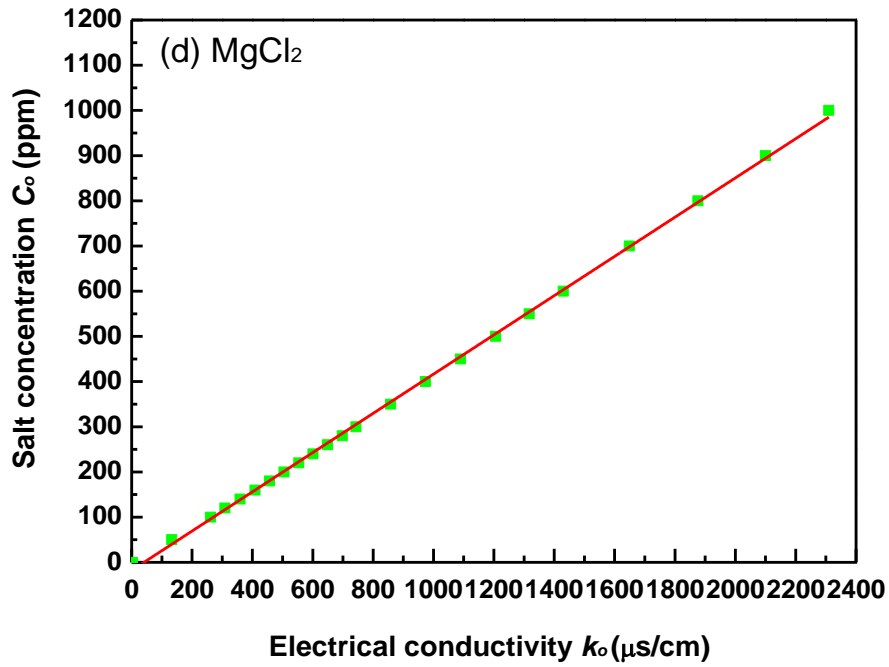
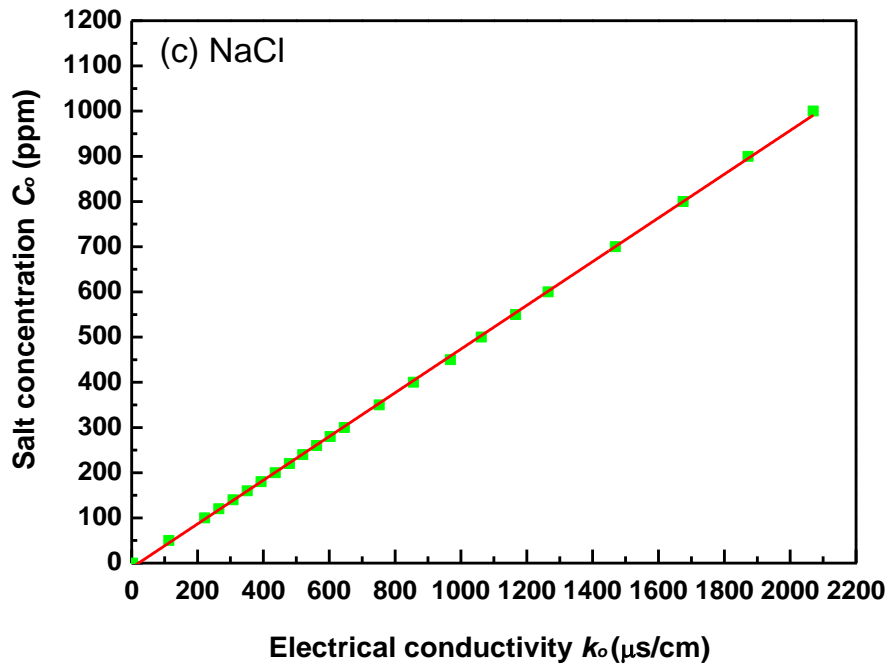


Figure A-1 Linear relationship between salt concentration and its electrical conductivity

A-2. Yates Algorithm for a 2^k factorial Design to compute the linear contrasts of the effects and their sum of squares (S.S.)

Samples calculations for the effects of three crosslinking factors and their interactions on permeation flux of the chitosan/PAA composite membrane for NaCl rejection.

Table A-1 Signs for calculating the effects in the 2^3 factorial Design

<i>Run</i>	<i>I</i>	<i>A</i>	<i>B</i>	<i>AB</i>	<i>C</i>	<i>AC</i>	<i>BC</i>	<i>ABC</i>	<i>Response</i>
<i>I</i>	+	+	+	+	+	+	+	+	6.31
<i>a</i>	+	-	+	-	+	-	+	+	6.60
<i>b</i>	+	+	-	-	+	+	-	-	6.42
<i>ab</i>	+	-	-	+	+	-	-	-	6.80
<i>c</i>	+	+	+	+	-	-	-	-	7.14
<i>ac</i>	+	-	+	-	-	+	-	-	9.54
<i>bc</i>	+	+	-	-	-	-	+	+	7.51
<i>abc</i>	+	-	-	+	-	+	+	+	10.2

Responses = permeation flux for NF with NaCl solution (L/(m² h)).

Table A-2 Yate's algorithm for the 2³ factorial design

<i>Run</i>	<i>Response</i>	<i>I</i>	<i>II</i>	<i>III</i>	<i>Factor</i>	<i>Effect</i>	<i>SS</i>
<i>I</i>	6.31	12.9	26.1	60.5	Total	7.56	15.5
<i>a</i>	6.60	13.2	34.4	5.76	A	1.44	4.15
<i>b</i>	6.42	16.7	0.67	1.30	B	0.33	0.21
<i>ab</i>	6.80	17.7	5.09	0.38	AB	0.10	0.02
<i>c</i>	7.14	0.29	0.30	8.30	C	2.08	8.61
<i>ac</i>	9.54	0.38	1.00	4.42	AC	1.11	2.44
<i>bc</i>	7.51	2.40	0.09	0.70	BC	0.18	0.06
<i>abc</i>	10.2	2.69	0.29	0.20	ABC	0.05	0.01

$$Effect_{total} = III_{total} / 8 ;$$

$$Effect_A = III_A / 4 \quad (\text{same calculation procedure for } B, AB, C, AC, AB \text{ and } ABC)$$

$$SS_A = III_A^2 / 8 \quad (\text{same calculation procedure for } B, AB, C, AC, AB \text{ and } ABC)$$

$$SS_{total} = SS_A + SS_B + SS_C + SS_{AC} + SS_{AB} + SS_{BC} + SS_{ABC}$$